Three Essays in Health Economics

Dominique Baril-Tremblay

Paris 1 Panthéon-Sorbonne

Doctoral Thesis

Three Essays in Health Economics

Author:
Dominique Baril-Tremblay

Supervisor:
Robert Gary-Bobo

A thesis submitted in partial fulfillment of the requirements for the degree of Doctor of Philosophy

May 9, 2023

Résumé

La recherche en économie de la santé n'a jamais été aussi pertinente. Les problèmes de santé publique se multiplient et menacent l'existence même de l'espèce humaine.

Au début de l'année 2020, le SRAS-CoV-2 a fait vaciller l'humanité en l'espace de quelques jours. Cette pandémie nous a permis de constater la vulnérabilité des systèmes de santé à travers le monde (hassan2021orchestrating). Précédemment, les pandémies étaient relativement rares Piret and Boivin (2021). Tout indique qu'avec l'étalement urbain, la hausse de la densité de la population et l'augmentation de la mobilité, celles-ci seront monnaie courante à l'avenir. En l'absence d'immunité à un nouveau pathogène, nos systèmes de santé peuvent rapidement être débordés ce qui multiplie les dommages collatéraux.

Il est impératif de développer des politiques publiques efficaces pour y faire face Dangerfield et al. (2022). Un des moyens pour y arriver est l'étude des modèles épidémiologiques. Ces outils décisionnels puissants se trouvent à la frontière entre l'épidémiologie et l'économie. Ces deux disciplines permettent de comprendre et prédire la dynamique de leur sujet d'étude respectif.

Nos recherches portent sur les outils épidémiologiques de modélisation de la dynamique des infections et de leur place dans les décisions sanitaires des agents économiques. À partir du modèle épidémiologique compartemental SIR *(Suceptible - Infecté - Recovered (immunisé en anglais))*, nous avons étudié trois contextes différents. Nos travaux s'inscrivent dans une littérature riche.

Depuis des décennies les chercheurs se sont intéressés aux modèles épidémiologiques. Kermack and McKendrick (1927) ont jeté les bases des modèles épidémiologiques SIS

(Susceptible - Infecté - Susceptible) et SIR. Ces modèles épidémiologiques sont toujours utiles et inspirent de nombreux modèles épidémiologiques. Ces modèles sont encore aujourd'hui utilisés pour étudier et prédire la propagation de nombreuses maladies telles que la rougeole (Matt J Keeling and Bryan T Grenfell (2002), L. Allen, M. Jones, and Martin (1991)), l'hépatite (Shahdoust et al. (2015)) et la tuberculose (Azeez et al. (2016)) .

Dans la littérature théorique, plusieurs articles ont analysé les effets des mesures de distanciation sociale dans un contexte de contrôle optimal (Sethi (1978), F. Chen et al. (2011) Rowthorn and Toxvaerd (2012)) et dans un contexte de décision stratégique individuelle (textcitereluga2010game, F. Chen (2012), Fenichel et al. (2011), Fenichel (2013), Toxvaerd (2019)). La pandémie de SRAS-CoV-2 a accéléré le développement de la littérature épi-économique. Devant cette menace infectieuse, les chercheurs se sont penchés sur le contrôle optimal de la pandémie sous les hypothèses du modèle épidémiologique SIR lorsque la population est homogène (Kruse and Strack (2020), Eichenbaum, Rebelo, and Trabandt (2022), Alvarez, Argente, and Lippi (2020), C. Jones, Philippon, and Venkateswaran (2021), Glover et al. (2020)) ou lorsque les risques pour une sous-population sont plus élevés (Acemoglu et al. (2021), Rampini (2020), Bairoliya and İmrohoroğlu (2022)). Toxvaerd (2020), Farboodi, Jarosch, and Shimer (2021) et Brotherhood et al. (2020) ont étudié, dans le modèle SIR, les choix des individus alors que ces derniers arbitrent les coûts et les bénéfices de l'auto-isolement. Il existe une littérature croissante en économie qui tente d'intégrer les décisions individuelles de distanciation sociale dans les modèles épidémiologiques.

Dans le premier chapitre, *Self-Isolation*, nous introduisons l'aspect d'apprentissage dans le modèle épidémiologique SIR. Nous analysons la dynamique de l'infection lorsque les individus choisissent leur niveau de confinement selon leur perception des coûts et bénéfices en fonction de leurs croyances subjectives. Dans le deuxième chapitre, *Self-Isolation Under Uncertainty* nous modifions le modèle précédemment décrit pour y ajouter de l'incertitude sur le paramètre épidémiologique. Cette modification nous permet de tirer des leçons quant au niveau d'information optimal en contexte de pandémie. Dans le troisième chapitre, *Swedish Paradox* nous utilisons un modèle épidémiologique

simplifié pour analyser l'effet des stratégies de mitigation des infections sur le rythme d'apparition des vagues d'infections. Vous trouverez dans les prochaines pages un bref résumé en français des contextes, méthodes et conclusions des chapitres qui composent cette thèse.

Self-isolation

Le niveau d'immunité collective d'une maladie infectieuse est défini comme la fraction de la population qui doit devenir immunisée pour que la propagation de la maladie diminue et s'arrête. Dans le modèle le plus simple, il est égal à $(R_0 - 1)/R_0$, où R_0 est le nombre de reproductions de base (*Basic Reproduction Number*)[1] de la maladie, qui est souvent estimé à environ 60% pour COVID-19. Ce chiffre de 60 % suppose que la population est homogène et passive, alors qu'il est bien documenté[2] entre autre par que le nombre d'infections secondaires causées par un seul individu infectieux introduit dans une population totalement susceptible varie entre les populations composées de personnes ayant des comportements différents. L'objet de la littérature épi-économique croissante est d'analyser les interactions bilatérales entre la dynamique des épidémies et les comportements individuels.

L'une des nombreuses caractéristiques de COVID-19 est la grande diversité des réponses à l'infection dans la population, certains individus étant totalement asymptomatiques, tandis que d'autres développent des formes mortelles en quelques jours. Comme les personnes symptomatiques, les patients asymptomatiques sont une source de propagation de l'infection. Avant d'être infecté, il n'y a aucun moyen de savoir si l'on est du type asymptomatique. C'est pourquoi les individus se forgent des croyances sur leur type, qu'ils actualisent en permanence en fonction de leur degré d'exposition au virus. Au même moment, ils décident leur niveau d'exposition au virus en tenant compte de

[1] Le nombre de reproductions de base est le nombre attendu de cas d'infection secondaire causés par un seul cas infectieux typique pendant toute sa période infectieuse au sein d'une population entièrement susceptible

[2] Delamater et al. 2019 ou Britton, Ball, and Trapman 2020 qui montrent que, pour COVID-19, le niveau d'immunité collective est ramené à 43% lorsque le modèle englobe la possibilité que les individus soient plus actifs socialement dans certains groupes que dans d'autres.

leur croyance actualisée. Par exemple, une personne qui interagit avec de nombreuses personnes sans développer de symptômes de la COVID-19 devient plus optimiste quant au fait d'être du type asymptomatique. Par conséquent, elle peut être tentée de rencontrer encore plus de personnes et d'oublier mesures de distanciation sociale. La contribution de cet article à la littérature épi-économique est d'introduire l'apprentissage dans un modèle épidémiologique et d'analyser la dynamique d'une épidémie lorsque les individus arbitrent entre les coûts et les bénéfices de l'auto-isolement sur la base de leurs croyances subjectives.

Pour analyser cette question, nous modifions le modèle épidémiologique classique SIR (*Susceptible - Infected - Recover*) de Kermack and McKendrick 1927 de deux manières. Dans sa version classique, le modèle SIR divise une population homogène en trois groupes : susceptible, infecté et guéri (*recovered* en anglais), les individus transitant d'un groupe à l'autre à des taux exogènes donnés qui dépendent de la taille de chaque groupe. Nous nous écartons de l'hypothèse d'homogénéité en considérant deux types d'individus possibles dans la population : *sévère* et *asymptomatique*. Les individus du type sévère présentent les symptômes de la maladie immédiatement après avoir été infectés. En revanche, les individus du type *asymptomatique* ne présentent aucun symptôme. Les personnes présentant des symptômes s'auto-isolent immédiatement, mais les personnes asymptomatiques peuvent être contagieuses sans le savoir. Par conséquent, la maladie se propage dans la population par les individus de types asymptomatiques. En outre, nous supposons que les personnes ne présentant pas de symptômes peuvent influencer le taux de transition de la catégorie susceptible à la catégorie infectée en réduisant stratégiquement le temps qu'elles passent à l'extérieur. Rester à la maison permet d'éviter d'être infecté, mais cela a un coût (ennui, coût d'opportunité de ne pas travailler ou de travailler dans de moins bonnes conditions, manque d'activité physique, etc.). Être infecté est également coûteux pour les individus du type sévère. Par conséquent, les individus arbitrent continuellement entre le coût de l'auto-isolement et le bénéfice escompté de l'absence de symptômes sur la base de leur conviction d'être du type sévère. Enfin, nous supposons qu'un vaccin arrivera à un moment connu de tous T.

Pourquoi les individus s'engageraient-ils volontairement dans un confinement coûteux? Un confinement accru diminue la probabilité de souffrir des symptômes et augmente la probabilité d'obtenir le gain de continuation d'un individu en bonne santé. Par conséquent, l'auto-isolement peut valoir le coût à certaines dates, mais pas à d'autres. Nous prouvons que les individus ne s'isolent jamais complètement à l'équilibre : si le reste de la population reste à la maison, les chances d'être infecté sont nulles, et chaque individu peut donc économiser le coût de l'isolement sans risquer l'infection. Intuitivement, lorsque l'auto-isolement est plus coûteux que l'apparition de symptômes, les individus ne s'auto-isolent pas du tout à l'équilibre, et la dynamique de l'épidémie est la même que dans le modèle SIR. Cependant, lorsque le coût du confinement est relativement faible, la stratégie d'équilibre n'est pas stationnaire et peut être *intérieur*, c'est-à-dire que les individus s'auto-isolent partiellement à chaque date. Nous prouvons qu'il ne peut y avoir qu'un seul équilibre intérieur symétrique.

Nous calibrons notre modèle sur les valeurs disponible au mois de mars 2020 de l'épidémie COVID-19 afin d'illustrer l'impact des comportements d'auto-isolement sur la dynamique de l'épidémie et de mettre en évidence les leçons politiques qui peuvent être tirées de nos résultats. Nous nous concentrons sur l'équilibre où les individus s'isolent partiellement à chaque date et nous simulons la dynamique de l'épidémie dans ce cas précis. Nous constatons que la population réagit à l'annonce de l'épidémie en s'isolant radicalement, ce qui entraîne une baisse du pourcentage de personnes infectées (Figure (1)). Ensuite, les individus augmentent progressivement le temps qu'ils passent à l'extérieur, en maintenant le R_e nombre de reproductions effectif (*Effective Reproduction Number*)[3] en dessous de la valeur qui accélère l'épidémie. En conséquence, la courbe épidémique est décroissante entre le moment de l'annonce de l'épidémie et l'arrivée du vaccin, contrairement à la courbe en forme de cloche bien connue du modèle SIR.

Nous constatons qu'une annonce tardive de l'épidémie augmente le nombre de décès,

[3]Le nombre de reproductions effectif est le nombre attendu de cas d'infection secondaire causés par un seul cas infectieux typique pendant toute sa période infectieuse dans une population où certain individu ne sont plus susceptible.

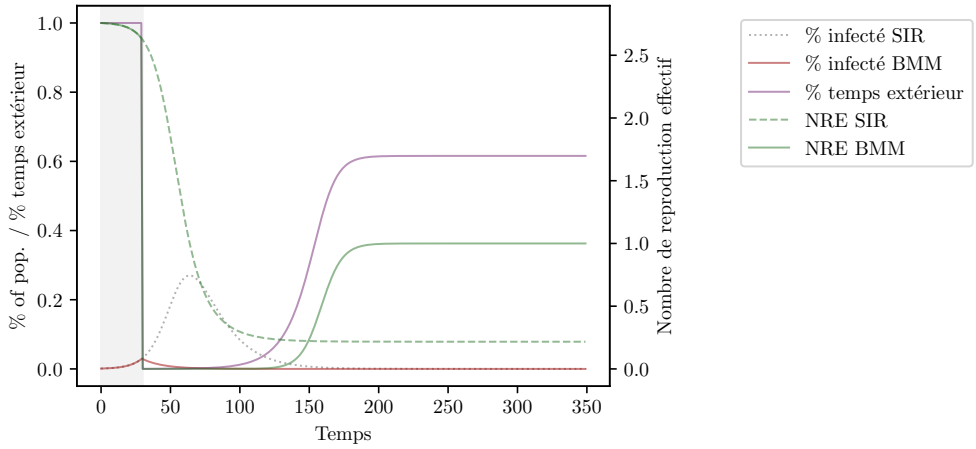

Figure 1: Dynamique de l'épidémie dans l'équilibre intérieur.

conformément aux résultats de Silverio et al. (2020), qui trouvent une corrélation positive entre le nombre de cas avant le confinement et le taux de mortalité en Italie. Nous analysons également l'impact des politiques visant à atténuer la transmission du virus, telle que la distribution de masques, la diffusion de messages sur les mesures d'hygiène, etc. Nous constatons que les individus compensent la diminution du risque d'infection en réduisant les distances sociales, mais pas au point d'accélérer l'épidémie. Dans l'ensemble, nous constatons que ces politiques réduisent le nombre de décès. Nous montrons également qu'un système de santé plus performant entraîne moins d'auto-isolement mais diminue globalement le nombre de décès. Enfin, les politiques de subvention de l'auto-isolement aplatissent la courbe économique, mais nous ne trouvons pas de différence substantielle lorsque l'auto-isolement est encouragé au début ou à la fin de l'épidémie.

Self-Isolation Under Uncertainty

Il est désormais bien documenté que la dynamique d'une épidémie dépend du comportement de la population en termes de distanciation sociale et d'application de mesures prophylactiques[4]. À l'inverse, de nombreux articles ont montré que les in-

[4]Delamater et al. (2019) et Britton, Ball, and Trapman (2020) montrent que le niveau d'immunité du groupe contre COVID-19 est réduit lorsque le modèle englobe la possibilité que certains groupes sociaux d'individus

dividus adaptent leurs comportements aux variables épidémiques (taux d'incidence, niveau d'hospitalisation, etc.)[5]. Par exemple, Farboodi, Jarosch, and Shimer (2021) montrent que la fréquentation des lieux publics a baissé dès l'annonce par l'OMS de l'existence d'une pandémie en mars 2020, donc avant la mise en place des politiques de confinement et de fermeture. L'objet de la littérature épi-économique stratégique croissante est d'analyser les interactions bilatérales entre la dynamique de l'épidémie et le comportement de la population. Dans cette littérature, les individus arbitrent entre le coût et le bénéfice des comportements préventifs en fonction de leur évaluation du risque d'entrer en contact avec une personne contagieuse, qui dépend naturellement du taux de prévalence. On suppose que les individus sont capables de déduire ce taux avec précision.

Cependant, il arrive souvent qu'il ne soit pas parfaitement observable, en particulier lorsqu'une proportion importante de la population est asymptomatique. De plus, pour que les individus puissent le déduire correctement, ils doivent avoir une connaissance détaillée des caractéristiques de la maladie, telles que la contagiosité et le taux de prévalence initial. Cette hypothèse est difficile à défendre lors de l'apparition d'un nouveau virus ou de la réapparition d'une maladie. Ces situations sont loin d'être anecdotiques et l'actualité récente regorge d'exemples : le COVID-19 et ses différents mutants, la grippe qui revient chaque hiver dans les zones tempérées, l'Ebola qui est réapparu plusieurs fois en RDC, mais aussi en Guinée en 2021, etc...

La contribution de cet article est d'analyser un modèle épidémiologique dans lequel les individus prospectifs sont incertains de certaines caractéristiques de l'épidémie et sont donc incapables de déduire la fraction de la population qui est infectée. Les

soient plus actifs socialement. Cowling, Chan, et al. (2009) et Aiello et al. (2010) montrent que les masques et le lavage des mains peuvent réduire la transmission domestique des infections respiratoires dans les petites zones. Cowling, Ali, et al. (2020) montrent que les restrictions aux frontières et les changements dans les comportements individuels sont en partie responsables de la réduction de la transmission à Hong Kong en février 2020.

[5]Par exemple, T. J. Philipson and Posner (1993) montre que la demande de vaccins contre la rougeole, les oreillons et la rubéole augmente lorsque le nombre de cas de rougeole dans une communauté est en forte hausse. Ahituv, Hotz, and T. Philipson (1996) montre que la demande de préservatifs augmente dans les régions où le VIH est répandu.

individus se forgent des croyances sur l'épidémie, qu'ils mettent continuellement à jour en fonction de leur degré d'exposition au virus. Simultanément, ils décident de leur degré d'exposition au virus en échangeant les coûts et les bénéfices de l'auto-isolement sur la base de leurs croyances subjectives.

Précisément, nous modifions le modèle classique Susceptible-Infecté-Récouvert (SIR ci-après) de Kermack and McKendrick (1927). Dans sa version classique, le modèle SIR divise une population homogène en trois groupes : {susceptible}, {infecté} et {récupéré}, les individus passant d'un groupe à l'autre à des taux exogènes donnés qui dépendent de la taille de chaque groupe. Comme dans Baril-Tremblay, Marlats, and Ménager (2021), nous considérons deux types d'individus possibles dans la population : *symptomatique* et *asymptomatique*. Les individus du type symptomatique présentent les symptômes de la maladie immédiatement après avoir été infectés. En revanche, les individus du type *asymptomatique* ne présentent aucun symptôme. Au départ, les individus ne connaissent pas leur type. Nous nous écartons de Baril-Tremblay, Marlats, and Ménager (2021) en supposant que les individus sont incertains de certains paramètres déterminant la dynamique du taux de prévalence. Ainsi, les agents, qui n'observent pas ce taux, savent que différents niveaux de prévalence sont possibles, mais ils ne les connaissent pas exactement.

Les individus influencent le taux de transition de {susceptible} à {infecté} en s'isolant, c'est-à-dire en réduisant stratégiquement leur activité sociale. Comment un individu qui n'a jamais eu de symptômes peut-il arbitrer entre le coût et le bénéfice de l'auto-isolement ? Du côté des avantages, l'auto-isolement permet d'éviter d'être infecté en réduisant la probabilité d'entrer en contact avec une personne contagieuse. L'aspect coût est plus subtil. En effet, une personne qui ne présente pas de symptômes alors qu'elle a une activité sociale devient plus optimiste à la fois sur le taux de prévalence et sur le fait d'être du type asymptomatique. Les coûts de l'auto-isolement sont donc doubles : il y a le coût direct de l'auto-isolement (ennui, coût d'opportunité de ne pas travailler ou de travailler dans de moins bonnes conditions, manque d'activité physique, etc.) et le coût d'opportunité de ne pas apprendre sur son type et sur le taux de prévalence.

Nous caractérisons l'équilibre symétrique dans lequel les individus s'auto-isolent partiellement. Dans cet équilibre, le niveau d'activité sociale est égal au rapport entre, d'une part, le coût direct de l'auto-isolement et, d'autre part, le coût d'opportunité attendu de l'activité sociale, qui est égal au bénéfice informationnel moins la perte de bien-être attendue en cas d'infection.

Nous calibrons notre modèle sur le COVID-19 et nous simulons la dynamique de l'épidémie lorsque la population a connaissance de deux épidémies possibles avec des taux de pénétration initiaux différents. Ce paramètre est l'un des éléments déterminant la dynamique du taux de prévalence. Ainsi, les agents, qui ont une incertitude sur ce paramètre, sont conscients que différents niveaux de prévalence sont possibles, mais ils ne le savent pas exactement. L'impact de l'incertitude est ambigu. Quelle que soit la croyance préalable, les individus s'isolent fortement après l'annonce de l'épidémie, ce qui entraîne une baisse de la fraction infectée ; ensuite, ils augmentent progressivement le niveau des interactions sociales. La vitesse à laquelle l'activité sociale augmente varie en fonction de l'hypothèse selon laquelle le taux de pénétration initial de l'épidémie est faible. Lorsque l'a priori augmente, les individus s'isolent moins au début de l'épidémie et plus à la fin. Cette inversion s'explique notamment par le fait que les individus pensent avoir été moins exposés à la maladie au début de l'épidémie lorsque le taux de pénétration initial est faible. Par conséquent, ils sont moins convaincus d'être immunisés contre la maladie et s'isolent davantage à la fin de l'épidémie.

Comme illustré dans la figure (2), dans l'épidémie la plus agressive, pour tout a priori, les individus s'auto-isolent suffisamment pour maintenir le nombre de reproductions effectives en dessous de la valeur qui accélère l'épidémie, de sorte que la courbe épidémique diminue continuellement jusqu'à l'arrivée du vaccin. Dans l'épidémie moins agressive, lorsque l'a priori initial est faible, il y a une deuxième vague d'infections avec un deuxième pic qui est d'autant plus élevé que les croyances sont erronées. Cette deuxième vague est due au fait que, pour ces antécédents, les individus choisissent un niveau d'activité sociale plus élevé à partir d'une certaine date.

Cela conduit à une réaction inadéquate au niveau réel de l'épidémie qui peut induire une augmentation effective de la fraction totale des individus infectés. Par conséquent,

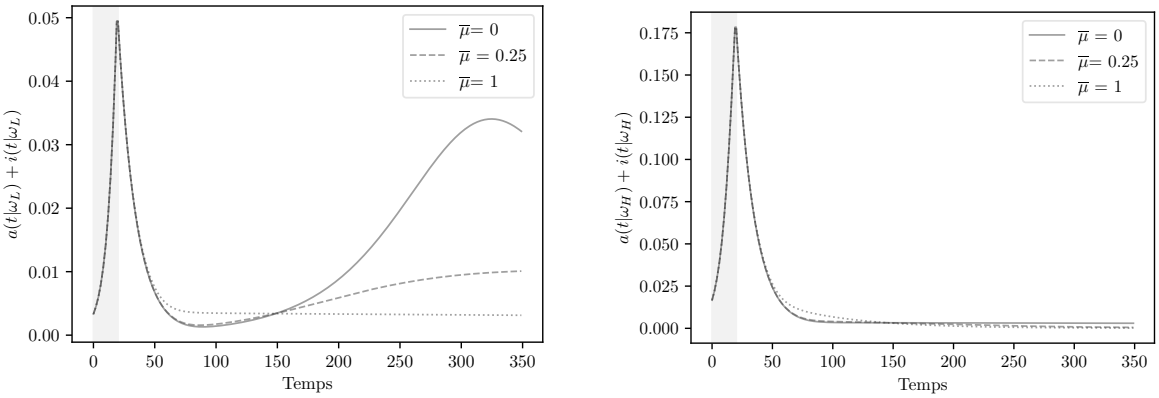

Figure 2: Droite: Dynamique de la fraction d'individus infectés en ω_L lorsque $\bar{\mu} \in \{0, 0.25, 1\}$. Gauche: Dynamique de la fraction d'individus infectés en ω_H lorsque $\bar{\mu} \in \{0, 0.25, 1\}$.

la valeur sociale de l'information dépend de l'état initial de l'épidémie. Nous constatons dans la figure (3) que la transparence n'améliore le bien-être que dans le cas de l'épidémie la moins agressive, à la fois en termes de fraction de décès et de gains. Pour tous les prieurs que nous considérons, la fraction ex-ante des décès est plus petite lorsque les individus sont incertains de l'état que sans incertitude, ce qui suggère que l'opacité peut prévenir les décès. En termes de gains, la valeur de l'information est négative lorsque la population est relativement confiante dans l'agressivité initiale de l'épidémie.

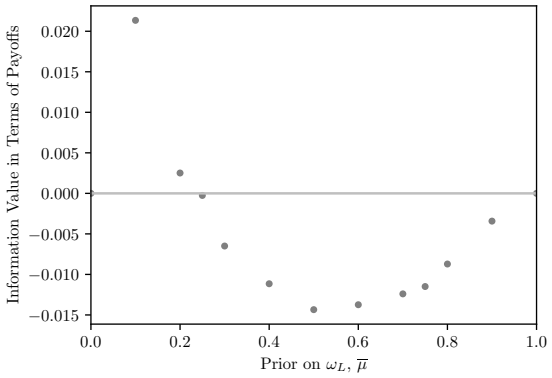

Figure 3: Valeur de l'information en termes de gains

The Swedish Paradox

Le SRAS-CoV-2 s'est propagé rapidement partout sur terre, même en Antarctique. La réduction des contacts entre individus est la clé pour ralentir la propagation de l'infection (Bavel et al. (2020), Min W Fong et al. (2020)). Plusieurs pays ont choisi de freiner la propagation de l'infection en adoptant une série d'interventions non pharmaceutiques, notamment le lavage des mains, le port de masques, l'isolement, la distanciation sociale et le confinement. (Wilder-Smith and Freedman (2020)). Toutefois, la portée et la rigueur de l'application des mesures d'atténuation des infections varient considérablement d'un pays à l'autre, en particulier en ce qui concerne le confinement. (Petherick, Kira, et al. (2020)).

La Suède a fait couler beaucoup d'encre au mois de mars 2020. Alors que les pays scandinaves voisins ont adopté des mesures strictes pour "aplanir la courbe", l'épidémiologiste d'état suédois a refusé d'imposer des mesures de distanciation sociale (Born, Dietrich, and Müller (2021), Cho (2020) et Juranek and Zoutman (2020)). Pourquoi, face à une menace infectieuse similaire, les gouvernements ont-ils adopté des stratégies diamétralement opposées? Ces stratégies diamétralement opposées peuvent être expliquées par plusieurs facteurs: risques locaux perçus, la capacité hospitalière (Kandel et al. (2020)) ainsi que la nature des institutions et le contexte culturel du pays (Matthews Pillemer et al. (2015)). Dans ce chapitre, nous proposerons une réponse à partir du modèle épidémiologique SIR avec dynamique vitale close, qui repose sur le caractère oscillatoire du système.

Dans notre article nous explorerons la nature périodique des épidémies provoquant l'émergence de vagues successives d'infection au fil du temps et l'effet des différentes mesures de mitigation des infections sur la longueur et l'amplitude de ces vagues. Il est essentiel de comprendre ce phénomène et les effets des différentes stratégies d'atténuation des infections sur ce dernier afin de prévoir et contrôler les vagues d'infections futures.

Les données historiques épidémiologiques démontrent que les épidémies ont un caractère périodique, c'est-à-dire que plusieurs vagues d'infections se succèdent. La péri-

odicité est une composante normale des épidémies et intéresse les chercheurs depuis des décennies (Webster (1799), Soper (1929), Hethcote and Levin (1989), Baryarama, Luboobi, and Mugisha (2005) par exemple). Les chercheurs ont proposé différents mécanismes, endogènes et exogènes, pour intégrer le comportement oscillatoire dans des modèles épidémiologiques (London and Yorke (1973), Bryan Thomas Grenfell and Roy Malcolm Anderson (1989), Bolker and Bryan Thomas Grenfell (1993), N. M. Ferguson, Nokes, and Roy M Anderson (1996), Hethcote (1997) et Earn et al. (2000)). Ces modèles permettent de tirer des conclusions intéressantes. Toutefois, ils sont mathématiquement lourds à manipuler. Earn (2008) a jeté les bases de l'apparition naturelle d'un comportement oscillatoire au sein d'un modèle épidémiologique. Greer et al. (2020) démontre formellement que des oscillations apparaissent naturellement lorsque le modèle inclut un processus de régénération de la population, soit via la dynamique vitale des naissances et des décès, soit via le déclin de l'immunité (Giannitsarou, Kissler, and Toxvaerd (2021)). À l'instar de Greer et al. (2020), nous avons choisi d'adopter un modèle simple et flexible.

Nous avons utilisé les valeurs du SRAS-CoV-2, disponible en mars 2020 pour calibrer notre modèle et analyser deux stratégies de distanciation sociale: des mesures permanentes et des mesures temporaires. Nos simulations donnent un aperçu de l'impact des différentes stratégies d'atténuation de l'infection sur l'apparition de différentes vagues d'infection. Nous avons concentré notre analyse sur deux types de stratégies d'atténuation de l'infection : les mesures de distanciation sociale permanentes et temporaires. Comme illustré à la figure (4), la persistance des mesures dans le temps a un impact sur le taux d'apparition des vagues d'infection suivantes. La répercussion de la mesure de distanciation sociale sur le schéma des vagues d'infection est assez intuitive : plus le niveau des mesures de distanciation sociale est élevé, plus le nombre cumulé d'individus infectés est faible. Toutefois, ce n'est pas le cas lorsque les mesures sont temporaires.

Les mesures d'atténuation des infections nécessitent un changement fondamental du comportement humain. Il peut être difficile pour le planificateur social de maintenir ces mesures sur une longue période. Les mesures temporaires ont pour effet, à court terme,

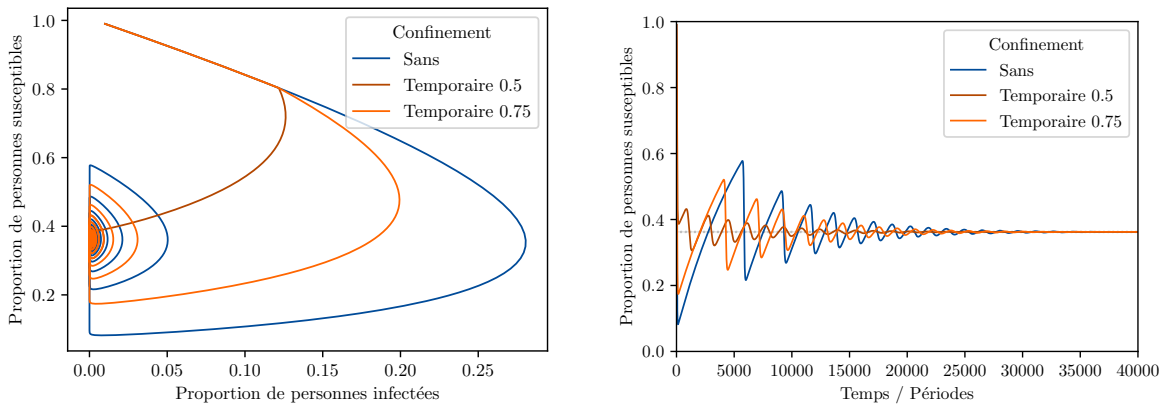

Figure 4: Illustration of the convergence of the various endemic equilibriums according to different social distancing scenario.

de ralentir la propagation de l'infection tout en protégeant la population. Toutefois, lorsqu'elles sont levées, la population précédemment protégée est exposée à l'infection. Comme l'infection est alimentée par le réservoir de personnes susceptible, les vagues d'infection surviennent plus rapidement. Ces vagues successives d'infection conduisent à une augmentation marquée du nombre cumulé d'individus infectés. Nous observons que, dans certaines conditions, comme observé à la figure (5), le nombre cumulé d'infections lorsque des mesures temporaires de distanciation sociale ont été prises est plus élevé que lorsqu'aucune mesure de distanciation sociale n'a été imposée. Le planificateur social qui souhaite minimiser le nombre cumulé d'infections doit tenir compte de ce phénomène, appelé le *Paradoxe Suédois*, et anticiper le moment probable de l'arrivée du vaccin.

Les oscillations amorties autour de l'équilibre endémique donnent naissance à plusieurs vagues successives d'infections. Ces vagues apparaissent au fur et à mesure que la population se régénère via la dynamique vitale. Puisque sous les hypothèses du modèle, la dynamique infectieuse est plus grande que la dynamique vitale, l'épuisement du bassin d'individus susceptibles, et donc l'amplitude des oscillations, diminue avec le temps. Le caractère oscillatoire du système donne naissance à plusieurs phases du *Paradoxe Suédois*, tel qu'illustré à la figure (6).

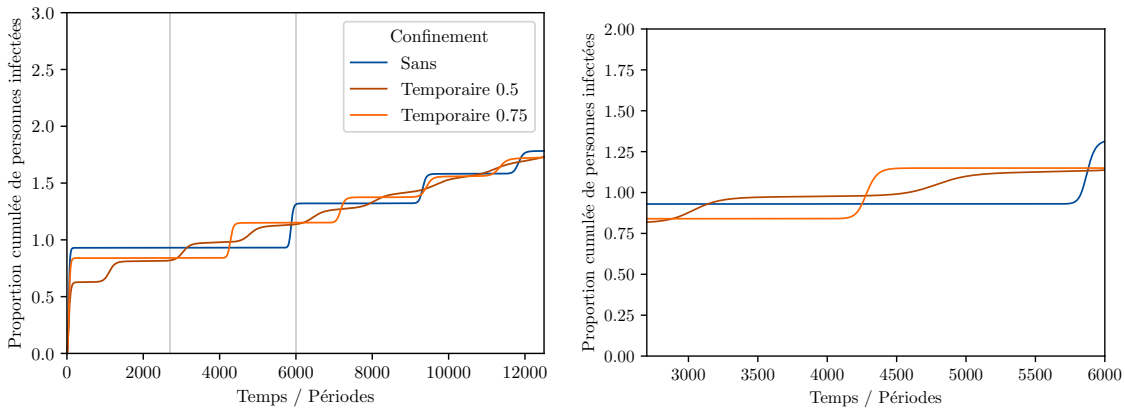

Figure 5: Illustration graphique du paradoxe suédois en comparant le nombre cumulé d'infections sans mesures de distanciation sociale (bleu) à différents scénarios de mesures temporaires de distanciation sociale (orange) pour les périodes de 0 à 12 000 (haut) et pour les périodes de 2700 à 6000 (bas).

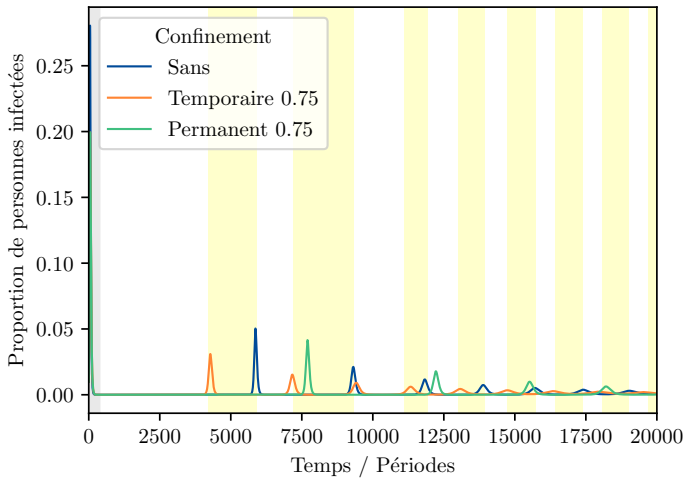

Figure 6: Illustration graphique de la récurrence des phases du *Paradoxe Suédois* en relation avec les oscillations de la proportion de personnes infectées entre les périodes 0 et 20000. Les zones jaunes indiquent les cas où le nombre cumulé d'individus infectés est plus élevé après une imposition de mesures temporaires de distanciation sociale que le nombre cumulé d'individus infectés sans mesures de distanciation sociale.

Acknowledgements

The Oak Tree

by Johnny Ray Ryder Jr.

A mighty wind blew night and day.
It stole the Oak Tree's leaves away.
Then snapped its boughs
and pulled its bark
until the Oak was tired and stark.

But still the Oak Tree held its ground
while other trees fell all around.
The weary wind gave up and spoke,
How can you still be standing Oak?"

The Oak Tree said, I know that you
can break each branch of mine in two,
carry every leaf away,
shake my limbs and make me sway.

But I have roots stretched in the earth,
growing stronger since my birth.
You'll never touch them, for you see
they are the deepest part of me.

Until today, I wasn't sure
of just how much I could endure.
But now I've found with thanks to you,
I'm stronger than I ever knew.

I can't think of a better way to express the importance of my friends and family in this adventure than this poem by Johnny Ray Ryder Jr. I thank you from the bottom of my heart, to you, my roots:

Ghislaine, Jean-François, Julien, Maude, Delphine, Frédérique-Emmanuelle, Lars, Maxime, Adriano, Jorunn, Leif, Robert, Nicolas, Chantal, Lucie, Tom, Michel, Catherine, Audrey, Pénélope, Sandra, Sably, Thank you!

Contents

List of Figures

Chapter 1

Self-Isolation

Dominique Baril-Tremblay[1], Chantal Marlats[2] and Lucie Ménager[3]

Abstract[4]

We analyze the spread of an infectious disease in a population when individuals strategically choose how much time to interact with others. Individuals are either of the severe type or of the asymptomatic type. Only severe types have symptoms when they are infected, and the asymptomatic types can be contagious without knowing it. In the absence of symptoms, individuals do not know their type and continuously tradeoff the costs and benefits of self-isolation on the basis of their belief of being the severe type. We show that all equilibria of the game involve social interaction, and we characterize the unique symmetric equilibrium in which individuals partially self-isolate at each date. We calibrate our model to the COVID-19 pandemic and simulate the dynamics of the epidemic to illustrate the impact of some public policies.

[1]Université Paris 1 - Panthéon Sorbonne, doumbaril@gmail.com.

[2]LEMMA, Université Paris 2 Panthéon-Assas, chantal.marlats@u-paris2.fr.

[3]LEMMA, Université Paris 2 Panthéon-Assas, lucie.menager@u-paris2.fr.

[4]We have greatly benefited from discussions with Sidartha Gordon, Nicolas Klein and Nicolas Vieille, and from comments by seminar participants at the Game theory seminar in Paris. We are particularly indebted to Jean-François Blanchette for his support in the programming process of our simulations. We thank two anonymous referees for their very constructive suggestions that led to many new results and a more insightful paper. This research was supported by the French National Research Agency (ANR-17-CE38-0005-01) and by the Labex MME-DII (ANR11-LBX-0023-01).

Keywords: SIR model; Self-isolation; COVID-19 epidemic.
JEL codes: C73; D84, I12.

1.1 Introduction

The herd immunity level of an infectious disease is defined as the fraction of the population that must become immune for the spread of the disease to decline and stop. Under the simplest model, it is equal to $(R_0-1)/R_0$, where R_0 is the basic reproduction number[5] of the disease, which is often estimated to be approximately 60% for COVID-19. The figure of 60% assumes that the population is homogenous and passive, while it is well-documented[6] that the herd immunity level varies between populations consisting of people with different behaviors. The object of the growing epi-economic literature is to analyze the two-sided interactions between the dynamics of epidemics and individual behaviors.

One of the many features of COVID-19 is the wide variety of responses to the infection in the population, with some individuals completely asymptomatic, and others developing fatal forms within a few days. As with symptomatic individuals, asymptomatic patients are a source of the spread of infection[7]. Before being infected, there is no way of knowing whether one is of the asymptomatic type. Therefore, individuals form beliefs about their type, which they continuously update on the basis of how much they might have been exposed to the virus. At the same time, they decide how much to expose themselves to the virus in function of their updated belief. For instance, an individual who interacts with many people without developing COVID-19 symptoms becomes more optimistic about being the asymptomatic type. As a result, she may be tempted to meet even more people and forget about social distancing. The contribution of this paper to the epi-economic literature is to introduce learning into an

[5]The basic reproduction number is the average number of secondary infections caused by a single infectious individual introduced into a completely susceptible population.

[6]See e.g. Delamater et al. 2019 or Britton, Ball, and Trapman 2020 who show that, for COVID-19, the herd immunity level is reduced to 43% when the model encompasses the possibility that individuals are more socially active in some groups than in others.

[7]See Nishiura et al. 2020 and Han et al. 2020, among others.

epidemiological model, and to analyze the dynamics of an epidemic when individuals tradeoff the costs and benefits of self-isolation on the basis of their subjective beliefs.

To analyze this question, we amend the classical Susceptible-Infected-Recovered (SIR hereafter) model of Kermack and McKendrick 1927 in two ways. In its classical version, the SIR model divides an homogeneous population into three groups: susceptible, infected and recovered, with individuals transiting from one group to another one at given, exogenous rates that depend on the size of each group. We depart from the homogeneity assumption by considering two possible types of individuals in the population: *severe* and *asymptomatic*. Individuals of the severe type experience the symptoms of the disease immediately after being infected. In contrast, individuals of the *asymptomatic* type do not have symptoms. Individuals with symptoms immediately self-isolate, but asymptomatic individuals can be contagious without knowing it. Therefore, the disease is spread in the population by asymptomatic types. Moreover, we assume that individuals without symptoms can influence the transition rate from susceptible to infected by strategically reducing the fraction of time they spend outside. Staying home prevents one from being infected, but comes at a cost (boredom, opportunity cost of not working, or of working in poorer conditions, lack of physical activity, etc.). Being infected is also costly for individuals of the severe type. Therefore, individuals continuously tradeoff the cost of self-isolation and the expected benefit of not having the symptoms on the basis of their belief of being the severe type. Finally, we assume that a vaccine will arrive at known time T.

Why would individuals voluntary engage in costly confinement? More confinement decreases the probability of suffering from the symptoms and increases the probability of getting the continuation payoff of a healthy individual. Therefore, self-isolation may be worth the cost at some dates, but may not at some other dates. We prove that individuals never completely self-isolate in equilibrium: if the rest of the population stays at home, the chances of being infected are 0, thus each individual can spare the confinement cost without risking infection. Intuitively, when self-isolating is costlier than having symptoms, individuals do not self-isolate at all in equilibrium, and the dynamics of the epidemic are the same as in the SIR model. When the confinement

cost is relatively small, however, the equilibrium strategy is non-stationary and may be *interior*, i.e. such that individuals partially self-isolate at each date. We prove that there can be only one interior, symmetric equilibrium.

We calibrate our model to the COVID-19 epidemic in order to illustrate the impact of self-isolation behaviors on the dynamics of the epidemic, and to highlight the policy lessons that can be drawn from our findings. We focus on the equilibrium where individuals partially self-isolate at each date and we simulate the dynamics of the epidemic in this case. We find that the population reacts to the epidemic announcement by self-isolating drastically, which results in a drop in the percentage of infected. Then individuals gradually increase the time they spend outside, maintaining the effective reproduction number below the value that accelerates the epidemic. As a result, the epidemic curve is decreasing between the time of announcement of the epidemic and the arrival of the vaccine, contrary to the well-known bell-shaped curve of the SIR model. We find that a later announcement of the epidemic increases the number of deaths, in line with the results of Silverio et al. (2020), who find a positive correlation between the number of cases before lockdown and the mortality rate in Italy. We also analyze the impact of policies aiming at mitigating the transmission of the virus such as mask distributions, messaging about hygiene measures, etc. We find that individuals compensate the decrease in the risk of infection by reducing social distances, but not to the point of accelerating the epidemic. Overall, we find that these policies reduce the number of deaths. We also show that a more performing health system results of less self-isolation but overall decreases the number of deaths. Finally, policies subsidizing self-isolation flatten the economic curve, but we find no substantial difference when self-isolation is encouraged at the beginning or at the end of the epidemic.

Related literature. Many papers have documented that individuals adapt their behavior when facing a risk of infection. For instance, T. J. Philipson and Posner (1993) show that the demand for measles, mumps and rubella vaccines increases when there is a large increase in measles cases in a community, and Ahituv, Hotz, and T. Philipson (1996) show that the demand for condoms increases in regions where HIV is prevalent. Some

papers[8] also prove that individual behaviors impact the spread of infectious diseases. In the case of COVID-19, Cowling, Ali, et al. (2020) show that border restrictions and changes in individual behavior are partly responsible for reduced transmission in Hong Kong in February 2020.

In the theoretical literature, some models analyze the effect of social distance in SIR or SIS epidemiological models, either in a social optimum approach (e.g. Sethi (1978), F. Chen et al. (2011)) or also with strategic individual decisions (Reluga (2010), F. Chen (2012), Fenichel et al. (2011) and Fenichel (2013), Toxvaerd (2019), Rowthorn and Toxvaerd (2020)). This literature has grown considerably with the COVID-19 crisis. A strand of papers analyze the optimal control of the epidemics in the SIR model, either in the case of an homogenous population (Kruse and Strack (2020), Eichenbaum, Rebelo, and Trabandt (2022), Alvarez, Argente, and Lippi (2020), C. Jones, Philippon, and Venkateswaran (2021), Glover et al. (2020)), or when older people are more likely to die from the disease (Acemoglu et al. (2021), Favero, Ichino, and Rustichini (2020), Rampini (2020) and Bairoliya and İmrohoroğlu (2022)). The problem of individuals who tradeoff the costs and benefits of self-isolation in the SIR model has been studied notably by Toxvaerd (2020), Farboodi, Jarosch, and Shimer (2021) and Brotherhood et al. (2020). In an infinite horizon model, Toxvaerd (2020) characterizes the exposure level at the symmetric equilibrium and shows that self-isolation flattens the epidemic curve. Farboodi, Jarosch, and Shimer (2021) prove that individuals do not self-isolate enough with respect to what would be socially optimal, and Brotherhood et al. (2020) analyze the effect of testing and age-specific policies in an heterogeneous population with observable characteristics. Our model is one of the first in which the trade-off that individuals face also depends on their subjective belief that they are the asymptomatic type.

The remainder of this paper is organized as follows. Section 2 sets up the model. In Section 3, we solve the best-response problem of a player, analyze some properties of the equilibrium and characterize equilibria in which there is no confinement at all, or

[8]For instance, Cowling, Chan, et al. (2009) and Aiello et al. (2010) show that masks and hand washing can reduce household transmission of respiratory infections in small areas.

always partial confinement. In Section 4, we calibrate our model to fit the COVID-19 pandemic, we simulate the dynamics of the epidemic in equilibrium and provide some policy analysis. Section 5 concludes and technical proofs are gathered in the Appendix.

1.2 An epidemiological model with voluntary confinement

The population. Time $t \in [0, +\infty)$ is continuous and discounted at a common rate $r > 0$. There is a rampant disease in the population, against which a vaccine will arrive at time $T > 0$. The population is a continuum of individuals who must continuously decide what fraction of their time they spend outside. An individual who stays home is protected from infection, while an individual who goes out may be infected by other individuals, with a probability that will be described later. For simplicity, we assume that an individual is contagious as long as she is infected. People know whether they have been infected only if they experience the symptoms of the disease. There are two types of individuals in the population. Individuals of type θ_s, the *severe* type, who experience the symptoms of the disease immediately after being infected. In contrast, individuals of type θ_a, the *asymptomatic* type, who do not have symptoms, thus never realize that they have been infected. The proportion $\mu \in (0, 1)$ of asymptomatic types in the population is common knowledge, but individuals do not know their own type, unless they are of type θ_s and become infected.

We assume that an individual who gets symptoms self-isolates immediately until the end of the symptoms, either to protect others, or simply because she is too sick to go out. Therefore, a strategy for player i is a measurable function $k_i : \mathbb{R}_+ \to [0, 1]$, with the interpretation that $k_i(t)$ is the proportion of time spent outside at time t, absent symptoms by time t.

Evolution of the epidemic. To model the spread of the disease, we use the SIR model from Kermack and McKendrick (1927). At each time t, the population is divided into three groups: susceptible $S(t)$, infected $I(t)$ and recovered $R(t)$, i.e., those who died from the disease or recovered and are now immune to it[9]. Accordingly, $s(t)$ is the

[9]The idea is that an individual cannot be infected after being matched with an individual in $R(t)$, either

fraction of the population that is healthy but susceptible to be infected at time t, $i(t)$ the fraction of the population that is infected at time t, and $r(t) = 1 - s(t) - i(t)$ the fraction of the population that has died or recovered from the disease at t.

The disease is transmitted to a susceptible individual through contact with an infected individual at rate $\beta \in (0,1)$, which measures the contagiousness of the disease. Therefore, the mass of susceptible individuals who become infected between t and $t+dt$ depends on β, but also on the size of groups $S(t)$ and $I(t)$ and on the behavior of the population in each group. Given a strategy profile $\mathbf{k} := ((k_j)_j)$, this mass equals $\beta \times \int_{j \in S(t)} k_j(t)dj \times \int_{j \in I(t)} k_j(t)dj$, thus the group of susceptible evolves according to the dynamics:

$$\dot{s}(t) = -\beta \bar{k}_S(t) s(t) \bar{k}_I(t) i(t), \text{ with } s(0) = s_0 \in (0,1), \tag{1.1}$$

where $\bar{k}_I(t) := \frac{1}{i(t)} \int_{j \in I(t)} k_j(t)dj$ and $\bar{k}_S(t) = \frac{1}{s(t)} \int_{j \in S(t)} k_j(t)dj$ denote the average fraction of time spent outside at t by infected and susceptible individuals, respectively. When infected, asymptomatic individuals do not die and heal from the disease at rate $\gamma^a \in (0,1)$. In contrast, individuals of the severe type die at rate ν and heal at rate γ^s. We assume the same recovery rate for both types of individuals, i.e., $\gamma^a = \nu + \gamma^s$, which guarantees that, at each point in time, there is a fraction μ of asymptomatic among infected people. We denote by $\gamma := \mu\gamma^a + (1-\mu)\gamma^s$ the average healing rate in the population. As the fraction of infected is also increased by $-\dot{s}(t)$, the group of infected evolves according to the following dynamics:[10]

$$\dot{i}(t) = \beta \bar{k}_S(t) s(t) \bar{k}_I(t) i(t) - (\gamma + (1-\mu)\nu) i(t), \text{ with } i(0) = i_0 = 1 - s_0. \tag{1.2}$$

Evolution of subjective beliefs. At time t, individual i holds a subjective belief $p_i(t)$ of being type θ_s, with a common prior belief $p_i(0) = 1 - \mu$ for all individuals[11]. In this

because this individual has recovered from the disease and is not contagious anymore, or because this individual is dead.

[10] Asymptomatic infected recover at rate γ^a, while severe infected recover at rate $\gamma^s + \nu$. Therefore, the fraction of infected decreases by $\mu\gamma^a + (1-\mu)(\gamma^s + \nu)$, which equals $\gamma + (1-\mu)\nu$ by definition of γ.

[11] The common prior belief assumption is very strong in the case of the COVID-19 epidemic for two reasons. First, as of today the proportion of asymptomatic has yet to be precisely estimated, not to mention commonly known. Second, even if the distribution of types in the population is still unknown, there are already evidences that the probability of being asymptomatic is conditional to individual characteristics. We discuss the

model, no news is good news: the subjective belief of being the severe type decreases as time passes without the arrival of symptoms, and jumps to 1 the first time the symptoms occur. Let us now describe the law of motion of $p_i(t)$. A susceptible individual i develops symptoms in $[t, t+dt)$ with probability 0 when she is of type θ_a; when she is of type θ_s, she develops symptoms if she meets and is infected by some individual in $I(t)$, which occurs with instantaneous probability[12] $k_i(t) \times \beta \bar{k}_I(s) i(s) dt$. By Bayes' rule, the law of motion of the subjective belief of individual i is thus[13]:

$$\dot{p}_i(t) = -p_i(t)(1 - p_i(t))k_i(t)\beta \bar{k}_I(t) i(t), \text{ with } p_i(0) = 1 - \mu. \tag{1.3}$$

Payoffs Staying home prevents one from being infected, but comes at a cost (boredom, opportunity cost of not working or working in poorer conditions, lack of physical activity, etc.). Being infected is also costly for individuals of the severe type because they suffer from the symptoms, and, in the worst case, because they die from the disease. Therefore, at each time t, individuals tradeoff the cost of self-isolating and the expected benefit of not having the symptoms. We denote by c_H the flow cost per unit of time spent at home, by c_I the flow cost of having symptoms and by c_D the flow cost of being dead.

Fix some strategy profile $\mathbf{k}$ and let us describe the expected payoff to individual i at time $t \leq T$ when she plays some strategy k_i, denoted by $v_i(t; k_i)$. Uncertainty is solved for individual i the first time she has symptoms. In that event, she knows that she is the severe type, thus that she will stay at home until she recovers or passes away, thereby incurring a total cost of $\int_0^{\min\{\tau_H, \tau_D\}} e^{-rt}(c_H + c_I)dt$, with τ_H and τ_D standing for the random times of healing and death, respectively. If she recovers (i.e., if $\tau_H < \tau_D$),

implications of relaxing this assumption in section 5.3.

[12] A possible interpretation of this probability is as follows. When she goes out, individual i is randomly matched with another individual who also went out, according to the uniform distribution. The probability of being matched with an infected agent at time t is thus exactly the mass of infected agents who are outside at time t, i.e., $\bar{k}_I(t)i(t)$. Finally, conditional on being matched with an infected individual, an individual has a probability β of being contaminated.

[13] By Bayes' rule, player i's probability of being type θ_s conditionally on having no symptoms between t and $t + dt$ is $p_i(t + dt) = \frac{(1-k_i(t)\beta \bar{k}_I(t) i(t) dt) p_i(t)}{(1-k_i(t)\beta \bar{k}_I(t) i(t) dt) p_i(t) + 1 - p_i(t)}$. Expression (1.3) is obtained by simplifying $\frac{p_i(t+dt) - p_i(t)}{dt}$ and taking dt to 0.

she becomes immune to the disease, plays $k(t) = 1$ forever after, thus obtains the continuation payoff 0. If she dies (i.e., if $\tau_D < \tau_H$), she incurs the flow cost c_D forever after, thus obtains the continuation payoff $-c_D/r$. Therefore, the expected continuation payoff to individual i the first time she has symptoms is[14]:

$$v_I = -E\left[\int_0^{\min\{\tau_H,\tau_D\}} e^{-rt}(c_H + c_I)dt + \frac{c_D}{r}e^{-r\tau_D}\mathbb{1}_{\tau_D<\tau_H}\right] = -\frac{1}{r+\gamma^s+\nu}(c_H+c_I+\nu\frac{c_D}{r}) \tag{1.4}$$

Conditionally on having no symptoms before $s \in [t, T]$, the instantaneous payoff to player i at time s is v_I if she has symptoms, which occurs with subjective probability $p_i(s)k_i(s)\beta\bar{k}_I(s)i(s)$, minus the cost c_H scaled with the proportion of time spent in isolation, $1 - k_i(s)$. At time t, the subjective probability of not having any symptoms before s is $1 - p_i(t) + p_i(t)e^{-\int_t^s k_i(u)\beta\bar{k}_I(u)i(u)du}$, which reduces to $e^{-\int_t^s p_i(u)k_i(u)\beta\bar{k}_I(u)i(u)du}$ after standard simplifications[15]. Finally, individual i is vaccinated at time T, thus plays $k_i(t) = 1$ for every $t \geq T$ and obtains the continuation payoff $V_i(T) = 0$. Therefore,

$$v_i(t; k_i) = \int_t^T e^{-r(s-t)}e^{-\int_t^s p_i(u)k_i(u)\beta\bar{k}_I(u)i(u)du}\left(p_i(s)k_i(s)\beta\bar{k}_I(s)i(s)v_I - c_H(1-k_i(s))\right)ds, \tag{1.5}$$

where functions $s(.)$, $i(.)$ and $p_i(.)$ are defined by (1.1), (1.2) and (1.3).

1.3 Equilibrium analysis

Fix a strategy profile $\mathbf{k}$ in all possible strategy profiles $\mathcal{K}$ and an individual i. The best-response problem faced by i is the optimal control problem:

$$\begin{cases} \max\limits_{k_i\in\mathcal{K}} & v_i(0; k_i) \\ \text{s.t.} & \dot{p}_i(t) = -p_i(t)(1-p_i(t))k_i(t)\beta\bar{k}_I(t)i(t)\ \forall\ t \text{ and } p_i(0) = 1-\mu, \end{cases}$$

which we solve in the Appendix using Pontryagin's principle. Here, we explain the intuition of the solution with a heuristic dynamic programming argument, using the time and the individual's current belief p as the state variable. At time t, the optimal

[14] See Lemma 1 in the Appendix for the detailed calculations.

[15] Using the law of motion of beliefs described by (1.3), we can establish two equalities. First, $e^{-\int_t^s k_i(u)\beta\bar{k}_I(u)i(u)du} = e^{\int_t^s \frac{\dot{p}_i(u)}{p_i(u)(1-p_i(u))}du} = \frac{1-p_i(t)}{p_i(t)}\frac{p_i(s)}{1-p_i(s)}$. Second, $e^{-\int_t^s p_i(u)k_i(u)\beta\bar{k}_I(u)i(u)du} = e^{\int_t^s \frac{\dot{p}_i(u)}{1-p_i(u)}du} = \frac{1-p_i(t)}{1-p_i(s)}$. Therefore, $1 - p_i(t) + p_i(t)e^{-\int_t^s k_i(u)\beta\bar{k}_I(u)i(u)du} = \frac{1-p_i(t)}{1-p_i(s)} = e^{-\int_t^s p_i(u)k_i(u)\beta\bar{k}_I(u)i(u)du}$.

level of social interaction of an individual maximizes the sum of her current expected payoff and of her discounted continuation payoff, should no symptoms occur in the interval $[t, t+dt)$. The best-response payoff to player i at time t and belief p thus satisfies the Bellman equation:

$$V(t,p) = \max_{k\in[0,1]} \left\{ \big(-(1-k)c_H + pk\beta\bar{k}_I(t)i(t)v_I \big)dt + \big(1 - pk\beta\bar{k}_I(t)i(t)dt\big)e^{-rdt}V(t+dt, p+dp) \right\}.$$

After standard simplifications and the elimination of terms to the order $(dt)^2$, the latter expression is rewritten:

$$rV(t,p) = V_t(t,p) - c_H + \max_{k\in[0,1]} k\big(\underbrace{c_H}_{\text{cost of confinement}} \underbrace{- p\beta\bar{k}_I(t)i(t)(V(t,p) - v_I - (1-p)V_p(t,p))}_{\text{cost of social interaction}} \big)dt. \tag{1.6}$$

To interpret this expression, note that two things can happen for an individual who does not self-isolate at time t: either she develops symptoms, thus obtains the payoff v_I "today", or she does not. In that case, she becomes more confident in being the asymptomatic type, and she obtains "tomorrow" the continuation payoff $V(t+dt, p+dp)$, approximated by $V(t,p)$ at time t. Her best response thus depends on whether the direct cost of confinement, c_H, exceeds the expected cost of social interaction, which has two parts: $p\beta\bar{k}_I(t)i(t)(V(t,p) - v_I)$ is the expected cost of the jump to v_I in case of symptoms; $-p\beta\bar{k}_I(t)i(t)(1-p)V_p(t,p)$ is the positive effect on the overall payoff should the individual develop no symptom, via the negative effect on the probability of being the severe type.

Proposition 1 (Best response)**.** *Given a strategy profile* $\mathbf{k}$*, the best-response problem of player* i *admits a solution* k_i^**, which is characterized by the pair of* C^1 *functions* $\psi_i^* : \mathbb{R}_+ \to \mathbb{R}$ *and* $p_i^* : \mathbb{R}_+ \to [0,1]$ *such that, for all* t*,*

$$k_i^*(t) \begin{cases} = 1 & \text{if } p_i^*(t)\beta\bar{k}_I(t)i(t)(\psi_i^*(t) - v_I) - c_H < 0, \\ \in [0,1] & \text{if } p_i^*(t)\beta\bar{k}_I(t)i(t)(\psi_i^*(t) - v_I) - c_H = 0, \\ = 0 & \text{if } p_i^*(t)\beta\bar{k}_I(t)i(t)(\psi_i^*(t) - v_I) - c_H > 0, \end{cases} \tag{1.7}$$

with

$$\dot{\psi}_i^*(t) - r\psi_i^*(t) = c_H + k_i^*(t)\left(\beta\bar{k}_I(t)i(t)(\psi_i^*(t) - v_I) - c_H\right),\ \psi_i^*(T) = 0 \quad (\textit{Euler condition}),$$
$$\dot{p}_i^*(t) = -p_i^*(t)(1 - p_i^*(t))k_i^*(t)\beta\bar{k}_I(t)i(t),\ p_i^*(0) = 1 - \mu \quad (\textit{Belief dynamics}).$$

Proof. See the Appendix. □

An immediate corollary of Proposition 1 is that all equilibria feature social interaction, in the sense that, at every time, there is a mass of individuals who do not self-isolate. The reason is simple: if the rest of the population stays at home, each individual can spare the confinement cost c_H by going out without risking infection.

Proposition 2. *Let $(k_i^*)_i$ be an equilibrium. At every time t, there is a non-empty set of individuals such that $k_i^*(t) > 0$ for every i in this set.*

Proof. Fix time t and suppose that $k_i(t) = 0$ for all i, i.e., $\bar{k}_I(t) = 0$. By condition (1.7) in Proposition 1, the best response of each individual i to $\bar{k}_I(t) = 0$ is to play $k_i(t) = 1$. This contradicts $\bar{k}_I(t) = 0$. □

Because the expected marginal benefit of confinement depends on t in expression (1.7), self-isolation may be worth the confinement cost at some dates, but may not at some other dates. Intuitively, when c_H is relatively large with respect to v_I, going out at every date is a dominant strategy for the population.

Proposition 3 (The no-confinement equilibrium)**.** *If $(1-\mu)\beta\mu v_I + c_H > 0$, the game admits a unique equilibrium, where all individuals play $k^*(t) = 1$ for every $t \in [0,T]$. In this equilibrium, the players' payoff at time t is*

$$v(t;k^*) = v_I(1-\mu)\beta \frac{\int_t^T e^{-r(u-t)} i(u) e^{-\beta\mu\int_0^u i(v)dv} du}{\mu + (1-\mu)e^{-\beta\mu\int_0^t i(u)du}},$$

where $i(.)$ is the unique solution of the system

$$\begin{cases} i(0) = 1 - s(0) = i_0 \text{ and, } \forall\, t \in [0,T], \\ \dot{i}(t) = \beta\mu s(t) i(s) - (\gamma + (1-\mu)\nu) i(t), \\ \dot{s}(t) = -\beta\mu s(t) i(t). \end{cases}$$

Proof. See the Appendix. □

When c_H is so large that nobody self-isolates, the epidemic ends quickly but results in a large number of deaths. As a vaccine will arrive at time T, the government may want to implement policies to reduce the cost of confinement, in order to create the conditions under which individuals consider self-isolation. We thus investigate the

existence of *interior equilibria*, in which individuals partially self-isolate at every date. We prove that there can exist only one symmetric and interior equilibrium.

Proposition 4 (The symmetric interior equilibrium)**.** *Let $\hat{k}$ be the strategy defined for every $t \in [0,T]$ by the system of equations:*

$$\begin{cases} \hat{k}(t) = \dfrac{c_H}{p(t)\beta\mu i(t)(\psi(t) - v_I)}, \\ \dot{p}(t) = -p(t)(1-p(t))\beta\mu i(t)\hat{k}(t)^2, \\ \dot{s}(t) = -\beta\mu s(t) i(t)\hat{k}(t)^2, \\ \dot{i}(t) = \beta\mu s(t) i(t)\hat{k}(t)^2 - (\gamma + (1-\mu)\nu) i(t), \\ \dot{\psi}(t) = r\psi(t) + c_H + c_H \dfrac{1-p(t)}{p(t)}\hat{k}(t), \\ p(0) = 1-\mu,\ i(0) = 1 - s(0) = i_0 \text{ and } \psi(T) = 0. \end{cases} \tag{1.8}$$

If $\hat{k}(t) < 1$ for every $t \in [0,T]$, then the game has a unique symmetric and interior equilibrium where all individuals play $\hat{k}$.

Proof. See the Appendix. □

1.4 Illustration

The purpose of this section is to illustrate the impact of self-isolation behaviors on the dynamics of the epidemic and to highlight the policy lessons that can be drawn from our findings. To do so, we simulate the dynamics of the epidemic when the population plays the interior equilibrium described in Proposition 4, and we compare it with the dynamics of the *standard* SIR model (referred to as the SIR model in the rest of the section), i.e., the model described by equations (1.1) and (1.2) with $\bar{k}_S(t) = \bar{k}_I(t) = 1$. We calibrate the epidemiological parameters β, γ^a, μ and ν to the COVID-19 pandemic and we chose the behavioral parameters c_I, c_H and c_D arbitrarily in such a way that the interior equilibrium exists given the epidemiological parameters.

Throughout our simulations, we assume that individuals are not aware of the epidemic until some time $\tau \in (0,T)$, which can be interpreted as the moment at which the government makes the epidemic common knowledge in the population via a public announcement. Before time τ, individuals play $k(t) = 1$. After time τ, they commonly

know the epidemiological parameters as well as the current fraction of susceptible and infected, and adapt their behavior accordingly.

The system (1.8) is well defined by initial values $p(0)$, $i(0)$ and $s(0)$. However, the algorithm we construct to simulate (1.8) also requires the specification of $\psi(0)$, which cannot be taken arbitrarily since ψ is determined by the terminal condition $\psi(T) = 0$. To determine $\psi(0)$, we use an adaptation of the *Simulated Annealing algorithm* – a stochastic search-based algorithm described by Lewis (2007), whose principle is to solve (1.8) for several possible values of $\psi(0)$ and to select the one that minimizes the distance between $\psi(T)$ and 0.[16]

1.4.1 Calibration

We assume that initially $\boldsymbol{i_0 = 0.1}\%$ of the population is infected, and that individuals discount time at rate $\boldsymbol{r = 0.014}\%$, in line with in Fenichel et al. (2011)[17]. We also assume that the population learns on day $\boldsymbol{\tau = 30}$ that a virus has been spreading since day 0, against which a vaccine will be available on day $\boldsymbol{T = 350}$.

In the absence of exhaustive testing campaigns, it is very difficult to have a satisfactory estimate of the proportion of asymptomatic in the population. In a nationwide study of over 61 000 participants, Pollán et al. (2020) find that the proportion of asymptomatic individuals in the Spanish population who developed antibodies to the SARS CoV-2 ranges from 21.9% to 35.8%. Therefore, we set μ to the middle of this interval: $\boldsymbol{\mu = 0.2885}$.

To calibrate the contagion rate β and the recovery rate γ^a, we use the estimates of A. Remuzzi and G. Remuzzi (2020)'s, i.e., a basic reproduction number of $\mathcal{R}_0 = 2.76$

[16]Precisely, at stage 1 a value $\psi(0)[1]$ is uniformly drawn from an interval of *reasonable* values and is temporarily designed "best candidate". The final value of ψ given $\psi(0)[1]$, i.e., $\psi(T)[1]$, is computed. At stage 2, another value $\psi(0)[2]$ is drawn at random. If the corresponding final value $\psi(T)[2]$ is closer to 0 than $\psi(T)(1)$, then $\psi(0)[2]$ becomes the new *best candidate*. The process does on iteratively and stops after a deterministic number of rounds N, which is large enough to guarantee that $\psi(T)[N]$ is almost 0 with the final best candidate.

[17]Precisely, Fenichel et al. (2011) study a discrete-time model in which they set the discount rate to $\delta = 0.99986$, which corresponds to a 5% annual discount rate. The analog of δ in a continuous-time model is $r = -\ln(\delta)$, thus we set $r = -\ln(0.99986)$.

and an infection duration of 15 days. The infection duration directly yields: $\boldsymbol{\gamma^a = 1/15}$. Some precautions must be taken to infer β from $\mathcal{R}_0$. By definition, the basic reproduction number is the average number of secondary infections produced by a typical case of an infection in a population where everyone is susceptible. It is affected by the rate of contacts in the population, the probability of infection being transmitted during contact and the duration of infectiousness. In our model, $\mathcal{R}_0 = \beta\mu/\gamma^a$. Let us explain why. As infected self-isolate when they are the severe type, a randomly chosen infected individual contaminates a susceptible only if she is asymptomatic (which happens with probability μ) and if the virus is transmitted during contact (which happens with probability β). As she is infectious during a period of expected length $1/\gamma^a$, the average number of new infections caused by an infected is $\beta\mu/\gamma^a$. Therefore, we set: $\boldsymbol{\beta = 2.76\gamma^a/\mu}$.

On March 3, 2020, the Director General of the WHO declared that approximately 3.4% of reported cases of COVID-19 died from the disease. As only patients with severe symptoms were tested at the beginning of the outbreak, we believe that the mortality rates measured in March 2020 are a valid estimate of the probability of death for an individual of the severe type infected by the disease[18], i.e., $\nu/(\nu + \gamma^s)$. Therefore, we set: $\boldsymbol{\nu/\gamma^a = 0.034}$.

Finally, we set the costs arbitrarily to $\boldsymbol{c_H = 0.0009}$, $\boldsymbol{c_I = 0.09}$ and $\boldsymbol{c_D = 9}$. These values are such that the interior equilibrium exists given the COVID-19 epidemiological parameters.

1.4.2 The dynamics of the epidemic in the interior equilibrium

We begin by analysing the impact of strategic self-isolation on the dynamics of the epidemic, which is illustrated in Figure 1.1.

Contrary to the now well-known bell-shaped curve of the SIR model, the epidemic curve (i.e., the graph of the percentage of infected plotted against time) continuously

[18]In our model, an infected of the severe type dies if the event "Death" occurs for her before the event "Healing". Therefore, the probability of death (conditional on being infected and the severe type) is $P(\tau_D < \tau_H)$, with τ_H and τ_D denoting the random times of healing and death, respectively. Straightforwardly, $P(\tau_D < \tau_H) = \int_0^\infty F_{\tau_D}(t) f_{\tau_H}(t) dt = \nu/(\gamma^s + \nu)$ since $f_{\tau_D}(t) = \nu e^{-\nu t}$ and $f_{\tau_H}(t) = \gamma^s e^{-\gamma^s t}$.

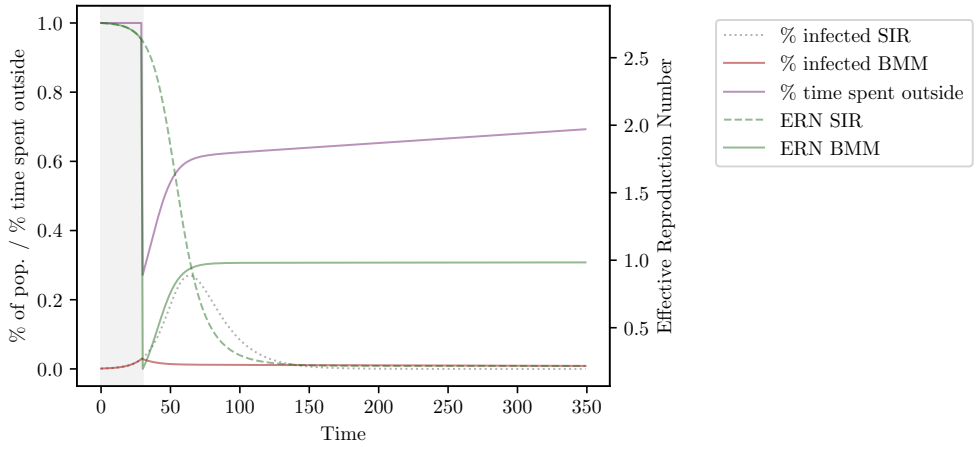

Figure 1.1: Dynamics of the epidemic in the interior equilibrium.

decreases on $[\tau, T]$. Therefore, the epidemic peak is reached before the population is informed about the epidemic, while in the SIR model, the fraction of infected continues to increase after time τ, reaching later a higher peak. The reason is that the population reacts to the epidemic announcement by self-isolating drastically after time τ, which results in a rapid decline in the percentage of infected. As the probability of being infected decreases, the marginal benefit of confinement decreases and individuals gradually increase the time they spend outside between $t = 97$ and $t = 203$ as a result. As $\hat{k}(t)$ sort of stabilizes to 0.615 after $t = 203$, there is no rebound of the epidemic.

One of the parameters monitored by health authorities is the effective reproduction number, i.e., the average number of secondary cases per infectious case in a population made up of both susceptible and recovered individuals. In the SIR model, the effective reproduction number is $\mathcal{R}_e^{SIR}(t) = \mu\beta s(t)/\gamma^a$. As the fraction of susceptible continuously decreases on $[0, T]$ (see equation (1.1)), the effective reproduction number in the SIR model decreases on $[0, T]$ and stabilizes to $\mathcal{R}_e^{SIR}(350) = 0.217$. In the interior equilibrium, an infected of the asymptomatic type has a "probability" $\hat{k}(t)$ of going out, and when she is out, a "probability" $\hat{k}(t)s(t)$ of meeting a susceptible. Therefore, the effective reproduction number in the interior equilibrium equals $\mathcal{R}_e^{BMM}(t) = \mu\beta\hat{k}(t)^2 s(t)/\gamma^a$. This explains why, contrary to the SIR model, the effective reproduction number in equilibrium falls after the epidemic announcement, then gradually increases and stabilizes

approximately[19] to 1 once people stop self-isolating, thus after $t = 210$.

Finally, one can see in Figure 1.2 that the SIR model overestimates the number of deaths compared to a model with strategic self-isolation. This should not be interpreted in favor of strategies pursuing herd immunity, however, because even the smaller number of cases predicted by our model may well overwhelm hospital capacity.

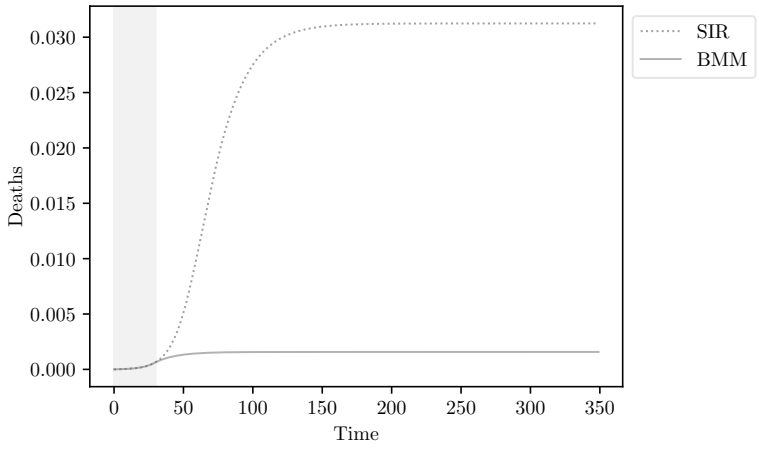

Figure 1.2: Cumulative number of deaths.

1.4.3 Policy analysis

Experts are still debating which public interventions should be imposed to manage the COVID-19 crisis. When it comes to public policies, not taking into account the fact that people react strategically to their environment might be counter productive. In this section, we illustrate how our results can inform some of the current debates over policies to control COVID-19.

The timing of announcement

We begin by analysing the impact of the announcement time on the epidemic course. As the epidemic peak is reached in τ, a later announcement mechanically increases the proportion of infected when the population learns about the epidemic. This has two opposite effects on the marginal benefit of confinement for an individual. On the positive

[19] Precisely, $\mathcal{R}_e^{BMM}(210) = 0.999$.

side, it increases the risk of being infected, which gives her more incentives to self-isolate. On the negative side, it increases her confidence[20] in being the asymptomatic type after she realizes that she has developed no symptoms during $[0, \tau]$, which gives her more incentives to go out.

These opposite effects explain the form of the graphs in Figure 1.3: when the epidemic announcement is delayed, the population starts deconfining later (the risk effect) but the percentage of time spent outside stabilizes at a higher level (the confidence effect).

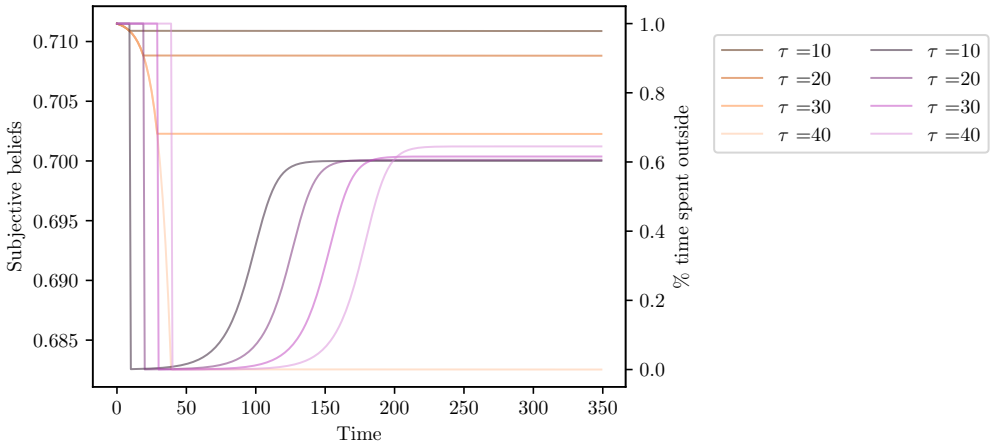

Figure 1.3: Impact of τ on the percentage of time spent outside and the subjective beliefs.

However, we find that a later announcement increases the number of deaths, as illustrated in Figure 1.4.

This is consistent with the findings of Silverio et al. (2020), who analyze the relationship between the penetration of COVID-19 at the time of lockdown and the mortality in the different Italian regions. They find a significant, positive correlation between the number of cases before lockdown and the mortality up to sixty days, and show that every day of delay in containment was associated with increased mortality.

[20] When an individual with no symptoms learns at time τ that the epidemic has been spreading since time 0, she updates her belief of being type θ_s to $p_i(\tau) = (1-\mu)/(1-\mu+\mu e^{\beta \int_0^\tau i(t)dt})$. Therefore, the larger τ, the smaller $p_i(\tau)$.

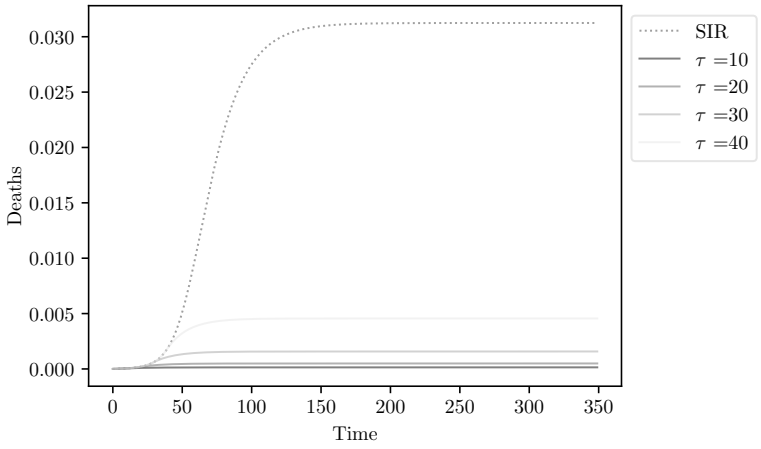

Figure 1.4: Impact of τ on the cumulative number of deaths.

Mitigating the transmission of the virus

The aim of lockdown policies is to flatten the economic curve by reducing the frequency of contacts in the population. Another way to do so is to mitigate the probability of transmission of the virus per contact, i.e., β. Governments can reduce β by subsidizing face masks, installing hand sanitizers in public spaces, messaging about hygiene measures such as hand washing, use of disposable tissues, etc. Governments can also organize screening campaigns to detect infected but asymptomatic people. Formally, if a fraction x of the population is tested for COVID-19 (and if asymptomatic people who test positive self-isolate), then only a fraction $(1-x)\mu$ of the infected people can infect susceptible individuals. In terms of the dynamics of the epidemic, this is equivalent to assuming that the marginal rate of infection decreases to $\beta(1-x)\mu$. Let us refer to the policies reducing $\beta\mu$ as *mitigating policies*.

In the SIR model, mitigating policies unambiguously flatten the epidemic curve[21]. In our model, however, the effect of these policies is more subtle. First, mitigating policies have two opposite effects on the marginal benefit of confinement for an individual. On the negative side, they decrease the risk of infection per contact, which gives her less incentives to self-isolate. On the positive side, they slow down[22] the learning process at

[21]The dynamics of the infected in the SIR model are $\dot{i}(t) = \beta\mu s(t)i(t) - (\gamma + (1-\mu)\nu)i(t)$, hence decreasing $\beta\mu$ flattens the epidemic curve.

[22]The law of motion of an individual's belief is $\dot{p}_i(t) = -p_i(t)(1-p_i(t))\beta\mu i(t)\hat{k}(t)^2$, hence decreasing $\beta\mu$

work in the model, hence decrease her confidence in being the asymptomatic type, which gives her less incentives to go out. The risk compensating behavior can be observed in Figure 1.5 for the three smallest values of $\beta\mu$. Interestingly, a decrease from $\beta\mu = 0.276$ to $\beta\mu = 0.230$ make individuals deconfining earlier (the risk effect) but the percentage of time spent outside stabilizes at a smaller level (the confidence effect).

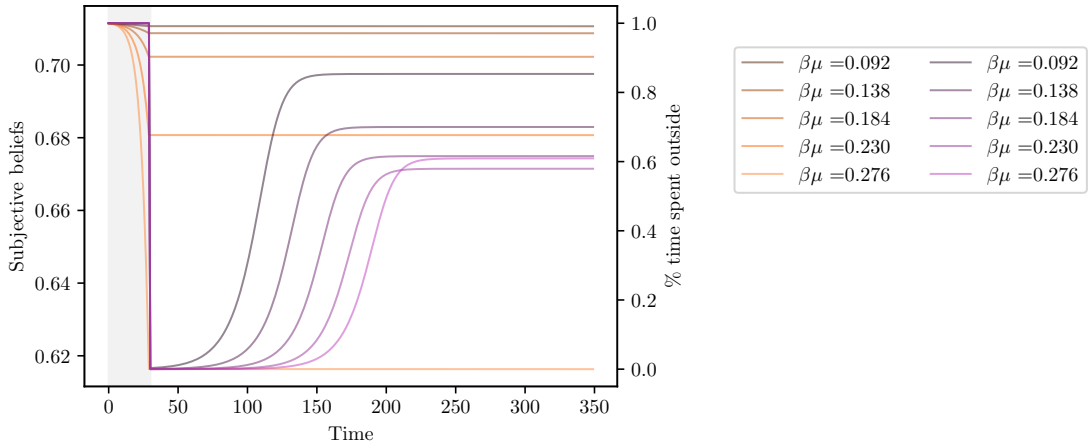

Figure 1.5: Impact of $\beta\mu$ on the percentage of time spent outside and the subjective beliefs.

This is in line with the empirical findings of Yan et al. (2020), who use SafeGraph smart device location data to investigate the consequences of wearing face masks on self-isolation behavior in the American population. They find evidence that masks enable disinhibition behavior and that Americans spend 20-30 minutes less time at home and more time in moderate to high-risk locations following orders to wear masks.

However, we find that mitigating policies are efficient in reducing the number of deaths, as illustrated in Figure 1.6.

Improving health system performance

The COVID-19 crisis has highlighted important differences between countries in terms of health system performance, even within the OECD group. It is reasonable to assume that the state of the health system (intensive care beds capacity, possibility of inter-hospital patient transfers or of setting up field hospitals, etc.) influences the healing rate γ^s and the mortality rate $\nu/(\nu + \gamma^s)$. We analyze the impact of the health

decreases the growth rate of $p_i(t)$ in absolute value.

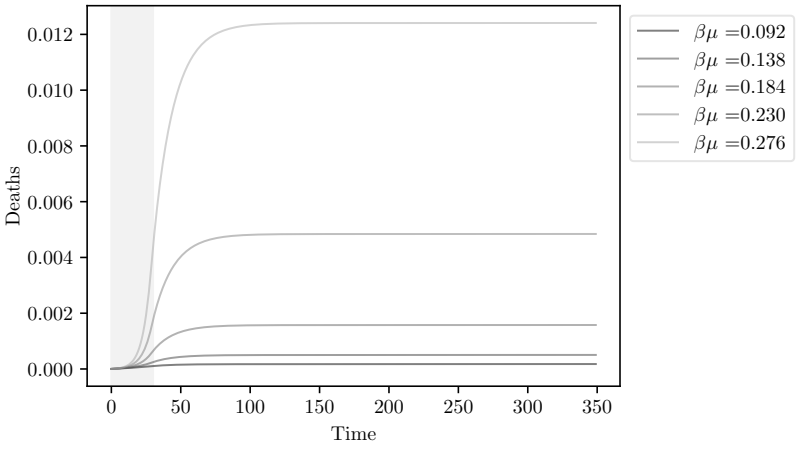

Figure 1.6: Impact of $\beta\mu$ on the cumulative number of deaths.

system performance on the dynamics of the epidemic by comparing our baseline system ($\gamma^a = 1/15$ and $\nu = 0.002267$) with a more performing system where $\gamma^a = 0.07334$ and $\nu = 0.0011335$.

Given a fixed percentage of time spent out by individuals, a better health system directly flattens the epidemic curve and decreases the number of deaths. However, with strategic self-isolation a better health system has also a perverse effect via the increase in the continuation payoff[23] in case of infection. Since the expected cost of having symptoms decreases with the quality of the health system, the marginal benefit of confinement decreases and individuals have less incentives to self-isolate. One can observe this risk compensating behavior in Figure 1.7: in a more performing health system, individuals deconfine earlier and the percentage of time spent outside stabilizes at a higher level.

However, we find that the performance of the health system decreases the number of deaths, as illustrated in Figure 1.8.

Subsidizing self-isolation.

The policy insight of Proposition 3 is that reducing the cost of confinement is also a means to be considered in controlling the spread of an infectious disease. To reduce c_H, governments can e.g. set up partial unemployment compensation schemes, subsidize the

[23]One can see in expression 1.4 that v_I increases when γ^s increases or when ν decreases.

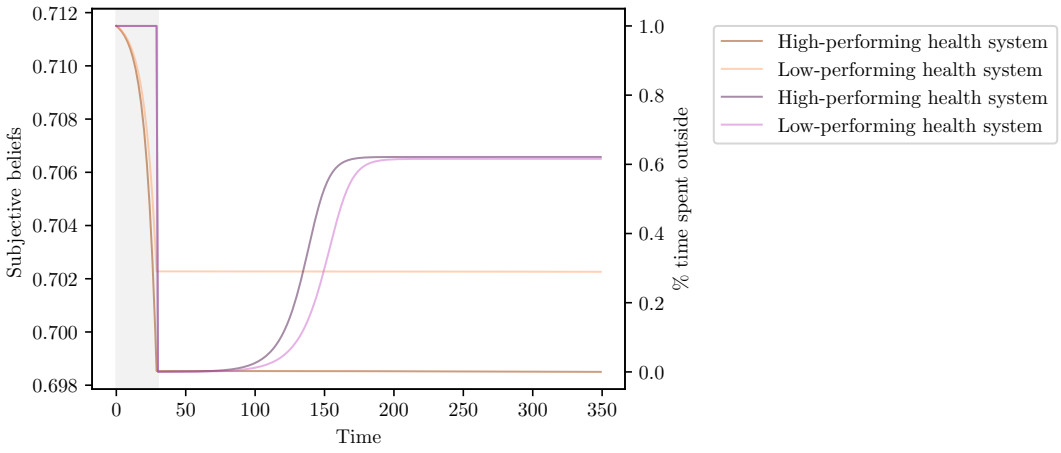

Figure 1.7: Dynamics of $\hat{k}(.)$ and $p(.)$ in a low-performing system and in a high-performing system.

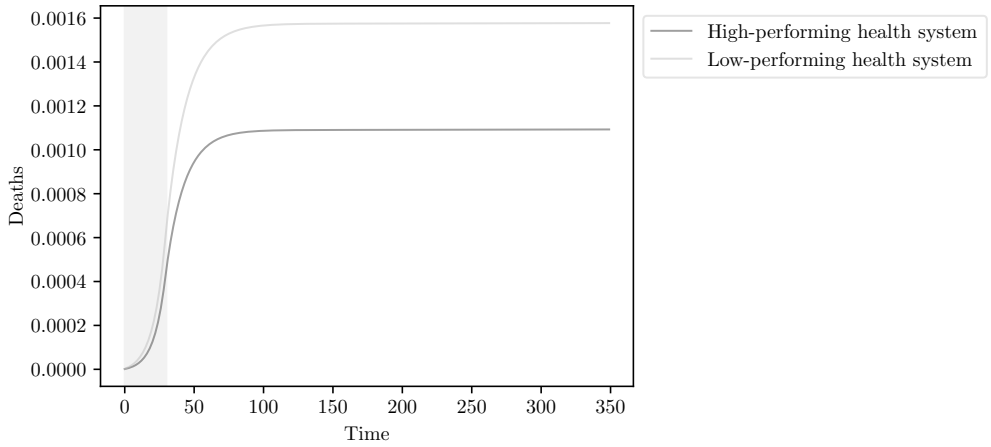

Figure 1.8: Cumulated number of deaths in a low-performing system and in a high-performing system.

purchase of computer equipment, etc. The impact of a decrease in c_H on the dynamics of the epidemic is immediate: it decreases the percentage of time spent outside, thus the number of deaths.

Since measures encouraging self-isolation are costly, it is conceivable that the government may not be able to cut back c_H until the vaccine arrives, but only for a certain period of time, which raises the question of the optimal timing of subsidizing policies. To address this question, we simulate two different scenarios that we compare to the baseline simulation. In the first scenario (*Public Policy 1*), the confinement cost is reduced to $c_H = 0.000675$ only between $t = 30$ and $t = 180$. In the second scenario (*Public Policy 2*), the confinement cost is reduced to $c_H = 0.000675$ only between

$t = 180$ and $t = 350$. As one can see in Figure 1.9, Policy 1 induces more self-isolation until $t = 180$. At $t = 180$, the time individuals spend outside skyrockets, then rapidly decreases and returns to the equilibrium level without public intervention. Right after the implementation of Policy 2, individuals self-isolate drastically, then the time they spend outside increases gradually until it returns to the equilibrium level without public intervention.

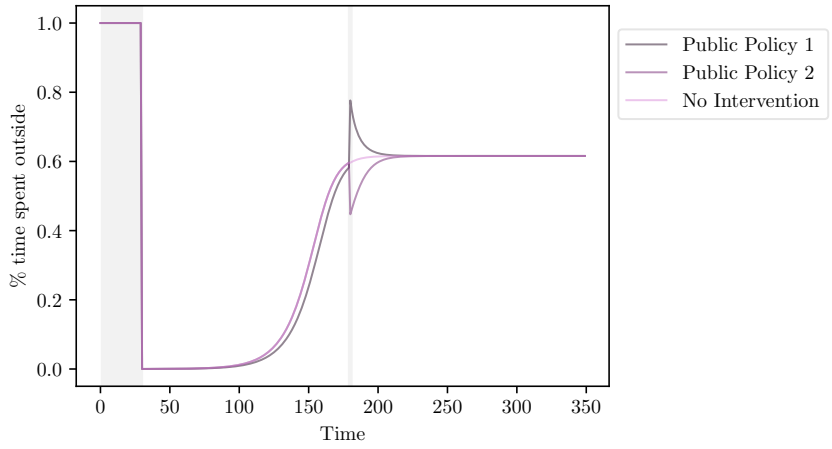

Figure 1.9: Percentage of time spent outside under Public Policy 1 and Public Policy 2.

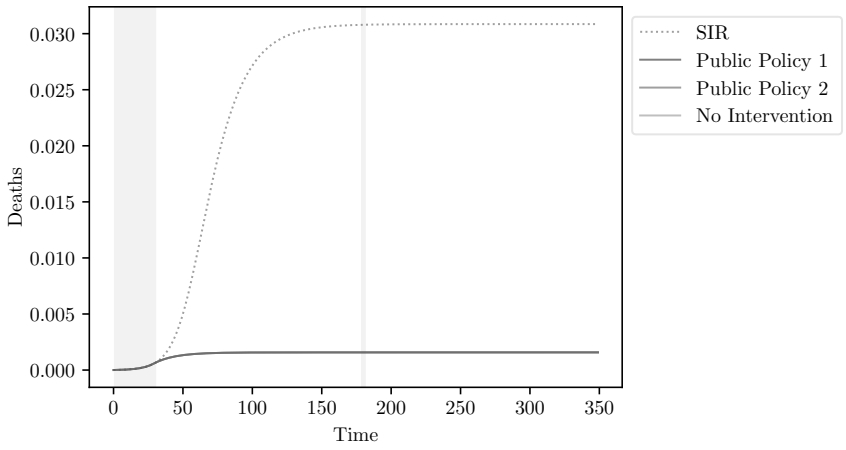

Figure 1.10: Cumulative number of deaths under Public Policy 1 and Public Policy 2.

Finally, these two policies only reduce the number of deaths at the margin (see Figure 1.10), because individuals already partially self-isolate in equilibrium. This should not be interpreted as evidence of inefficiency of policies subsidizing self-isolation. On the

contrary, these policies allow for a shift from equilibria in dominant strategies without self-isolation to equilibria with partial self-isolation.

1.5 Concluding remarks

This paper is a first attempt to analyze the spread of an infectious disease in a population when individuals strategically choose how much time to interact with others. In the absence of any symptoms, individuals are not sure whether they are susceptible or infected but asymptomatic, and they continuously tradeoff the costs and benefits of self-isolation on the basis of their belief of being the asymptomatic type. We prove that when the cost of confinement is small enough, there exists an equilibrium in which the population partially self-isolates at every date. This is consistent with the findings of Youpei Yan et al. (2021), who use smart device location data to show that people adopted avoidance behaviors following the announcement of the pandemic.

We calibrate the parameters of our model to the COVID-19 pandemic and simulate the impact of some public interventions on the dynamics of the epidemic. Calibration is very delicate in the case of an emerging disease for which knowledge is increasing daily. In particular, the choices of the proportion of asymptomatic and the basic reproduction number are questionable. To verify the robustness of our results, we perform a sensitivity analysis in the Appendix. To do so, we simulate our model with other reasonable values of the parameters and obtain qualitatively the same results. In particular, we show that the number of deaths increases when the population is informed later of the epidemic, and decreases under mitigating policies.

Two subjects have been particularly debated since the beginning of the COVID-19 crisis: the application, timing and duration of lockdowns and the use of face masks in the general population.

Most countries have implemented lockdown policies to slowdown the epidemic. As lockdowns cause huge collateral damage in terms of economic activity, education and access to care, some governments were tempted by strategies pursuing herd immunity at first. The optimal timing of lockdowns is a crucial question. In a theoretical model

where individuals do not chose how much time they interact with others, Kruse and Strack (2020) show that if the government has the possibility to lockdown the population during only 100 days, delaying the moment to start the lockdown might actually decrease the total number of deaths. The reason is that delaying the lockdown increases the level of herd immunity in the population, which works as a protection for those individuals who remain susceptible after the lockdown. In contrast, we find that the number of deaths increases with the announcement time. The reason is that, when individuals behave strategically, they flatten the epidemic curve by self-isolating more when the epidemic is too fast. Therefore, delaying the announcement time postpones the moment at which the population strategically controls the epidemic course.

At present, many governments have mandated the use of face masks in public spaces, arguing that face masks are low cost and might help prevent some transmission. At the beginning of the outbreak, however, WHO officials did not recommend mask wearing in the general population[24], stressing that 1) masks are commonly misused, and as a result, do not offer the intended protections, and 2) wearing a mask can provide a false sense of security, leading some to become less vigilant in more important hygiene measures, such as hand washing and self-isolation. Our results confirm that making masks mandatory leads individuals to reduce social distance, which can accelerate the epidemic. However, as individuals adapt to the level of the epidemic, this reduction is moderate, and the negative effect of a higher level of social interaction is more than offset by the positive effect on virus transmission, so that mandatory masks lead to a reduction in the number of deaths.

In our model we assume an homogenous population, full immunity after healing and no incubation period. These are strong assumptions in the case of the COVID-19 pandemic, which could be relaxed for future research.

Heterogeneous population. We assume that individuals have all the same prior belief

[24]On 30 March, 2020, Dr. Mike Ryan, executive director of the WHO health emergencies program declared: "There is no specific evidence to suggest that the wearing of masks by the mass population has any potential benefit. In fact, there's some evidence to suggest the opposite in the misuse of wearing a mask properly or fitting it properly."

of being the severe type, thus of dying from the disease. In the case of COVID-19, it is now clear and well documented[25] that the population is divided between those who are at high risk of dying from the disease (patients with co-morbidities) and those who are at lower risk. It is still unclear whether individuals with co-morbidities are less likely to be asymptomatic. However, they know that, if they catch the disease and are not asymptomatic, they will have more severe symptoms and a higher chance of dying than people without co-morbidities. To capture this observable intrinsic heterogeneity in the population, we can augment the model by assuming that each individual i is of medical condition $\epsilon_i \in \{c, \bar{c}\}$, with c standing for "co-morbidities" and $\bar{c}$ standing for "no co-morbidities". An individual knows her medical condition but not whether she is the asymptomatic type. In the Appendix, we prove that any equilibrium features social interaction, and that the game admits a unique equilibrium in which no individual self-isolates when the confinement cost is large enough. The main difference is that assuming an heterogeneous population precludes the existence of symmetric equilibria other than the no-confinement equilibrium.

Waning immunity. In our model, individuals who recover from the disease become perfectly immune to the virus. This is true for many infectious diseases, but likely not for COVID-19. Antibodies to other coronaviruses are known to wane over time (12 to 52 weeks from the onset of symptoms) and homologous re-infections have been observed (see e.g. Kellam and Barclay (2020)). SARS-CoV-2 IgM and IgG antibody levels may remain over the course of seven weeks or at least in 80% of the cases until day 49 (see Xiao et al. (2020) and Zeng et al. (2020)). Therefore, it is reasonable to assume that individuals are immune immediately after recovery, but may lose their immunity after a random period of time, probably before the vaccine arrives. One possible way to introduce waning immunity into our model would be to assume that healed individuals become susceptible again at some rate $\eta \in (0.1)$. This would change the dynamics of

[25] Underlying medical conditions, such as obesity, hypertension (Richardson et al. (2020)), cardiovascular disease (Sanyaolu et al. (2020)), chronic lung disease (S. Zhao et al. (2020)) and diabetes (Singh et al. (2020)) are clinical predictors of mortality and severity for SARS-CoV-2. In addition, older people are not only more at risk of contracting the disease but have an increased risk of death among these patient groups (K. Liu et al. (2020), B. Wang et al. (2020), F. Zhou et al. (2020)).

the epidemic[26] and also the continuation payoff in case of symptoms. Like in our model, an individual would learn that she is the severe type the first time she has symptoms. The difference is that she would face a new type of uncertainty after healing, as she would not know whether she is still immune to the virus. As a result, playing $k(t) = 1$ forever after healing would not be a dominant strategy, and she would face a non trivial dynamic optimization problem after healing. The technical analysis of this augmented model is challenging and left for future research.

Incubation period. The most critical assumption of our model is the absence of incubation period, which implies that the virus is spread in the population only by asymptomatic individuals. In the case of COVID-19, the time from exposure to the development of symptoms is estimated to be 5.2 days on average (see Q. Li et al. (2020)), hence severe types can also spread the virus during the incubation period. A simple way to introduce an incubation period in our model would be to assume that an individual infected at time t develops symptoms only at time $t + \Delta$, with Δ standing for the incubation period. The dynamics of the epidemic would be the same, except for the law of motion of beliefs. Indeed, in this variant of the model the probability of developing symptoms between t and $t + dt$ conditional on being type θ_s would be the probability of having been infected in $t - \Delta$. Therefore, the law of motion of player i's belief would be $\dot{p}_i(t) = -p_i(t)(1 - p_i(t))k_i(t - \Delta)\bar{k}_I(t - \Delta)i(t - \Delta)$. The best-response problem of individuals would be an optimal control problem with time lag in the control variable, which is very difficult to solve. However, we believe that the equilibria of the game would be similar, as the uncertainty that people might be infected and contagious but asymptomatic is already present in our model with the uncertainty about the type.

[26] In this augmented model would be governed by the system of ODE $\dot{s}(t) = -\beta\bar{k}_S(t)s(t)\bar{k}_I(t)i(t) + \eta r(t)$, $\dot{i}(t) = \beta\bar{k}_S(t)s(t)\bar{k}_I(t)i(t) - (\gamma + (1 - \mu)\nu)i(t)$ and $\dot{r}(t) = (\gamma^s + \nu)i(t) - \eta r(t)$.

Appendix

1.5.1 Proofs for Section 2 and Section 3

Lemma 1. *Let τ_H and τ_D be independent random variables distributed according to $f(t) = \gamma e^{-\gamma t}$ and $f(t) = \nu e^{-\nu t}$, respectively. The following equality holds:*

$$E\left[\int_0^{\min\{\tau_H,\tau_D\}} e^{-rt}(c_H + c_I)dt + \frac{c_D}{r}e^{-r\tau_D}\mathbb{1}_{\tau_D<\tau_H}\right] = \frac{1}{r+\gamma+\nu}(c_H + c_I + \nu\frac{c_D}{r}).$$

Proof. Let $g(\tau_H, \tau_D) := \int_0^{\min\{\tau_H,\tau_D\}} e^{-rt}(c_H + c_I)dt + \frac{c_D}{r}e^{-r\tau_D}\mathbb{1}_{\tau_D<\tau_H}$. Straightforwardly,

$$g(\tau_H, \tau_D) = \frac{c_H + c_I}{r}(1 - e^{-r\min\{\tau_H,\tau_D\}}) + \frac{c_D}{r}e^{-r\tau_D}\mathbb{1}_{\tau_D<\tau_H}.$$

The random variable $\min\{\tau_H, \tau_D\}$ is distributed according to $f(t) = (\gamma + \nu)e^{-(\gamma+\nu)t}$. Therefore,

$$E[e^{-r\min\{\tau_H,\tau_D\}}] = \frac{\gamma+\nu}{r+\gamma+\nu}.$$

Moreover,

$$E[e^{-r\tau_D}\mathbb{1}_{\tau_D<\tau_H}] = \int_0^\infty \left(\int_0^{\tau_H} e^{-(r+\nu)\tau_D}\nu d\tau_D\right)\gamma e^{-\gamma\tau_H}d\tau_H = \frac{\nu}{r+\gamma+\nu}$$

Therefore,

$$E[g(\tau_H, \tau_D)] = (c_H + c_I)\frac{1}{r+\gamma+\nu} + \frac{c_D}{r}\frac{\nu}{r+\gamma+\nu}.$$

□

Proof of Proposition 1

The best-response problem of player i is to determine the strategy k_i that maximizes her expected discounted payoff $v_i(0; k_i)$, the pair of functions $s(.)$ and $i(.)$ being fixed and defined by the dynamics

$$\begin{cases} s(0) = 1 - i(0) = s_0 \text{ and, } \forall\, t \in [0, T], \\ \dot{s}(t) = -\beta\bar{k}_S(t)s(t)\bar{k}_I(t)i(t), \\ \dot{i}(t) = \beta\bar{k}_S(t)s(t)\bar{k}_I(t)i(t) - (\gamma + (1-\mu)\nu)i(t) \end{cases}$$

Formally, it is the solution of the optimal control problem:

$$\begin{cases} \max\limits_{k_i\in\mathcal{K}} & \int_0^T e^{-rt}e^{-\int_0^t p_i(s)k_i(s)\beta\bar{k}_I(s)i(s)ds}\left(p_i(t)k_i(t)\beta\bar{k}_I(t)i(t)v_I - c_H(1-k_i(t))\right)dt \\ \text{w.r.t.} & \dot{p}_i(t) = -p_i(t)(1-p_i(t))k_i(t)\beta\bar{k}_I(t)i(t)\ \forall\, t \text{ and } p_i(0) = 1-\mu. \end{cases}$$

where $\mathcal{K}$ denotes the set of piecewise continuous functions from $\mathbb{R}_+$ into $[0,1]$. Making the change of variable $x(t) := e^{-\int_0^t p_i(s)k_i(s)\beta\bar{k}_I(s)i(s)ds}$, player i's problem can be rewritten as:

$$\mathcal{P}(\mathbf{k}): \begin{cases} \max\limits_{k\in\mathcal{K}} & \int_0^{+\infty} e^{-rt}F(t,x(t),k(t))dt \\ \text{w.r.t.} & \dot{x}(t) = f(t,x(t),k(t)) \text{ and } x(0)=1. \end{cases}$$

with $F(t,x(t),k(t)) := (x(t)-\mu)\,k(t)\beta\bar{k}_I(t)i(t)v_I - x(t)c_H(1-k(t))\big)$ and $f(t,x(t),k(t)) := -(x(t)-\mu)\,k(t)\beta\bar{k}_I(t)i(t)$.

As $F(t,x(t),k(t))$ is negative and bounded below by v_I, the objective is well defined. Furthermore, by standard results, the problem admits at least one solution. Applying Pontryagin's maximum principle, the optimal control k^* and the associated trajectory x^* must satisfy the following conditions:

Lemma 2 (**Necessary conditions**). *If (x^*,k^*) is a solution of $\mathcal{P}(\mathbf{k})$, then there exists a continuous, piecewise continuously differentiable function $\psi:\mathbb{R}_+\to\mathbb{R}$ such that:*

(i) $\dot{\psi}(t) - r\psi(t) = -H_x(t,x^*(t),k^*(t),\psi(t))$,

(ii) $H(t,x^*(t),k(t),\psi(t)) \le H(t,x^*(t),k^*(t),\psi(t))$ *for every admissible control k,*

(iii) $\psi(T)=0$,

where $H(t,x(t),k(t),\psi(t)) := F(t,x(t),k(t)) + \psi(t)f(t,x(t),k(t))$ is the (discounted[27]) Hamiltonian of the problem.

Observing that

$$H(t,x(t),k(t),\psi(t)) = (x(t)-\mu)k(t)\beta\bar{k}_I(t)i(t)(v_I-\psi(t)) - x(t)c_H(1-k(t)),$$

the necessary conditions are rewritten as

(i) $\dot{\psi}(t) - r\psi(t) = k^*(t)\beta\bar{k}_I(t)i(t)(\psi(t)-v_I) + c_H(1-k^*(t))$,

(ii) $(k^*(t)-k(t))\left[x^*(t)c_H - (x^*(t)-\mu)\beta\bar{k}_I(t)i(t)(\psi(t)-v_I)\right] \ge 0$ $\forall$ admissible control k.

[27]The Hamiltonian of the problem is $\widehat{H}(t,x(t),k(t),v(t)) := e^{-rt}F(t,x(t),k(t)) + v(t)f(t,x(t),k(t))$. For expositional reasons, we define $\psi(t) := e^{rt}v(t)$ and use the discounted Hamiltonian $H(t,x(t),k(t),\psi(t)) := e^{rt}\widehat{H}(t,x(t),k(t),v(t))$. The first necessary condition is adapted from the standard condition $v'(t) = -\widehat{H}_x(t,x(t),k(t),v(t))$.

The latter condition can be more conveniently rewritten as:

$$(ii)\ (k^*(t)-k(t))\left[c_H - p^*(t)\beta\bar{k}_I(t)i(t)(\psi(t)-v_I)\right] \geq 0,$$

with $p^*(t) = 1 - \frac{\mu}{x^*(t)}$. Accordingly, if $c_H - p^*(t)\beta\bar{k}_I(t)i(t)(\psi(t)-v_I) > 0$, then $k^*(t)$ must be larger than every admissible control, which is true only if $k^*(t) = 1$. If, on the contrary, $c_H - p^*(t)\beta\bar{k}_I(t)i(t)(\psi(t)-v_I) < 0$, $k^*(t)$ must be smaller than every admissible control, which is true only if $k^*(t) = 0$. Therefore, condition (ii) reduces to

$$(ii)\ k^*(t) = \begin{cases} 1, & \text{if } c_H - p^*(t)\beta\bar{k}_I(t)i(t)(\psi(t)-v_I) > 0, \\ 0, & \text{if } c_H - p^*(t)\beta\bar{k}_I(t)i(t)(\psi(t)-v_I) < 0, \\ \in [0,1], & \text{if } c_H - p^*(t)\beta\bar{k}_I(t)i(t)(\psi(t)-v_I) = 0. \end{cases}$$

Finally, we prove that $\psi(T) = 0$. For every belief p, at time T the best-response payoff satisfies the Bellman equation:

$$V(T,p) = \max_{k\in[0,1]} \left\{ \big(-(1-k)c_H + pk\beta\bar{k}_I(T)i(T)v_I \big)dt + \big(1 - pk\beta\bar{k}_I(T)i(T)dt\big)e^{-rdt}V(T+dt, p+dp) \right\}.$$

As the game stops at time T, $V(T,p) = V(T+dt, p+dp) = 0$, thus the latter expression is rewritten:

$$0 = \max_{k\in[0,1]} \left\{ -(1-k)c_H + pk\beta\bar{k}_I(T)i(T)v_I \right\},$$

which implies that the best-response at time T is:

$$k^*(T) = \begin{cases} 1, & \text{if } c_H + p^*(T)\beta\bar{k}_I(T)i(T)v_I > 0, \\ 0, & \text{if } c_H + p^*(T)\beta\bar{k}_I(T)i(T)v_I < 0, \\ \in [0,1], & \text{if } c_H + p^*(T)\beta\bar{k}_I(T)i(T)v_I = 0. \end{cases}$$

It follows that $\psi(T) = 0$ by condition (ii).

Let us now prove that necessary conditions are also sufficient.

Lemma 3 (**Sufficient conditions**). *Consider a continuous, piecewise continuously differentiable function $\psi : \mathbb{R}_+ \to \mathbb{R}$ and a pair (x^*, k^*) satisfying conditions (i), (ii) and (iii). For any admissible pair (x,k), $\int_0^{+\infty} e^{-rt}F(t, x(t), k(t)) \leq \int_0^{+\infty} e^{-rt}F(t, x^*(t), k^*(t))$.*

Proof. Using the change of variable $y(t) = \ln\left(\frac{\mu}{x(t)-\mu}\right)$, the maximization problem $\mathcal{P}(\mathbf{k})$ is rewritten as:

$$\mathcal{P}(\mathbf{k}): \begin{cases} \max\limits_{k\in\mathcal{K}} & \int_0^{+\infty} e^{-rt} F(t, \mu(1+e^{-y(t)}), k(t))dt \\ \text{w.r.t.} & y'(t) = k(t)\beta\bar{k}_I(t)i(t) \text{ and } y(0) = \ln\left(\frac{\mu}{1-\mu}\right). \end{cases}$$

Therefore, the Hamiltonian of the problem can be rewritten as:

$$H(t, y, k, \psi) = \mu e^{-y(t)} k(t)\beta\bar{k}_I(t)i(t)v_I - \mu(1+e^{-y(t)})c_H(1-k(t)) + \psi(t)k(t)\beta\bar{k}_I(t)i(t)$$

Let us define the function $\hat{H}(y) = \max_k H(t, y, k, \psi)$. Straightforwardly,

$$\hat{H}(y) = \begin{cases} \mu e^{-y}\beta\bar{k}_I(t)i(t)v_I + \psi(t)\beta\bar{k}_I(t)i(t) & \text{if } \mu e^{-y}\beta\bar{k}_I(t)i(t)v_I + \mu(1-e^{-y})c_H + \psi(t)\beta\bar{k}_I(t)i(t) > 0 \\ -\mu(1+e^{-y})c_H & \text{if } \mu e^{-y}\beta\bar{k}_I(t)i(t)v_I + \mu(1-e^{-y})c_H + \psi(t)\beta\bar{k}_I(t)i(t) \leq 0 \end{cases}$$

Since $v_I < 0$, $\hat{H}(y)$ is concave in y. Therefore, necessary conditions are also sufficient by the Arrow-Kurz theorem (see e.g. Arrow and Kurz (1970)). □

Proof of Proposition 3

Fix a player i, a date t and a value $\bar{k}_I(t)$. We shall use the following lemma:

Lemma 4. *If $\psi_i : \mathbb{R} \in \mathbb{R}$ satisfies the necessary conditions of Proposition 1, then $v_I < \psi_i(t) < 0$ for every $t \in [0, T]$.*

Proof. Let ψ_i such that

$$\dot{\psi}_i(t) - r\psi_i(t) = c_H + k_i(t)\left(\beta\bar{k}_I(t)i(t)(\psi_i(t) - v_I) - c_H\right),\ \psi_i(T) = 0, \tag{1.9}$$

with

$$k_i(t) \begin{cases} = 1 & \text{if } p_i(t)\beta\bar{k}_I(t)i(t)(\psi_i(t) - v_I) - c_H < 0, \\ \in [0,1] & \text{if } p_i(t)\beta\bar{k}_I(t)i(t)(\psi_i(t) - v_I) - c_H = 0, \\ = 0 & \text{if } p_i(t)\beta\bar{k}_I(t)i(t)(\psi_i(t) - v_I) - c_H > 0. \end{cases}$$

1) We first prove that $v_I < \psi_i(t)$ for every $t \in [0, T]$. Suppose that there exists $t' < t'' \leq T$ such that $\psi_i(t) \leq v_I$ for every $t \in [t', t'']$. It follows that, for every

$t \in [t', t'']$, $p_i(t)\beta\bar{k}_I(t)i(t)(\psi_i(t) - v_I) - c_H < 0$, which further implies that $k_i(t) = 1$. Plugged into condition (1.9), this yields

$$\dot{\psi}_i(t) - r\psi_i(t) = \beta\bar{k}_I(t)i(t)(\psi_i(t) - v_I) \; \forall \; t \in [t', t''],$$

thus $\dot{\psi}_i(t) < 0 \; \forall \; t \in [t', t'']$. As $\psi_i(t'') < v_I$, $\psi_i(t) < v_I$ in the right neighbourhood of t''. Therefore, the assumption that $\psi_i(t) \leq v_I$ for every $t \in [t', t'']$ implies that $\psi_i(t) < v_I$ and $\psi'(t) < 0$ for every $t \in [t', T]$. However, $\psi_i(T) = 0$, thus $\psi_i'(t) < 0$ on $[t', T]$ implies that $\psi_i(t) > 0$ on $[t', T]$, which contradicts $\psi_i(t) < v_I$ on $[t', T]$.

2) Now we prove that $\psi_i(t) \leq 0$ for every $t \in [0, T]$. Suppose that there exists $t' < t'' \leq T$ such that $\psi_i(t) > 0$ for every $t \in [t', t'']$. The, as $\psi_i(t) - v_I > 0$, $\psi_i'(t) > 0$ on $[t', t'']$ by (1.9). It follows that $\psi_i(t'') > 0$, thus that $\psi_i(t) > 0$ in the right neighbourhood of t'', thus $\psi_i(t)$ is increasing in the right neighborhood of t''. Extending this argument, this implies that $\psi_i(t) > 0$ and $\psi_i'(t) > 0$ for every $t \in [t', T]$. This contradicts $\psi_i(T) = 0$. $\square$

As infected individuals of the severe type completely self-isolate, $\bar{k}_I(t) \leq \mu$. Moreover, $p_i^*(t)$ is non increasing in t, thus $p_i^*(t) \leq 1-\mu$. Finally, $i(t) < 1$ and $v_I \leq \psi_i^*(t) \leq 0$ by Lemma 4. Therefore,

$$p_i^*(t)\beta\bar{k}_I(t)i(t)(\psi_i^*(t) - v_I) - c_H \leq (1-\mu)\beta\mu(-v_I) - c_H.$$

As a consequence, if $(1-\mu)\beta\mu v_I + c_H > 0$, then $p_i^*(t)\beta\bar{k}_I(t)i(t)(\psi_i^*(t) - v_I) - c_H < 0$, which implies that $k_i^*(t) = 1$ is the unique best response for player i to $\bar{k}_I(t)$ by condition (7) in Proposition 1. Therefore, the condition $(1-\mu)\beta\mu v_I + c_H > 0$ guarantees that the game has a unique equilibrium in dominant strategies, in which $k_i^*(t) = 1$ for every i, t.

We now determine the players' payoff in the equilibrium where $k^* = 1$. As a first step, we compute the players' belief at time t. Plugging $k_i(t) = 1$ and $\bar{k}_I(t) = \mu$ into the belief dynamics (3), we obtain the players' belief function as the solution of the ODE:

$$\dot{p}(t) = -p(t)(1 - p(t))\beta\mu i(t),$$

with initial condition $p(0) = 1 - \mu$. Integrating between 0 and t, we obtain

$$\ln\left(\frac{1-p(t)}{p(t)}\right) - \ln\left(\frac{\mu}{1-\mu}\right) = \int_0^t \beta\mu i(u)du,$$

which, after straightforward simplifications, yields:

$$e^{-\int_t^s p(u)\beta\mu i(u)du} = \frac{1-p(t)}{1-p(s)}, \text{ and}$$

$$p(t) = \frac{1-\mu}{1-\mu+\mu z(t)},$$

with $z(t) := e^{\beta\mu\int_0^t i(u)du}$. Using the latter findings and plugging $k_i(t) = 1$ and $\bar{k}_I(t) = \mu$ into the payoff expression (5) then simplifying, we obtain:

$$v(t;k^*) = v_I(1-\mu)\beta\mu\frac{\int_t^T e^{-r(s-t)}e^{-\beta\mu\int_0^s i(u)du}i(s)ds}{\mu+(1-\mu)e^{-\beta\mu\int_0^t i(u)du}}.$$

□

Proof of Proposition 4

Consider an interior, symmetric strategy profile where $k_i(t) = \hat{k}(t) \in (0,1)\ \forall\ i,\ t$. Since individuals self-isolate when they have symptoms, only susceptible and infected, asymptomatic individuals play $\hat{k}(t)$ at time t. As a result, $\bar{k}_S(t) = \hat{k}(t)$ and $\bar{k}_I(t) = \mu\hat{k}(t)$, which, once plugged into equations (1) and (2), yields:

$$\dot{s}(t) = -\beta\mu s(t)i(t)\hat{k}(t)^2,$$
$$\dot{i}(t) = \beta\mu s(t)i(t)\hat{k}(t)^2 - (\gamma+(1-\mu)\nu)i(t).$$

Moreover, plugging $k_i(t) = \hat{k}(t)$ and $\bar{k}_I(t) = \mu\hat{k}(t)$ into the individual belief dynamics, we obtain $p_i(t) = p(t)$ for every i, with

$$\dot{p}(t) = -p(t)(1-p(t))\beta\mu i(t)\hat{k}(t)^2.$$

Plugging $p_i(t) = p(t)$ and $\bar{k}_I(t) = \mu\hat{k}(t)$ into condition (7) in Proposition 1, we obtain $\psi_i(t) = \psi(t)$ for every i, with

$$p(t)\beta\mu\hat{k}(t)i(t)(\psi(t)-v_I) - c_H = 0 \tag{1.10}$$

Finally, plugging (1.10) into the Euler condition, we obtain:

$$\dot{\psi}(t) - r\psi(t) = c_H + c_H\frac{1-p(t)}{p(t)}\hat{k}(t).$$

The strategy $\hat{k}$ is interior strategy if and only if $\hat{k}(t) \in (0,1)$ for every $t \in [0,T]$.

□

1.5.2 An extension of the model with co-morbidities

Several assumptions have been made about the effect of co-morbidities on people's behavior. In this section, we will explore the effect of adding co-morbidities to the previously defined model and symmetric equilibrium. We augment the model by assuming that each individual i is of health condition $\epsilon_i \in \{c, \bar{c}\}$, with c standing for "presence of co-morbidities" and $\bar{c}$ for "absence of co-morbidities". An individual knows her health condition but not her type (asymptomatic or severe). For simplicity, we assume that the probability of being the asymptomatic type is independent of the health condition. Assuming that individuals with co-morbidities are more likely to be the severe type, though more realistic, would not change the form of the best-responses and the nature of our results.

All individuals of the asymptomatic type recover at rate γ^a when they are infected. Individuals of the severe type with health condition $\epsilon \in \{c, \bar{c}\}$ recover at rate γ^ϵ and die at rate ν^ϵ, with $\gamma^\epsilon + \nu^\epsilon = \gamma^a \in (0, 1)$. To capture the effect of co-morbidities on the course of the disease, we assume that individuals of the severe type without co-morbidities recover faster: $\gamma^{\bar{c}} \geq \gamma^c$, are less likely to die: $\nu^{\bar{c}} \leq \nu^c$, and suffer less from the disease: $c_I^{\bar{c}} \leq c_I^c$.

At each time t the population is divided into five groups: susceptible with and without co-morbidities: $S^c(t)$ and $S^{\bar{c}}(t)$, infected with and without co-morbidities: $I^c(t)$ and $I^{\bar{c}}(t)$, and recovered: $R(t)$. Using the same notation as in the main model, the dynamics of the epidemic are governed by the following equations for each $\epsilon \in \{c, \bar{c}\}$:

$$
\begin{aligned}
&s^\epsilon(0) = 1 - i^\epsilon(0) = s_0^\epsilon \in (0, 1) \text{ and, } \forall\, t \in [0, T], \\
&\dot{s}^\epsilon(t) = -\beta \bar{k}_{S^\epsilon}(t) s^\epsilon(t) \bar{k}_I(t) i(t), \\
&\dot{i}^\epsilon(t) = \beta \bar{k}_{S^\epsilon}(t) s^\epsilon(t) \bar{k}_I(t) i(t) - (\mu\gamma^a + (1-\mu)(\gamma^\epsilon + \nu^\epsilon)) i^\epsilon(t).
\end{aligned}
$$

where $i(t) = i^c(t) + i^{\bar{c}}(t)$, $\bar{k}_I(t) := \frac{1}{i(t)} \int_{j \in I(t)} k_j(t) dj$ and $\bar{k}_{S^\epsilon}(t) = \frac{1}{s^\epsilon(t)} \int_{j \in S^\epsilon(t)} k_j(t) dj$ denote the average fraction of time spent outside at time t by infected and susceptible people with condition ϵ, respectively. The continuation payoff of an individual with health condition ϵ the first time she has symptoms equals:

$$
v_I^\epsilon = -\frac{1}{r + \gamma^\epsilon + \nu^\epsilon} (c_H + c_I^\epsilon + \nu^\epsilon \frac{c_D}{r}).
$$

As v_I^ϵ increases with γ^ϵ and decreases with c_I^ϵ or ν^ϵ, it is smaller for an individual with co-morbidities, thus $v_I^c < v_I^{\bar{c}}$. Proposition 1 is unchanged in the case of an heterogenous population: each individual decides what fraction of her time to spend outside after comparing the confinement cost with her expected cost of social interaction. Therefore, Proposition 2 and (an adapted version of) Proposition 3 remain true in the augmented model: any equilibrium features social interaction and the game admits a unique equilibrium in which no individual self-isolates when the confinement cost is large enough, i.e., when $c_H + (1-\mu)\beta v_I^c \geq 0$. Not surprisingly, given the definition used for the symmetric equilibrium, the only equilibrium that exists when comorbidities are added to the model is the no self-isolation equilibrium. Unlike the case of a homogeneous population, the unconfined equilibrium is the only symmetric equilibrium in the augmented set, as the following proposition indicates.

Proposition 5. (1) *The only symmetric equilibrium is the no-confinement equilibrium where all individual play* $k(t) = 1$ *for every* $t \in [0, T]$.

(2) *The no-confinement equilibrium exists if and only if*

$$-v_I^c < \frac{c_H}{p(t)\beta\mu i(t)(1 - H(t))} \; \forall \; t \in [0, T],$$

where p *and* i *are defined by the system of equations*

$$\begin{aligned}
&p(0) = 1 - \mu, \; s^\epsilon(0) = 1 - i^\epsilon(0) = s_0^\epsilon \text{ for } \epsilon \in \{c, \bar{c}\} \text{ and, } \forall \; t \in [0, T], \\
&\dot{s}^\epsilon(t) = -\beta\mu s^\epsilon(t) i(t) \text{ for } \epsilon \in \{c, \bar{c}\}, \\
&\dot{i}^\epsilon(t) = \beta\mu s^\epsilon(t) i(t) - (\mu\gamma^a + (1-\mu)(\gamma^\epsilon + \nu^\epsilon)) i^\epsilon(t) \text{ for } \epsilon \in \{c, \bar{c}\}, \\
&i(t) = i^c(t) + i^{\bar{c}}(t), \\
&\dot{p}(t) = -p(t)(1 - p(t))\beta\mu i(t),
\end{aligned} \tag{1.11}$$

and $H(t) = \dfrac{1 - p(t)}{p(t)} \displaystyle\int_t^T e^{-r(u-t)} \beta\mu i(u) \frac{p(u)}{1 - p(u)} du.$

Proof. (1) We work towards a contradiction. Consider a symmetric equilibrium where all individuals play some strategy $\hat{k}$. Plugging $k_i(t) = \hat{k}(t)$ into the law of motion of individual beliefs, we obtain $p_i(t) = p(t)$ for every i. By Proposition 1, the best response of individual i at time t thus depends on the sign of the expression

$$Z_i(t) := p(t)\beta\bar{k}_I(t) i(t)(\psi_i(t) - v_I^{\epsilon_i}) - c_H.$$

Since $\hat{k}(t) = 0$ cannot be a mutual best response, in a symmetric equilibrium, either $\hat{k}(t) \in (0,1)$, i.e., $Z_i(t) = 0$ for every i, or $\hat{k}(t) = 1$, i.e, $Z_i(t) < 0$ for every i. If $Z_i(t) = 0$ on some interval $[t', t'']$, then

$$\psi_i(t) = v_I^{\epsilon_i} + \frac{c_H}{p(t)\beta\bar{k}_I(t)i(t)} \; \forall \; t \in [t', t''] . \tag{1.12}$$

This implies that for any i and j and every $t \in [t', t'']$, $\psi_i(t) - v_I^{\epsilon_i} = \psi_j(t) - v_I^{\epsilon_j}$ and $\psi_i'(t) = \psi_j'(t)$. Plugging this into the Euler condition in Proposition 1, we obtain $\psi_i(t) = \psi_j(t)$, which implies $v_I^{\epsilon_i} = v_I^{\epsilon_j}$ by (1.12). This proves that two individuals with different health condition cannot play the same interior strategy. It follows that, in a symmetric equilibrium, individuals play $k(t) = 1$ for almost every $t \in [0, T]$.

(2) Consider the no-confinement strategy profile where $k_i(t) = 1 \; \forall \; i, \; t$. Since individuals self-isolate when they have symptoms, only susceptible and infected, asymptomatic individuals play 1 at time t. As a result, $\bar{k}_S(t) = 1$ and $\bar{k}_I(t) = \mu$, which, once plugged into the equations governing the population dynamics, yields:

$$\begin{aligned}
&\dot{s}^{\epsilon}(t) = -\beta\mu s^{\epsilon}(t) i(t) \text{ for } \epsilon \in \{c, \bar{c}\}, \\
&\dot{i}^{\epsilon}(t) = \beta\mu s^{\epsilon}(t) i(t) - (\mu\gamma^a + (1-\mu)(\gamma^{\epsilon} + \nu^{\epsilon})) i^{\epsilon}(t) \text{ for } \epsilon \in \{c, \bar{c}\}, \\
&i(t) = i^c(t) + i^{\bar{c}}(t).
\end{aligned}$$

Moreover, plugging $k_i(t) = 1$ and $\bar{k}_I(t) = \mu$ into the individual belief dynamics, we obtain $p_i(t) = p(t)$ for every i, with

$$\dot{p}(t) = -p(t)(1 - p(t))\beta\mu i(t).$$

By Proposition 1, $k_i(t) = 1$ is a mutual best response in the population if and only if

$$c_H - p(t)\beta\mu i(t)(\psi_i(t) - v_I^{\epsilon_i}) > 0 \; \forall \; i, \tag{1.13}$$

where ψ_i is determined by the Euler condition:

$$\dot{\psi}_i(t) - r\psi_i(t) = \beta\mu i(t)(\psi_i(t) - v_I^{\epsilon_i}). \tag{1.14}$$

Integrating (1.14) between t and T and using the terminal condition $\psi_i(T) = 0$, we obtain:

$$\psi_i(t) = v_I^{\epsilon_i} \underbrace{\frac{1 - p(t)}{p(t)} \int_t^T e^{-r(u-t)} \beta\mu i(u) \frac{p(u)}{1 - p(u)} du}_{:= H(t)} .$$

The best-response condition (1.13) is rewritten:

$$c_H - p(t)\beta\mu i(t) v_I^{\epsilon_i}(H(t)-1) > 0 \; \forall \; i.$$

As $v_I^c < v_I^{\bar{c}} < 0$, the latter condition is satisfied if and only if it is satisfied for $\epsilon_i = c$. This proves the result. □

The next proposition gives conditions under which only individuals with co-morbidities self-isolate in equilibrium.

Proposition 6. *The game has an equilibrium where $k_i(t) = \mathbb{1}_{\epsilon_i=\bar{c}} \; \forall \; t \in [0,T]$ if and only if*

$$p^{\bar{c}}(t) v_I^{\bar{c}}(H(t)-1) < \frac{c_H}{\beta\mu i^{\bar{c}}(t)} < (1-\mu)(-\frac{c_H}{r}(1-e^{-r(T-t)}) - v_I^c) \; \forall \; t \in [0,T],$$

where $p^{\bar{c}}$ and $i^{\bar{c}}$ are defined by the system of equations:

$$\begin{cases} p^{\bar{c}}(0) = 1-\mu, \; s^{\bar{c}}(0) = 1 - i^{\bar{c}}(0) = s_0^{\bar{c}} \text{ and, } \forall \; t \in [0,T], \\ \dot{s}^{\bar{c}}(t) = -\beta\mu s^{\bar{c}}(t) i^{\bar{c}}(t), \\ \dot{i}^{\bar{c}}(t) = -\dot{s}^{\bar{c}}(t) - (\mu\gamma^a + (1-\mu)(\gamma^{\bar{c}} + \nu^{\bar{c}})) i^{\bar{c}}(t), \\ \dot{p}^{\bar{c}}(t) = -p^{\bar{c}}(t)(1-p^{\bar{c}}(t))\beta\mu i^{\bar{c}}(t), \end{cases}$$

and $H(t) = \dfrac{1-p^{\bar{c}}(t)}{p^{\bar{c}}(t)} \displaystyle\int_t^T e^{-r(u-t)} \beta\mu i^{\bar{c}}(u) \frac{p^{\bar{c}}(u)}{1-p^{\bar{c}}(u)} du.$

Proof of Proposition 6

Consider the strategy profile where $k_i(t) = \mathbb{1}_{\epsilon_i=\bar{c}}$ for every $t \in [0,T]$. Given this strategy profile, $\bar{k}_I(t) i(t) = \mu i^{\bar{c}}(t)$, $\bar{k}_{S^c}(t) = 0$ and $\bar{k}_{S^{\bar{c}}}(t) = 1$, thus the population of individuals without co-morbidities evolves as follows:

$$\begin{aligned} \dot{s}^{\bar{c}}(t) &= -\beta\mu s^{\bar{c}}(t) i^{\bar{c}}(t), \\ \dot{i}^{\bar{c}}(t) &= \beta\mu s^{\bar{c}}(t) i^{\bar{c}}(t) - (\mu\gamma^a + (1-\mu)(\gamma^{\bar{c}} + \nu^{\bar{c}})) i^{\bar{c}}(t). \end{aligned}$$

Moreover, the belief of every individual i such that $\epsilon_i = \bar{c}$ follows:

$$\dot{p}^{\bar{c}}(t) = -p^{\bar{c}}(t)(1-p^{\bar{c}}(t))\beta\mu i^{\bar{c}}(t).$$

By Proposition 1, playing $k_i(t) = 1$ is thus a best response to $i^{\bar{c}}(t)$ for an individual i with $\epsilon_i = \bar{c}$ if and only if

$$c_H - p^{\bar{c}}(t)\beta\mu i^{\bar{c}}(t)(\psi_{\bar{c}}(t) - v_I^{\bar{c}}) > 0 \; \forall \; t \in [0, T], \tag{1.15}$$

where $\psi_{\bar{c}}$ is determined at each t by the Euler condition:

$$\dot{\psi_{\bar{c}}}(t) - r\psi_{\bar{c}}(t) = \beta\mu i^{\bar{c}}(t)(\psi_{\bar{c}}(t) - v_I^{\bar{c}}). \tag{1.16}$$

Integrating (1.16) between t and T and using the terminal condition $\psi_{\bar{c}}(T) = 0$, we obtain:

$$\psi_{\bar{c}}(t) = v_I^{\bar{c}} \underbrace{\frac{1 - p^{\bar{c}}(t)}{p^{\bar{c}}(t)} \int_t^T e^{-r(u-t)} \beta\mu i^{\bar{c}}(u) \frac{p^{\bar{c}}(u)}{1 - p^{\bar{c}}(u)} du}_{:=H(t)}.$$

The best-response condition (1.15) is thus rewritten:

$$\frac{c_H}{\beta\mu i^{\bar{c}}(t)} > p(t) v_I^{\bar{c}} (H(t) - 1) \; \forall \; t \in [0, T].$$

As individuals with co-morbidities never get infected, they hold belief $1 - \mu$ at each date. By Proposition 1, playing $k_i(t) = 0$ is a best response to $i^{\bar{c}}(t)$ for an individual i with $\epsilon_i = c$ if and only if

$$c_H - (1 - \mu)\beta\mu i^{\bar{c}}(t)(\psi_c(t) - v_I^c) < 0 \; \forall \; t \in [0, T], \tag{1.17}$$

where ψ_c is determined at each t by the Euler condition:

$$\psi_c'(t) - r\psi_c(t) = c_H. \tag{1.18}$$

Integrating (1.18) between t and T and using the terminal condition $\psi_c(T) = 0$, we obtain:

$$\psi_c(t) = -\frac{c_H}{r}(1 - e^{-r(T-t)}).$$

The best-response condition (1.17) is thus rewritten:

$$\frac{c_H}{\beta\mu i^{\bar{c}}(t)} < (1 - \mu)(-\frac{c_H}{r}(1 - e^{-r(T-t)}) - v_I^c) \; \forall \; t \in [0, T].$$

□

1.5.3 Sensitivity analysis

Because epidemiological parameter measurement (β, γ^a, R_0 and μ) is sensitive to the context, it is natural to ask whether the main insights of the baseline simulation are sensitive to these measures. In this section, we conduct a sensitivity analysis in which we consider other couples (R_0,μ). The first one, our upper bound, is the one of Acemoglu et al. (2021): (2.14, 40%). The second one, our lower bound, are the values observed by Mizumoto et al. (2020) and Sheng Zhang et al. (2020) on the Diamond Princess: (2.28, 17.9%). In the rest of the section, we refer to the *set of values A* for the values used in Acemoglu et al. (2020) and to the *set of values DP* for the values observed on the Diamond Princess. Below we explain the context of study for each set of values.

Set of values *A*: Acemoglu et al. (2021) have proposed a set of parameters to describe the Covid-19 infection based on the report of N. Ferguson et al. (2020). These results, obtained in mid-March 2020 with very preliminary data, have since been strongly criticized for the pessimistic nature of their estimates. However, several governments (including U.K. and Canada) have based their lockdown decisions on these estimates, hence we have chosen to use them as an upper bound.

Set of values *DP*: In February 2020, at the very start of the pandemic, the Diamond Princess cruise ship, following the diagnosis of 10 of its passengers with COVID-19, was quarantined. The 3,711 passengers and crew were tested and at least 712 of them were diagnosed positive for Covid-19 – of this number 14 have died. This natural experiment in a small environment where the population density is high, offered a unique opportunity for researchers to study the dynamics of the infection and to determine its key values. Mizumoto et al. (2020) determined, using statistical analysis adjusted for infection delay, that the proportion of asymptomatic individuals aboard the Diamond Princess as of February 20, 2020 was 17.9%. However, they did not estimated the epidemiological parameters. We therefore turned to Sheng Zhang et al. (2020). They estimated the value of R_0 for the Diamond Princess's crew members and passengers to be $R_0 = 2.28$, using the maximum likelihood method and assuming $\gamma^a = 1/7.5$.

As a preliminary, we have checked that the interior strategy profile is an equilibrium with the set of values A and DP. We first simulate the dynamics of the epidemic with each set of values. We observe that the fraction of infected, the fraction of time spent outside, the effective reproduction number and the fraction of deaths of the baseline simulation is framed between the two alternative set of values, and that the curves have the same shape (see Figure 1.11, Figure 1.12, Figure 1.13 and Figure 1.14). As R_0 is greater with the set $\boldsymbol{A}$ than with the set $\boldsymbol{DP}$, individuals self-isolate more with the former set than in the later. However, in all cases, individuals drastically reduce their contacts after the announcement; when the spread of the epidemic is under control, they gradually increase the time spent outside to a plateau, which maintains the effective reproduction number close to 1, thus containing the spread of infection.

Next, we simulate our policy analysis with the two alternative set of values and obtain the same qualitative results:

- Delaying the epidemic announcement accelerates the epidemic (see Figure 1.15) and increases the number of deaths (see Figure 1.17). This is because individuals drastically self-isolate after the announcement, then gradually reduce their level of self-isolation to a level maintaining the effective reproduction number approximately equal to 1 (see Figure 1.16).

- We multiply the value of $\beta\mu$ by 0.75, 1 and 1.25 for each set of values (which yields $\beta\mu \in \{0.1005, 0.134, 0.1667\}$ in set $\boldsymbol{A}$ and $\beta\mu \in \{0.228, 0.304, 0.38\}$ in set $\boldsymbol{DP}$). We find also find that decreasing $\beta\mu$ induces less self-isolation and reduces the number of deaths (see Figure 1.19 and Figure 1.20).

- We multiply the value of γ^a by 1.1 for each set of values and the value of ν by 0.5 in each set of values. While the dynamics of the infection follow a very similar trajectory in the two scenarios, the infection is stronger in set $\boldsymbol{A}$ than in set $\boldsymbol{DP}$ (see Figure 1.21). We also find that a better health system induces less self-isolation (Figure 1.22) but reduces the number of deaths (see Figure 1.23).

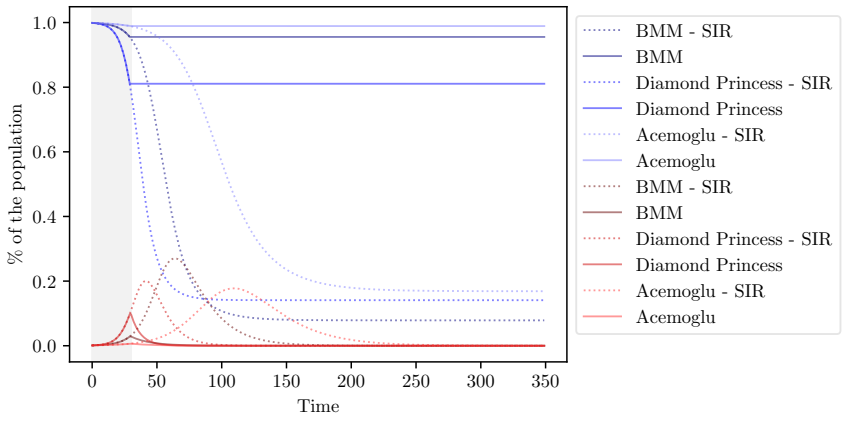

Figure 1.11: Sensitivity analysis: fraction of infected.

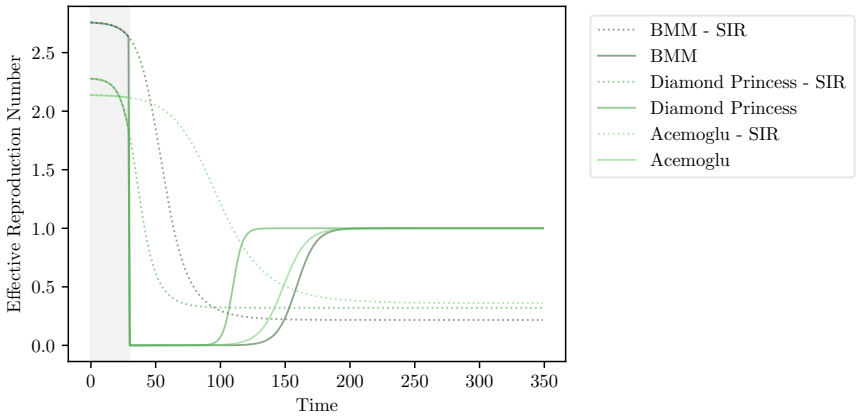

Figure 1.12: Sensitivity analysis: Effective Reproduction Number.

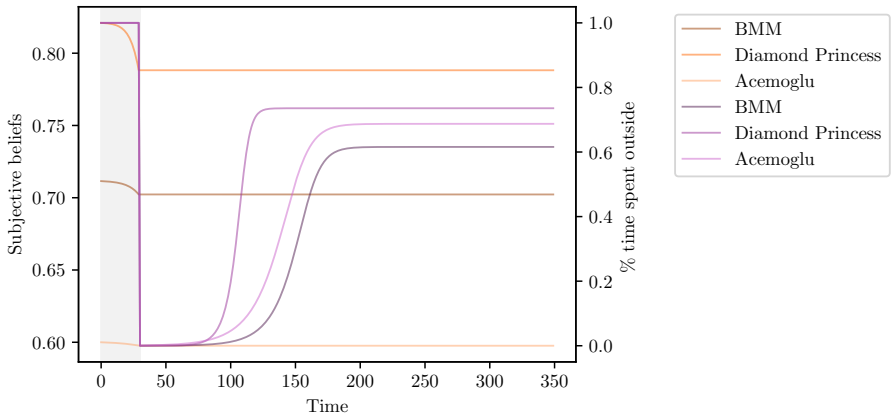

Figure 1.13: Sensitivity analysis: beliefs and behaviors.

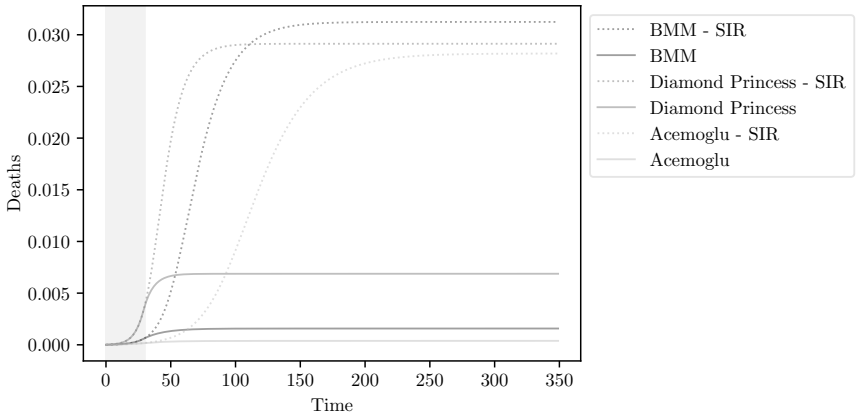

Figure 1.14: Sensitivity analysis: deaths.

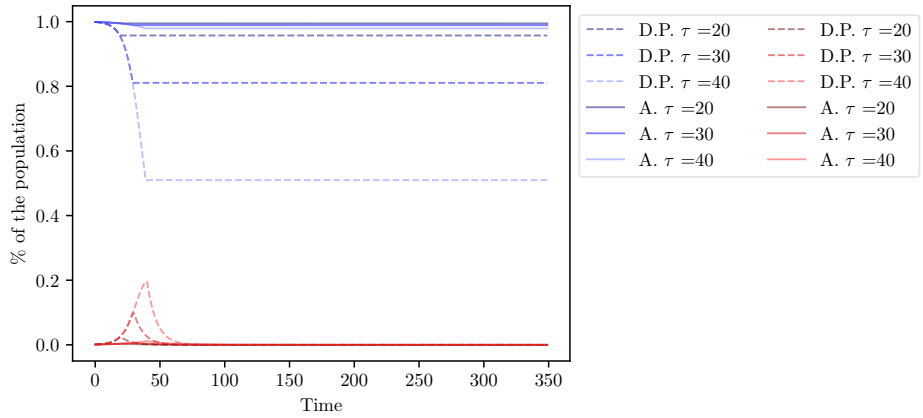

Figure 1.15: Sensitivity analysis: effect of a variation of τ on the fraction of infected.

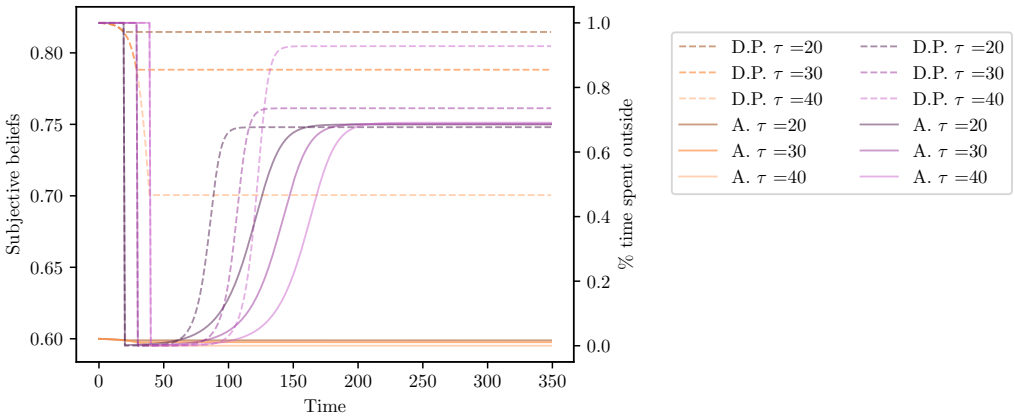

Figure 1.16: Sensitivity analysis: effect of a variation of τ on behaviors and beliefs.

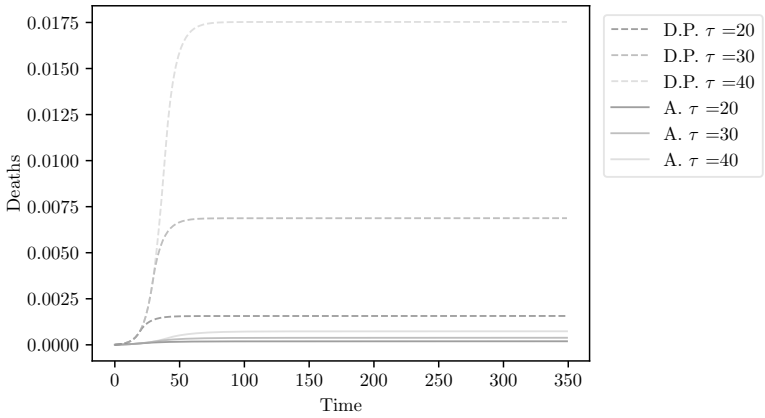

Figure 1.17: Sensitivity analysis: effect of a variation of τ on deaths.

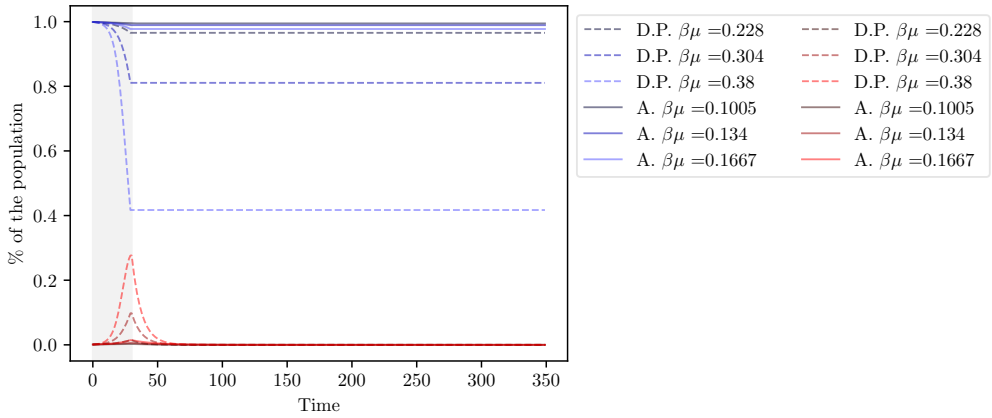

Figure 1.18: Sensitivity analysis: effect of a variation of $\beta\mu$ on the fraction of infected.

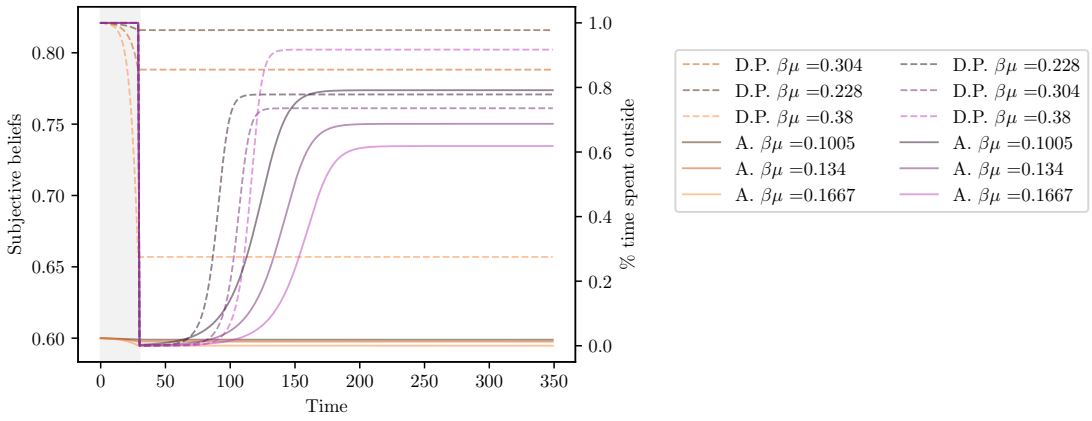

Figure 1.19: Sensitivity analysis: effect of a variation of $\beta\mu$ on beliefs and behaviors.

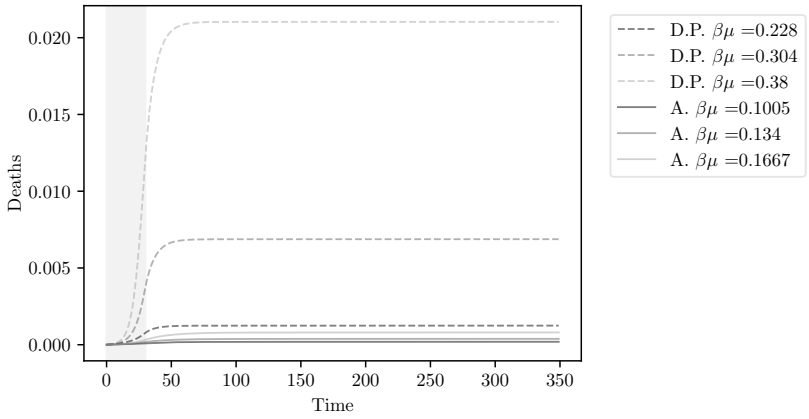

Figure 1.20: Sensitivity analysis: effect of a variation of $\beta\mu$ on deaths.

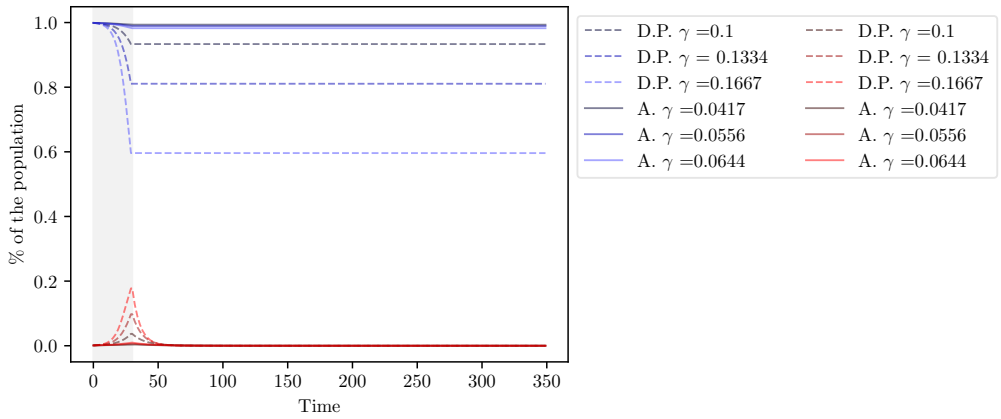

Figure 1.21: Sensitivity analysis: effect of a variation of γ on the the fraction of infected.

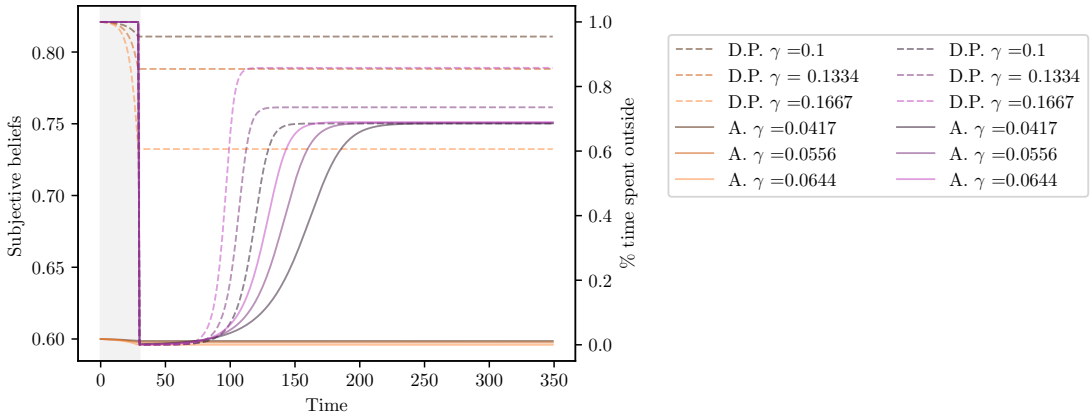

Figure 1.22: Sensitivity analysis: effect of a variation of γ on beliefs and behaviors.

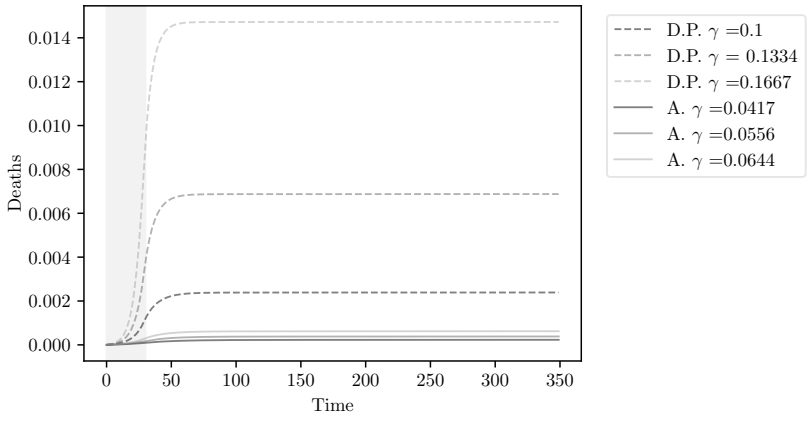

Figure 1.23: Sensitivity analysis: effect of a variation of γ on deaths.

Chapter 2

Self-Isolation Under Uncertainty

Dominique Baril-Tremblay[1], Chantal Marlats[2] and Lucie Ménager[3]

Abstract[4]

We analyze an epidemiological model where forward-looking individuals trade off the costs and benefits of self-isolation while being uncertain about the dynamics of the epidemic. We characterize the interior symmetric equilibrium and we identify necessary conditions of the optimal solution. We calibrate our model to the COVID-19 pandemic and simulate the dynamics of the epidemic under various scenarios to illustrate the impact of uncertainty on self-isolation behaviors. We show that uncertainty may cause a second wave of infection and that the average level of social activity can decrease with uncertainty. Finally, uncertainty about the epidemic dynamics may be welfare improving, both in terms of fraction of deaths and average payoff.

Keywords: SIR model; Self-isolation; Uncertainty; COVID-19 epidemic.

JEL codes: C73; D84, I12.

[1]Université Paris 1 - Panthéon Sorbonne, doumbaril@gmail.com.

[2]LEMMA, Université Paris 2 Panthéon-Assas, chantal.marlats@u-paris2.fr.

[3]LEMMA, Université Paris 2 Panthéon-Assas, lucie.menager@u-paris2.fr.

[4]This research was supported by the French National Research Agency (ANR-17-CE38-0005-01) and by the Labex MME-DII (ANR11-LBX-0023-01).

2.1 Introduction

It is now well-documented that the dynamics of an epidemic depend on the behavior of the population in terms of social distancing and application of prophylactic measures[5]. Conversely, many papers have documented that individuals adapt their behaviors to epidemic variables (incidence rate, level of hospitalizations, etc)[6]. For example, Farboodi, Jarosch, and Shimer (2021) show that attendance in public places declined as soon as the WHO announced the existence of a pandemic in March 2020, thus before the implementation of lockdown and closure policies. The object of the growing *strategic epi-economic* literature is to analyze the two-sided interactions between the dynamics of epidemic and the population behavior. In this literature, individuals trade off the cost and benefit of preventive behaviors based on their assessment of the risk of coming into contact with a contagious person, which naturally depends on the prevalence rate[7]. It is assumed that individuals are able to infer this rate accurately. However, it is often the case that it is not perfectly observable, especially when a significant proportion of the population is asymptomatic. Moreover, for individuals to be able to infer it correctly, they must have detailed knowledge of the characteristics of the disease, such as contagiousness and initial prevalence rate. This assumption is difficult to defend when a new virus appears or a disease resurfaces. These situations are far from being anecdotal and recent events are full of examples: the COVID-19 and its different mutants, influenza which returns every winter in temperate zones, ebola which has reappeared several times in DRC, but also in Guinea in 2021, etc...

The contribution of this paper is to analyze an epidemiological model where forward-

[5]Delamater et al. (2019) and Britton, Ball, and Trapman (2020) show that the herd immunity level against COVID-19 is reduced when the model encompasses the possibility that some social groups of individuals are more socially active. Cowling, Chan, et al. (2009) and Aiello et al. (2010) show that masks and hand washing can reduce household transmission of respiratory infections in small areas. Cowling, Ali, et al. (2020) show that border restrictions and changes in individual behaviors are partly responsible for reduced transmission in Hong Kong in February 2020.

[6]For instance, T. J. Philipson and Posner (1993) show that the demand for measles, mumps and rubella vaccines increases when there is a large increase in measles cases in a community. Ahituv, Hotz, and T. Philipson (1996) show that the demand for condoms increases in regions where HIV is prevalent.

[7]The prevalence rate is the fraction of infected individuals in the population

looking individuals are uncertain about certain characteristics of the epidemic and are therefore unable to infer the fraction of the population that is infected. Individuals form beliefs about the epidemic, that they continuously update on the basis of how much they might have been exposed to the virus. Simultaneously, they decide their degree of exposure to the virus by trading off the costs and benefits of self-isolation on the basis of their subjective beliefs.

Precisely, we amend the classical Susceptible-Infected-Recovered (SIR hereafter) model of Kermack and McKendrick (1927). In its classical version, the SIR model divides an homogeneous population into three groups: {susceptible}, {infected} and {recovered}, with individuals transiting from one group to another one at given, exogenous rates that depend on the size of each group. As in Baril-Tremblay, Marlats, and Ménager (2021), we consider two possible types of individuals in the population: *symptomatic* and *asymptomatic*. Individuals of the symptomatic type experience the symptoms of the disease immediately after being infected. In contrast, individuals of the *asymptomatic* type do not have symptoms. Initially, individuals do not know their type. We depart from Baril-Tremblay, Marlats, and Ménager (2021) by assuming that individuals are uncertain about some parameter determining the dynamics of the prevalence rate. Thus, the agents, who do not observe this rate, are aware that different levels of prevalence are possible but they do not know it exactly.

Individuals influence the transition rate from {susceptible} to {infected} by self-isolating, i.e., strategically reducing social activity. How does an individual who never had symptoms tradeoff the cost and the benefit of self-isolation? On the benefits side, self-isolation prevents one from being infected by reducing the likelihood of coming into contact with a contagious person. The costs side is more subtle. Indeed, an individual who does not get symptoms while having social activity becomes more optimistic both on the prevalence rate and on being the asymptomatic type. The costs of self-isolation are thus twofold: there is the direct cost of self-isolate (boredom, opportunity cost of not working, or of working in poorer conditions, lack of physical activity, etc..) and the opportunity cost of not learning about one's type and about the prevalence rate.

We characterize the symmetric equilibrium in which individuals partially self-isolate.

At this equilibrium, the level of social activity is equal to the ratio between, on the one hand, the direct cost of self-isolation, and on the other hand, the expected opportunity cost of the social activity, which is equal to the informational benefit minus the expected welfare loss in case of infection.

We calibrate our model to the COVID-19 and we simulate the dynamics of the epidemic when the population is aware of two possible epidemics with different initial penetration rates. This parameter is one of the elements determining the dynamics of the prevalence rate. Thus, the agents, who have uncertainty about this parameter, are aware that different levels of prevalence are possible but they do not know it exactly. The impact of uncertainty is ambiguous. For any prior belief, individuals self-isolate drastically after the epidemic announcement, which results in a drop in the fraction of infected; then, they gradually increase the level of social interactions. The rate at which social activity increases varies with the prior that the epidemic has a low initial penetration rate. When the prior increases, individuals self-isolate less at the beginning of the epidemic and more at the end. One reason for this reversal is that individuals believe they have been less exposed to the disease at the beginning of the epidemic when the initial penetration rate is low. As a result, they are less confident in being immune to the disease, and self-isolate more at the end of the outbreak. In the more aggressive epidemic, for any prior, individuals self-isolate enough to maintain the effective reproduction number below the value that accelerates the epidemic, thus the epidemic curve continuously decreases until the arrival of the vaccine. In the less aggressive epidemic, when the initial prior is small there is a second wave of infections with a second peak that is higher the more erroneous the beliefs are. This second wave arises because, for these priors, individuals choose a higher level of social activity from some date on. This leads to an inadequate reaction to the true level of the epidemic that may induce an effective rise of the total fraction of infected individuals. Therefore, the social value of information depends on the initial state of the epidemic. We find that transparency is welfare improving only in the less aggressive epidemic, both in terms of fraction of deaths and payoffs. For all the priors we consider, the ex-ante fraction of deaths is smaller when individuals are uncertain about the state than

without uncertainty, suggesting that opacity can prevent deaths. In terms of payoffs, the information value is negative when the population is relatively confident that the epidemic is initially aggressive.

Related literature. Many papers in economics have documented that individuals adapt their behavior when facing a risk of infection. Before COVID-19, concern was mainly on AIDS, thus papers analyzed steady-states of Susceptible-Infected models (see for instance Kremer (1996), T. J. Philipson and Posner (1993) and Toxvaerd (2019)).

To analyze an infectious disease like COVID-19, recent papers are based on SIR models in continuous time with either forward-looking or myopic individuals. Carnehl, Fukuda, and Kos (2023) analyze a SIR model with infinite horizon and myopic agents. The infection risk is linear in the average level of social interaction and the isolation cost are quadratic. They show that there exists a unique symmetric equilibrium and that a second wave is impossible. Surprisingly, if the initial faction of infected individuals is sufficiently small, an epidemic may not start if the virus is very contagious. In a companion paper (Carnehl, Fukuda, and Kos (2022)), they assume non stationary isolation cost to capture the lockdown fatigue phenomenon, and give sufficient conditions for the existence of a second wave. Dasaratha (2020) assumes that infected individuals do not observe their health status but know when they are recovered. The infection risk is a quadratic function of the average level of social activity. In the main part of the paper, agents are supposed to be myopic. The author shows that, because agents adapt their behavior, an exogenous marginal increase of the infected individuals can have a negative effect on the number of new cases. Phelan and Toda (2022) analyze a model in which infected individuals can be asymptomatic with a certain probability. The population is finite and agents ignore the effect of their choice on the infection rate. A vaccine arrives at some random date. They show that there is a unique value function that satisfies the Bellman Equation and that there exists a Markovian equilibrium. They derive the optimal lockdown policy. Toxvaerd (2022) considers a model in which players are can be of two types: asymptomatic and symptomatic. An agent's type determines whether he will develop symptoms or not when infected. When an individual is infected and develops symptoms, he chooses the maximal social interaction level. When types

are not observable, individuals can infer their type only when they develop symptoms. The author shows that when types are not observable, the total number of infection cases is higher but the number of infected with symptoms is lower. Consequently, the welfare is higher when types are not observable. A comparison between the effect of infection and the immunity tests on the dynamic of the epidemic reveals that, except in the early stages, the latter have a higher private value. Finally, our model generalizes Baril-Tremblay, Marlats, and Ménager (2021) by introducing uncertainty. In both papers, we assume that each agent can be of two types, as in Matthies and Toxvaerd (2022), the infection risk is a quadratic function of the average level of social activity, the self-isolation costs are linear and the horizon is finite (the underlying assumption is that a vaccine is available after some date).

Several papers compare the competitive equilibrium with the confinement effectiveness. Farboodi, Jarosch, and Shimer (2021) assume quadratic matching and imperfect observation of the health status. They compare the dynamics obtained at the decentralized equilibrium with the one obtained under the optimal policy and show that the competitive equilibrium is suboptimal. Brotherhood et al. (2020) assume that agents are heterogenous with respect to age and the older people are more likely to die. Rachel et al. (2020) considers a lockdown problem and provides analytical results.

Several papers put aside the question of individuals' responses to an epidemic risk and focus exclusively on optimal mitigation policies by assuming that a planner control the transmission rate (see for instance Kruse and Strack (2020), Alvarez, Argente, and Lippi (2020) ...). Acemoglu et al. (2021) assume that agents are heterogenous. Giannitsarou, Kissler, and Toxvaerd (2021) analyze the dynamics of epidemics under waning immunity.

It is well known that in SIR models without decentralized self-isolation choice and policy intervention, a second wave cannot emerge in a closed population. In Carnehl, Fukuda, and Kos (2022) it arrises because the self-isolation costs are not stationary. Farboodi, Jarosch, and Shimer (2021) and Rachel et al. (2020) show that a second wave can occur after a lockdown. Giannitsarou, Kissler, and Toxvaerd (2021) show that waning immunity induces oscillations. In our paper, the second wave is not due

to non stationary self-isolation costs, waning immunity or lockdown release but only to uncertainty.

The remainder of this paper is organized as follows. Section 2 sets up the model. In Section 3, we solve the best-response problem of a player, analyze some properties of the equilibrium and characterize the symmetric equilibrium. In Section 4, we calibrate our model to fit the COVID-19 pandemic, we simulate the dynamics of the epidemic in equilibrium and investigate the impact of uncertainty. In Section 5, we analyze the problem of a government who must decide upon the optimal isolation policy. Proofs are gathered in the Appendix.

2.2 An epidemiological model with uncertainty

The population. Time $t \in [0, +\infty)$ is continuous and discounted at a common rate $r > 0$. There is a rampant disease in the population, against which a vaccine will arrive at time $T > 0$. The population is a continuum of individuals $j \in [0, 1]$ who must continuously choose a level of *social activity*, which can be interpreted as the fraction of their time they do not spend at home. An individual who stays home is protected from infection, while an individual who goes out may be contaminated by contact with an infected individual.

Infection may be totally asymptomatic. Whether an individual develops symptoms or not when she is infected is an idiosyncratic characteristic described by her *type*. There are two types of individuals in the population: Individuals of type θ_s –the *symptomatic type*– who experience the symptoms of the disease immediately after being infected, and individuals of type θ_a –the *asymptomatic type*– who do not have symptoms in case of infection, thus never realize when they have been infected. Individuals do not know their type unless they are of type θ_s and catch the disease. There is a proportion $\alpha \in (0, 1)$ of asymptomatic types in the population. The infection period ends by recovery at rate γ_a for asymptomatic types, and by either recovery or death for symptomatic types, at rates γ_s and ν. However, infection stops for both types of individuals at the same rate, i.e., $\gamma_a = \nu + \gamma_s$[8]. Therefore, at each time there is a proportion α of infected individuals

[8]This is a simplifying technical assumption that can be released by adding a compartment to the model as

who have no symptoms. Finally, individuals are contagious as long as they are infected, and are immune to the disease after recovering.

We assume that an individual who gets symptoms self-isolates immediately until the end of the symptoms, either to protect others, or simply because she is too sick to go out. Therefore, a strategy for player j is a measurable function $k_j : \mathbb{R}_+ \to [0,1]$, with the interpretation that $k_j(t)$ is the proportion of time spent outside at time t, absent symptoms by time t[9]. Therefore, the disease is spread in the population by asymptomatic infected individuals.

The epidemic. An epidemic is characterized by its initial penetration level in the population $(\bar{s}, \bar{a}, \bar{r})$, where $\bar{s} \in [0,1]$ is the proportion of individuals who are not immune to the disease at time 0, $\bar{a} \in [0,1]$ is the proportion of individuals infected without symptoms at time 0 and $\bar{r} \in [0,1]$ the proportion of individuals who already recovered from the disease at time 0 and are now immune to it. As the share of asymptomatic types in the general population is α, the proportion of individuals infected with symptoms at time 0 is $\bar{i} = \frac{1-\alpha}{\alpha}$, and the proportion of dead individuals is $\bar{d} = 1 - \bar{s} - \bar{a} - \bar{r} - \bar{i} \in [0,1]$[10]. We identify an epidemic ω with the tuple $\{\bar{s}, \bar{a}, \bar{r}\}$ and we denote by Ω the finite set of possible epidemics.

Dynamics of the epidemic. To model the spread of epidemic ω, we use the classical Susceptible-Infected-Recovered (SIR) model by Kermack and McKendrick (1927), that we amend to introduce individual behaviors and uncertainty.

At each time t, the population is divided into five groups: the group of *susceptible* individuals who have never been infected by the disease, denoted by $S(t \mid \omega)$ and of size $s(t \mid \omega) := \int_{j \in S(t|\omega)} dj$; the group of *symptomatic infected* individuals who are infected with symptoms at time t, denoted by $I(t \mid \omega)$ and of size $i(t \mid \omega) := \int_{j \in I(t|\omega)} dj$; the group of *asymptomatic infected* individuals who are infected without symptoms at

in the previous chapter.

[9]The usual assumption in the literature is that infected individuals chose a constant social activity level $\bar{k}$ during the symptomatic period. Assuming $\bar{k} = 0$ is without loss of generality for the purpose of this paper and lightens the analytic expressions.

[10]By the law of large numbers, the initial proportion of infected individuals with symptoms represents a share $1 - \alpha$ of the population of infected people, thus $\bar{i} = (1 - \alpha)(\bar{i} + \bar{a})$.

time t, denoted by $A(t \mid \omega)$ and of size $a(t \mid \omega) := \int_{j \in A(t|\omega)} dj$; the group of *recovered* individuals who already healed from the disease (with or without symptoms), denoted by $R(t \mid \omega)$ and of size $r(t \mid \omega) := \int_{j \in R(t|\omega)} dj$ and the group of *dead* individuals, denoted by $D(t \mid \omega)$ and of size $d(t \mid \omega) = 1 - s(t \mid \omega) - i(t \mid \omega) - a(t \mid \omega) - r(t \mid \omega)$.

The evolution of the epidemic penetration depends on the behavior of the population. Here we explain how by using a probabilistic argument. What is the mass of individuals who become infected in the interval $[t, t+dt)$, in expectation? Fix some date t, some strategy profile $\mathbf{k} := (k_j)_{j \in [0,1]}$ and some small $dt > 0$. The probability that a susceptible individual $s \in S(t \mid \omega)$ meets and is infected by some infected asymptomatic individual $a \in A(t \mid \omega)$ during the interval $[t, t + dt)$ is $k_s(t)k_a(t)\beta dt$. Therefore, the probability that s becomes infected in $[t, t + dt)$ is $k_s(t) \left(\int_{j \in A(t|\omega)} k_j(t) dj \right) \beta dt$, and the expected mass of newly infected individuals is $\int_{s \in S(t|\omega)} \left(k_s(t) \int_{a \in A(t|\omega)} k_a(t) da \beta dt \right) ds$. Therefore, the fraction of susceptible individuals evolves as follows:[11]

$$\dot{s}(t \mid \omega) = -\beta \bar{k}_S(t \mid \omega) s(t \mid \omega) \bar{k}_A(t \mid \omega) a(t \mid \omega), \tag{2.1}$$

where $\bar{k}_S(t \mid \omega) = \frac{1}{s(t|\omega)} \int_{j \in S(t|\omega)} k_j(t) dj$ and $\bar{k}_A(t \mid \omega) = \frac{1}{a(t|\omega)} \int_{j \in A(t|\omega)} k_j(t) dj$ denote the average behavior of susceptible and asymptomatic infected individuals, respectively. At each time t, the fraction of newly infected $-\dot{s}(t \mid \omega)$ is split between $A(t \mid \omega)$ and $I(t \mid \omega)$, in proportions α and $1 - \alpha$, respectively. The other groups of the population thus evolve as follows:

$$\begin{aligned}
\dot{a}(t \mid \omega) &= -\alpha \dot{s}(t \mid \omega) - \gamma_a a(t \mid \omega), && (2.2)\\
\dot{i}(t \mid \omega) &= -(1 - \alpha) \dot{s}(t \mid \omega) - (\gamma_s + \nu) i(t \mid \omega), && (2.3)\\
\dot{r}(t \mid \omega) &= \gamma_a a(t \mid \omega) + \gamma_s i(t \mid \omega), && (2.4)\\
\dot{d}(t \mid \omega) &= \nu i(t \mid \omega), && (2.5)
\end{aligned}$$

with $s(0 \mid \omega) = \bar{s}$, $i(0 \mid \omega) = \bar{i}$, $a(0 \mid \omega) = \bar{a}$, $r(0 \mid \omega) = \bar{r}$ and $d(0 \mid \omega) = \bar{d}$. The assumptions $\gamma_a = \nu + \gamma_s$ and $\bar{i} = \frac{1-\alpha}{\alpha} \bar{a}$ guarantee that $i(t \mid \omega) = \frac{1-\alpha}{\alpha} a(t \mid \omega)$ for every t.

[11] As $s(t + dt \mid \omega) - s(t \mid \omega) = -\int_{j \in S(t|\omega)} k_j(t) dj \times \int_{j \in A(t|\omega)} k_j(t) dj \times \beta dt$. The result follows from the fact that $\dot{s}(t \mid \omega) = \lim_{dt \to 0} \frac{s(t+dt|\omega) - s(t|\omega)}{dt}$.

Uncertainty and beliefs. At time 0, individuals learn the existence of an epidemic, but do not know their own type nor which epidemic they are facing. Moreover, they never observe the current epidemic penetration, hence the only additional information they have at time t is whether they had or did not have symptoms before t.[12]

We denote by $p_j(t) : \Omega \to [0,1]$ the subjective belief of individual j at time t that she is the symptomatic type, with the interpretation that $p_j(t \mid \omega)$ is the probability of player j being type θ_s conditionally on the epidemic being ω and having experienced no symptom by time t. Individual j continuously updates her belief on the basis of whether she is having symptoms, conditionally on the strategy profile of the population and the dynamic system (2.1) and (2.2). Precisely, the law of motion of the subjective belief of individual j is[13]

$$\dot{p}_j(t \mid \omega) = -p_j(t \mid \omega)(1-p_j(t \mid \omega))k_j(t)\beta\bar{k}_A(t \mid \omega)a(t \mid \omega), \text{ with } p_j(0 \mid \omega) = 1-\alpha. \quad (2.6)$$

Moreover, we denote by $\mu_j(t) : \Omega \to [0,1]$ the subjective belief of individual j at time t over Ω, with the interpretation that $\mu_j(t,\omega)$ is the probability at time t for individual j that the epidemic is ω, conditional on having experienced no symptom by time t. At time 0, individuals hold the common belief $\mu^0 : \Omega \to [0,1]$. The subjective belief that the epidemic is ω depends on the subjective belief $p_j(t)$ as follows:[14]

$$\mu_j(t,\omega) = \frac{\mu^0(\omega)/(1-p_j(t \mid \omega))}{\sum_{\omega' \in \Omega} \mu^0(\omega')/(1-p_j(t \mid \omega'))}. \quad (2.7)$$

Payoffs. Staying home prevents one from being infected, but comes at a cost (boredom, opportunity cost of not working or working in poorer conditions, lack of physical activity, etc.). Being infected is also costly for individuals of the symptomatic type because they suffer from the symptoms, and, in the worst case, die from the disease. Therefore, at each time t, individuals tradeoff the cost of self-isolating and the expected benefit of

[12] In Section we describe a more general model where uncertainty pertains also to the epidemiological parameters β, α, γ^s, γ^a, ν. The analysis is similar with heavier notation.

[13] Fix $\omega \in \Omega$ and a strategy profile $\mathbf{k}$. A susceptible individual j develops symptoms in $[t, t+dt)$ with probability 0 when she is of type θ_a; when she is of type θ_s, she develops symptoms if she meets and is infected by some asymptomatic individual, which occurs with instantaneous probability $k_j(t)\bar{k}_A(t \mid \omega)a(t \mid \omega) \times \beta dt$. By Bayes' rule, the law of motion of the subjective belief of individual j is thus (2.6).

[14] See Lemma 5 in the Appendix.

having no symptoms. We denote by c_S the flow cost of self-isolation, by c_I the flow cost of having symptoms and by c_D the flow cost of being dead. The flow payoff of having social activity and being healthy is normalized to 0.

Uncertainty about her type is solved for an individual the first time she has symptoms. In that event, she knows that she is the symptomatic type, thus that she will stay at home until she heals or passes away, thereby incurring a total cost of $\int_0^{\min\{\tau_H,\tau_D\}} e^{-rt}(c_S+c_I)dt$, with τ_H and τ_D standing for the random times of healing and death, respectively. If she heals from the disease (i.e., if $\tau_H < \tau_D$), she becomes immune to it, plays $k(t)=1$ forever after, thus obtains the continuation payoff 0. If she dies (i.e., if $\tau_D < \tau_H$), she incurs the flow cost c_D forever after, thus obtains the continuation payoff $-c_D/r$. Therefore, the expected continuation payoff to an individual the first time she has symptoms is:[15]

$$v_I = -E\left[\int_0^{\min\{\tau_H,\tau_D\}} e^{-rt}(c_S+c_I)dt + \frac{c_D}{r}e^{-r\tau_D}\mathbb{1}_{\tau_D<\tau_H}\right] = -\frac{1}{r+\gamma^s+\nu}(c_S+c_I+\nu\frac{c_D}{r}) \tag{2.8}$$

Let us express the payoff increment at time $t \in (0,T)$ in epidemic ω. Conditionally on having no symptoms before t, player j obtains the continuation payoff v_I if she has symptoms, which occurs if she is the symptomatic type and gets infected, thus with probability $p_j(t \mid \omega)k_j(t)\beta\bar{k}_A(t \mid \omega)a(t \mid \omega)$. She also bares the confinement cost per unit of time in self-isolation, thus $c_S(1-k_j(t))$. After getting vaccinated at time T, she has a probability 0 of developing symptoms and plays $k_j(t)=1$ for every $t \geq T$, which yields the continuation payoff 0. Finally, the subjective probability of having no symptom before $t \in [0,T]$ in epidemic ω is $1-p_j(0 \mid \omega)+p_j(0 \mid \omega)e^{-\int_0^t k_j(s)\beta\bar{k}_A(s|\omega)a(s|\omega)]ds}$, which reduces to $e^{-\int_0^t p_j(s|\omega)k_j(s)\beta\bar{k}_A(s|\omega)a(s|\omega)ds}$ by integrating (2.6). After simplifications, the discounted expected payoff conditional on the epidemic being ω is:[16]

$$v(k_j \mid \omega) = \int_0^T e^{-rt}\underbrace{e^{-\int_0^t p_j(s|\omega)k_j(s)\beta\bar{k}_A(s|\omega)a(s|\omega)ds}}_{\substack{\text{Player } j\text{'s probability to}\\ \text{have no symptom before } t.}}\underbrace{\left(p_j(t \mid \omega)k_j(t)\beta\bar{k}_A(t \mid \omega)a(t \mid \omega)v_I - c_S(1-k_j(t))\right)}_{\substack{\text{Player } j\text{'s expected payoff increment at } t \text{ con-}\\ \text{ditional on having no symptom before } t.}}dt. \tag{2.9}$$

[15] See Lemma 6 in the Appendix for the detailed calculations.

[16] See Appendix 2.5.2 for the detailed calculation.

2.3 Equilibrium analysis

Fix a strategy profile $\mathbf{k}$. Player j's best-response problem is to maximize $E_{\mu^0}[v(k_j;.)]$, where the fraction of asymptomatic infected at time t is given for each ω by the system of o.d.e. $\{(2.1), (2.2)\}$. Formally, it is the solution of the optimal control problem:

$$\begin{cases} \max\limits_{k_j \in \mathcal{K}} & E_{\mu^0}[v(k_j \mid .)] \\ \text{s.t.} & \forall\, \omega \in \Omega,\ p_j(0 \mid \omega) = 1 - \alpha \text{ and, } \forall\, t \in [0,T], \\ & \dot{p}_j(t \mid \omega) = -p_j(t \mid \omega)(1 - p_j(t \mid \omega))k_j(t)\beta \bar{k}_A(t \mid \omega)a(t \mid \omega), \end{cases}$$

which we solve in the Appendix using Pontryagin's principle. Here, we explain the intuition of the solution with a heuristic dynamic programming argument, using the time and the player's current belief of being the symptomatic type p as the state variable. At time t, the optimal social activity level of an individual maximizes the sum of her current expected payoff increment and of her discounted continuation payoff, should no symptoms occur in the interval $[t, t+dt)$. Given the strategy profile $\mathbf{k}$, the best-response payoff to a player at time t and belief p satisfies the Bellman equation

$$V(t,p) = \max_{k \in [0,1]} \left\{ \big(-(1-k)c_S + v_I P(S(t) \mid p) \big) dt + \big(1 - P(S(t) \mid p) dt\big) e^{-rdt} V(t+dt, p+dp \mid \bar{S}(t)) \right\}, \tag{2.10}$$

where $S(t)$ stands for the event "having symptoms between t and $t+dt$" and $\bar{S}(t)$ for the complementary event. By Bayes' rule, the probability of developing symptoms between t and $t+dt$ is linear in the individual's action k, with

$$P(S(t) \mid p) = k \sum_{\omega} \mu(t,\omega) p(t \mid \omega) \beta \bar{k}_A(t \mid \omega) a(t \mid \omega).$$

Moreover,

$$V(t+dt, p+dp \mid \bar{S}(t)) = V(t,p) + V_t(t,p)dt + \sum_{\omega} V_{p(t|\omega)}(t,p)\dot{p}(t \mid \omega)dt.$$

Using (2.6), eliminating terms to the order $(dt)^2$ and simplifying, we can rewrite the Bellman equation (2.10) as follows:

$$rV(t,p) = V_t(t,p) - c_S$$
$$+ \max_{k \in [0,1]} k\big(c_S - \beta \underbrace{\sum_{\omega} \mu(t,\omega) p(t \mid \omega) \bar{k}_A(t \mid \omega) a(t \mid \omega) \left(V(t,p) - v_I + \frac{1 - p(t \mid \omega)}{\mu(t,\omega)} V_{p(t|\omega)}(t,p)\right)}_{\text{expected net cost of social activity}}\big).$$

To interpret this expression, note that two things might happen for the individual at time t: either she gets symptoms, or she does not. In the first case, she incurs a payoff loss of $V(t,p) - v_I$; in the second case, she becomes more confident in being the asymptomatic type, which increases her continuation payoff by $-V_{p(t|\omega)}(t,p)$. Therefore, the marginal benefit of more social activities is the difference between the direct cost of self-isolation, c_S, and the *expected cost of social activity*, composed of

- the expected cost of the jump to v_I in case of symptoms: $\beta \sum_\omega \mu(t,\omega) p(t \mid \omega) \bar{k}_A(t \mid \omega) a(t \mid \omega)(V(t,p) - v_I)$;
- the opportunity cost in terms of payoff of not becoming more optimistic about being the asymptomatic type in the absence of symptoms: $\beta \sum_\omega p(t \mid \omega)(1 - p(t \mid \omega)) \bar{k}_A(t \mid \omega) a(t \mid \omega) V_{p(t|\omega)(t,p)}$.

The next proposition gives necessary conditions for a strategy of player j to be a best response against a strategy profile $(k_{j'})_{j' \neq j} := \mathbf{k}_{-j}$:

Proposition 7 (Best response)**.** *If k_j^* the best-response of player j against the strategy profile $\mathbf{k}_{-j}$, then there exists functions $\psi_j : \mathbb{R}_+ \times \Omega \to \mathbb{R}$ and $p_j : \mathbb{R}_+ \times \Omega \to [0,1]$, C^1 in the first argument and such that, such that, for all $t \leq T$:*

$$k_j^*(t) \begin{cases} = 1 & \text{if } \ c_S > \beta \sum_\omega \mu_j(t,\omega) p_j(t \mid \omega) \bar{k}_A(t \mid \omega) a(t \mid \omega)(\psi_j(t \mid \omega) - v_I), \\ \in [0,1] & \text{if } c_S = \beta \sum_\omega \mu_j(t,\omega) p_j(t \mid \omega) \bar{k}_A(t \mid \omega) a(t \mid \omega)(\psi_j(t \mid \omega) - v_I), \\ = 0 & \text{if } \ c_S < \beta \sum_\omega \mu_j(t,\omega) p_j(t \mid \omega) \bar{k}_A(t \mid \omega) a(t \mid \omega)(\psi_j(t \mid \omega) - v_I), \end{cases} \tag{2.11}$$

where, for all $\omega \in \Omega$,

$$\dot{\psi}_j(t \mid \omega) - r\psi_j(t \mid \omega) = k_j^*(t)\beta \bar{k}_A(t \mid \omega) a(t \mid \omega)(\psi_j(t \mid \omega) - v_I) + (1 - k_j^*(t)) c_S, \ \psi_j(T \mid \omega) = 0,$$
$$\dot{p}_j(t \mid \omega) = -p_j(t \mid \omega)(1 - p_j(t \mid \omega)) k_j^*(t) \beta \bar{k}_A(t \mid \omega) a(t \mid \omega), \ p_j(0 \mid \omega) = 1 - \alpha,$$

and $\mu_j(t,\omega)$ is defined by (2.7).

Proof. See the Appendix. □

An immediate corollary of Proposition 7 is that all equilibria feature social interaction, in the sense that, at every period, there is a mass of individuals who do not self-isolate. The reason is simple: if the rest of the population stays at home, each individual can spare the self-isolation cost c_S by going out without risking infection. Therefore, in the symmetric equilibrium, at each date individuals either partially self-isolate or do not self-isolate at all. The strategy profile $\mathbf{k}$ is said to be symmetric interior if $k_j(t) = k_{j'}(t)$ for all players j, j' and $k_j(t) \in (0,1)$ for all t. The following lemma gives necessary and sufficient conditions for a symmetric interior strategy profile to be an equilibrium.

Proposition 8 (The symmetric equilibrium)**.** *Let $\hat{\mathbf{k}}$ be the symmetric strategy profile where all individuals play $\hat{k}$ defined by*

$$\hat{k}(t) = \frac{c_S}{\beta \sum_\omega \mu(t,\omega) p(t \mid \omega) a(t \mid \omega)(\psi(t \mid \omega) - v_I)}$$

where

$$\begin{cases} \forall\, t \in [0,T],\ \forall\, \omega \in \Omega, \\ \dot{\psi}(t \mid \omega) - r\psi(t \mid \omega) = \hat{k}^2(t)\beta a(t \mid \omega)(\psi(t \mid \omega) - v_I) + (1 - \hat{k}(t))c_S, \\ \dot{p}(t \mid \omega) = -p(t \mid \omega)(1 - p(t \mid \omega))\beta \hat{k}^2(t) a(t \mid \omega), \\ \dot{s}(t \mid \omega) = -\beta \hat{k}^2(t) s(t \mid \omega) a(t \mid \omega), \\ \dot{a}(t \mid \omega) = -\alpha \dot{s}(t \mid \omega) - \gamma_a a(t \mid \omega), \\ \mu(t,\omega) = \frac{\mu^0(\omega)/(1-p(t|\omega))}{\sum_{\omega'} \mu^0(\omega')/(1-p(t|\omega'))}, \end{cases} \tag{2.12}$$

and $\psi(T \mid \omega) = 0$.
The strategy profile $\hat{\mathbf{k}}$ is a symmetric interior equilibrium if and only if $\hat{k}(t) \in (0,1)$ for all t.

Proof. See the Appendix. □

When the confinement cost c_S is large relatively to the continuation payoff in case of infection, individuals have less incentives to self-isolate. The next proposition gives a sufficient condition such that there is no self-isolation at all in equilibrium.

Proposition 9 (The no-confinement equilibrium)**.** *If $(1-\alpha)\alpha\beta v_I + c_S > 0$, the game admits a unique equilibrium in dominant strategy, where all individuals play $\hat{k}(t) = 1$*

for every t. In this equilibrium, the players' payoff is

$$E_{\mu^0}[v(\hat{k} \mid .)] = v_I(1-\alpha)\beta \int_0^T e^{-rt} \sum_{\omega} \mu^0(\omega) a(t \mid \omega) e^{-\int_0^t \beta a(s|\omega) ds} dt,$$

where, for each ω, $a(. \mid \omega)$ is the unique solution of the system

$$\begin{cases} \forall\, t \in [0,T], \\ \dot{s}(t \mid \omega) = -\beta s(t \mid \omega) a(t \mid \omega),\ s(0 \mid \omega) = \bar{s}, \\ \dot{a}(t \mid \omega) = -\alpha \dot{s}(t \mid \omega) - \gamma_a a(t \mid \omega),\ a(0 \mid \omega) = \bar{a}. \end{cases}$$

Proof. See the Appendix. □

2.4 The effect of uncertainty

In this section we explore the role of uncertainty on the epidemic dynamics in the simplest possible setting where the population is aware of two possible epidemics: $\Omega = \{\omega_L, \omega_H\}$, and has prior belief $\mu^0(\omega_L) = 1 - \mu^0(\omega_H) = \bar{\mu}$. To do so, we simulate the dynamics of each epidemic ω for several values of $\bar{\mu}$ when the population plays the symmetric equilibrium described in Proposition 8. We denote by $\hat{k}_{\bar{\mu}}$ the symmetric interior equilibrium strategy when the prior is $\bar{\mu}$. We compare them with the dynamics of each epidemic without uncertainty, i.e., when $\bar{\mu} = 1$ in epidemic ω_L, and $\bar{\mu} = 0$ in epidemic ω_H. We calibrate the epidemiological parameters β, γ_a, γ_s and ν to the COVID-19 pandemic and we chose the behavioral parameters c_I, c_S and c_D arbitrarily.

2.4.1 Simulation strategy and calibration

In any epidemic, the first cases go unnoticed. For SARS-COV2, the first case was reported on December 11, 2019, whereas several phylodynamics studies date the onset of the epidemic between late August and early December.[17] Therefore, throughout our simulations we assume that individuals are not aware of the epidemic until some time $\tau \in (0,T)$, which can be interpreted as the moment at which the government makes the epidemic common knowledge in the population via a public announcement. Before

[17] See for instance Van Dorp et al. (2020).

time τ, individuals play $k(t) = 1$. After time τ, they form beliefs about the epidemic state and adapt their behavior accordingly.

The system (2.12) is well defined for each ω by initial values $p(0 \mid \omega)$, $a(0 \mid \omega)$ and $s(0 \mid \omega)$. However, the algorithm we construct to simulate (2.12) also requires the specification of $\psi(0 \mid \omega)$, which cannot be taken arbitrarily since ψ is determined by the terminal condition $\psi(T \mid \omega) = 0$. To determine $\psi(0 \mid \omega)$, we use an adaptation of the *Simulated Annealing algorithm*, a stochastic search-based algorithm described by Lewis (2007), whose principle is to solve the system (2.12) for several possible values of $\psi(0 \mid \omega)$ and to select the one that minimizes the distance between $\psi(T \mid \omega)$ and 0 for each ω.[18]

In line with Fenichel et al. (2011), we set the discount rate to $\boldsymbol{r = 0.014}\%$.[19]. The epidemiological parameters are calibrated to the SARS-COV-2:

- Absent an exhaustive testing campaign, the proportion of asymptomatic types in the population is rather difficult to estimate. In a nationwide study of over 61 000 participants, Pollán et al. (2020) find that the proportion of asymptomatic individuals in the Spanish population who developed antibodies to the SARS CoV-2 ranges from 21.9% to 35.8%. Therefore, we set $\boldsymbol{\alpha = 0.3}$.
- The recovery rate is usually estimated to two weeks, which implies $\boldsymbol{\gamma_a = 1/15}$.[20]
- To calibrate the contagiousness rate of the disease β, we use the value of the *basic reproduction number* $\mathcal{R}_0$, i.e., the average number of secondary infections produced by a typical infected individual in a population where everyone is susceptible.

[18]Precisely, at stage 1 a value $\psi(0 \mid \omega)[1]$ is uniformly drawn from an interval of *reasonable* values and is temporarily designed "best candidate". The final value of ψ given $\psi(0 \mid \omega)[1]$, i.e., $\psi(T \mid \omega)[1]$, is computed. At stage 2, another value $\psi(0 \mid \omega)[2]$ is drawn at random. If the corresponding final value $\psi(T \mid \omega)[2]$ is closer to 0 than $\psi(T \mid \omega)(1)$, then $\psi(0 \mid \omega)[2]$ becomes the new *best candidate*. The process does on iteratively and stops after a deterministic number of rounds N, which is large enough to guarantee that $\psi(T \mid \omega)[N]$ is almost 0 with the final best candidate.

[19]Precisely, Fenichel et al. (2011) study a discrete-time model in which they set the discount rate to $\delta = 0.99986$, which corresponds to a 5% annual discount rate. The analog of δ in a continuous-time model is $r = -\ln(\delta)$, thus we set $r = -\ln(0.99986)$.

[20]See e.g., A. Remuzzi and G. Remuzzi (2020).

In our model, $\mathcal{R}_0 = \beta\alpha/\gamma_a$. Indeed, as symptomatic individuals self-isolate, a randomly chosen infected individual contaminates a susceptible individual only if she is the asymptomatic type and if the virus is transmitted during contact, hence with probability $\alpha\beta$. As the individual is contagious during a period of expected length $1/\gamma_a$, the average number of infections caused by an infected is $\beta\alpha/\gamma_a$. For SARS-COV-2, the estimation of $\mathcal{R}_0$ ranges between 2.5 and 3.5, thus we set $\mathcal{R}_0 = 3.2$, and therefore set $\boldsymbol{\beta = 3.2\gamma_a/\alpha}$.

- There are various estimates of the Fatality-Infected ratio in the epidemiological literature. For instance, Verity et al. (2020) estimate this ratio to 0.7% percent and Gudbjartsson et al. (2020) to 0.3% We set a fatality rate $\boldsymbol{\nu/(\nu + \gamma^s) = 0.5\%}$.[21]

Finally, we arbitrarily set the costs to $\boldsymbol{c_S = 1}$, $\boldsymbol{c_I = 10}$ and $\boldsymbol{c_D = 100}$.

On day $\boldsymbol{\tau = 20}$, the population is informed that a virus has been spreading since day 0, and that a vaccine will be available on day $\boldsymbol{T = 350}$. Individuals do not know whether the initial penetration of the disease is low or high, that is if the epidemic is ω_L or ω_H with $a(0 \mid \omega_L) = 0.1\%$ and $a(0 \mid \omega_H) = 0.5\%$[22]. They know that nobody has died or recovered from the disease yet, thus that $r(0 \mid \omega) = d(0 \mid \omega) = 0$ and $s(0 \mid \omega) = 1 - \frac{1}{\alpha}a(0 \mid \omega)$ for each $\omega \in \{\omega_L, \omega_H\}$. We shall focus on the following epidemic indicators:

Total deaths. The total fraction of deaths in epidemic ω is $TD_{\bar{\mu}}(\omega) := \lim_{t\to\infty} d(t \mid \omega)$.

[21] In our model, an infected of the symptomatic type dies if the event "Death" occurs for her before the event "Healing". Therefore, the probability of death (conditional on being infected and the symptomatic type) is $P(\tau_D < \tau_H)$, with τ_H and τ_D denoting the random times of healing and death, respectively. Straightforwardly, $P(\tau_D < \tau_H) = \int_0^\infty F_{\tau_D}(t) f_{\tau_H}(t) dt = \nu/(\gamma^s + \nu)$ since $f_{\tau_D}(t) = \nu e^{-\nu t}$ and $f_{\tau_H}(t) = \gamma^s e^{-\gamma^s t}$.

[22] By definition, asymptomatic infections are difficult to detect and therefore, it is challenging to determine their magnitude in the population. The range of estimates in the literature is very wide. N. Ferguson et al. (2020) in a preliminary report, which has since been much criticized, estimated the percentage of asymptomatic infection to be between 40% to 50%. Other studies estimated the number of asymptomatic infections to be around 21.9% to 35.8% (Pollán et al. (2020)), 17.9% (Mizumoto et al. (2020)and 12.5% (Jefferson et al. (2022)). However, recent studies suggest that these figures are high since most of the Covid-19 infections were not persistently asymptomatic (Buitrago-Garcia et al. (2022)). Up to 50% of asymptomatic infections are in fact presymptomatic infections (Jefferson et al. (2022)). We have therefore chosen values at the extreme end of the spectrum of possible values for our illustration

By equation (2.5), $\int_0^\infty \dot{d}(t \mid \omega)dt + \bar{d} = \bar{d} + \nu\frac{1-\alpha}{\alpha}\int_0^\infty a(t \mid \omega)dt$. For all $t \geq T$, $\dot{s}(t \mid \omega) = 0$, hence $\dot{a}(t \mid \omega) = -\gamma_a a(t \mid \omega)$ and $a(t \mid \omega) = a(T \mid \omega)e^{-\gamma_a(t-T)}$. It follows that $\int_0^\infty a(t \mid \omega)dt = \int_0^T a(t \mid \omega)dt + \frac{1}{\gamma_a}a(T \mid \omega)$, thus the total fraction of deaths in epidemic ω is

$$TD_{\bar{\mu}}(\omega) = \bar{d} + \nu\frac{1-\alpha}{\alpha}\left(\int_0^T a(t \mid \omega)dt + \frac{1}{\gamma_a}a(T \mid \omega)\right).$$

Average transmission rate. The transmission rate of the disease is the rate at which a susceptible individual is contaminated. In average, the transmission rate in epidemic ω is $TR_{\bar{\mu}}(\omega) := \frac{1}{T}\int_0^T \beta a(t \mid \omega)\hat{k}^2_{\bar{\mu}}(t)dt$. By equation (2.1), $\beta a(t \mid \omega)\hat{k}^2_{\bar{\mu}}(t) = -\frac{\dot{s}(t|\omega)}{s(t|\omega)}$ hence

$$TR_{\bar{\mu}}(\omega) = \frac{1}{T}\left(\ln(\bar{s}) - \ln(s(T \mid \omega))\right).$$

Effective reproduction number The effective reproduction number is the expected proportion of the population contaminated by a randomly chosen infected individual. In our model, only asymptomatic individuals can effectively contaminate others, hence the effective reproduction number at time t in epidemic ω is $ERN_{\bar{\mu}}(t \mid \omega) = \frac{1}{\gamma_a}\frac{a(t|\omega)}{a(t|\omega)+i(t|\omega)}\beta s(t \mid \omega)\hat{k}_{\bar{\mu}}(t)^2$, which simplifies to $ERN(t \mid \omega) = \frac{1}{\gamma_a}\alpha\beta s(t \mid \omega)\hat{k}_{\bar{\mu}}(t)^2$.

2.4.2 The dynamics of the epidemics and behaviors without uncertainty.

As a benchmark, we simulate the dynamics of both epidemics without uncertainty. Figure 2.1 exhibits the dynamics of the fraction of infected individuals at the equilibrium and the equilibrium social activity level $\hat{k}_{\bar{\mu}}(t)$ in when individuals know the epidemic state ; if $\bar{\mu} = 1$ then they know that epidemic is ω_L and $\bar{\mu} = 0$ then they know that epidemic is ω_H.

In both epidemics, the equilibrium social activity level drops to $\hat{k}_1(20) = 0.042$ and $\hat{k}_0(20) = 0.012$ right after the announcement. Afterwards, the level of social activity increases in both epidemics, first rapidly then at a slower pace, and remains smaller than 1 until the arrival of the vaccine.

The initial risk of infection is larger in ω_H than in ω_L, this is why $\hat{k}_0(t)$ is smaller than $\hat{k}_1(t)$ at the beginning of the epidemic. Interestingly, after time 90, individu-

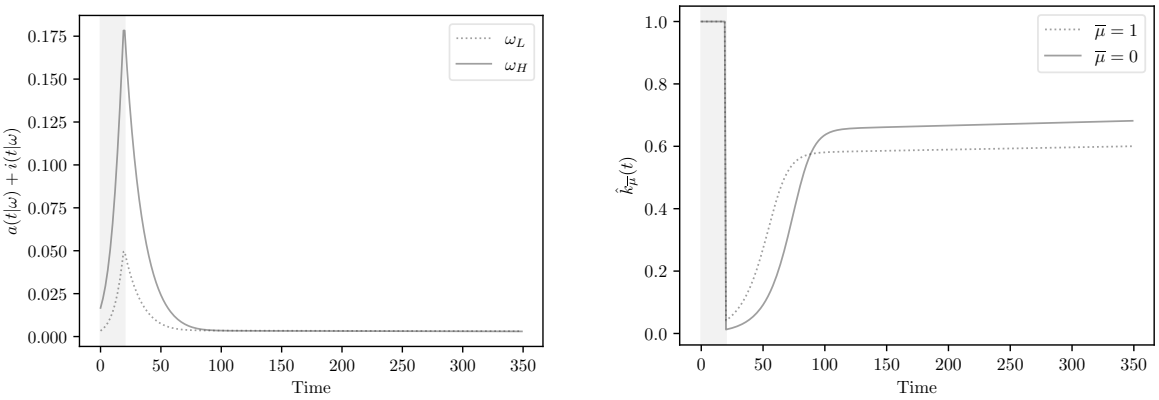

Figure 2.1: Dynamics of each epidemic without uncertainty.

als self-isolate more in epidemic ω_L than in epidemic ω_H. Let us explain why. The subjective probability of having symptoms depends on the fraction of infected individuals without symptoms $a(t|\omega)$ and the subjective belief of being the symptomatic type $p(t|\omega)$. Individuals are more confident in being of the asymptomatic type in epidemic ω_H $(p(t \mid \omega_H) < p(t \mid \omega_L))$, because, at the beginning, the virus circulated more intensively. Also, after date 100, the fraction of infected individuals with symptoms is higher in ω_L. Therefore, the subjective probability of having symptoms is smaller ω_H after date 90. Figure 2.2 illustrates this point.

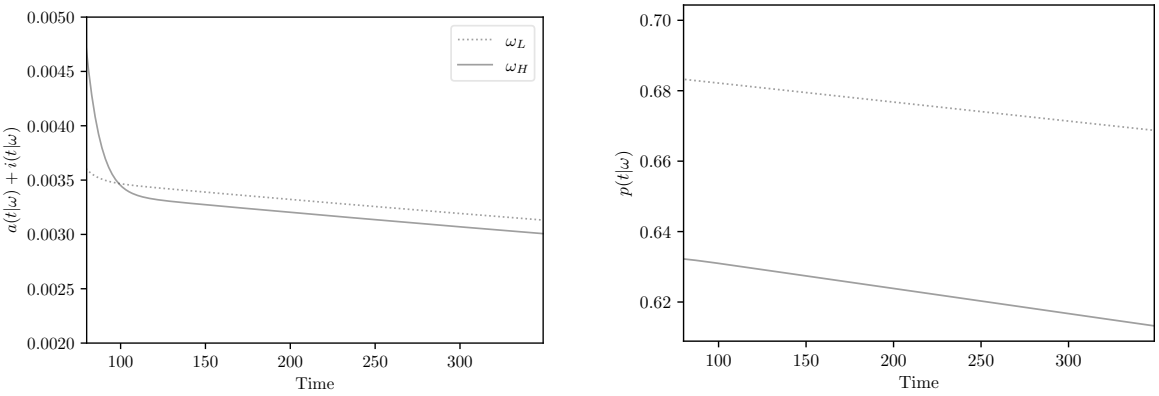

Figure 2.2: Dynamics of the epidemic and the subjective belief without uncertainty after date 90.

2.4.3 The dynamics of the epidemics and behaviors under uncertainty

We now simulate the dynamics of the two epidemics when the population has prior belief $\bar{\mu} \in \{0, 0.25, 1\}$ that the epidemic is ω_L. As illustrated in Figure 2.3, uncertainty has important consequences on the spread of the disease in ω_L but not in ω_H.

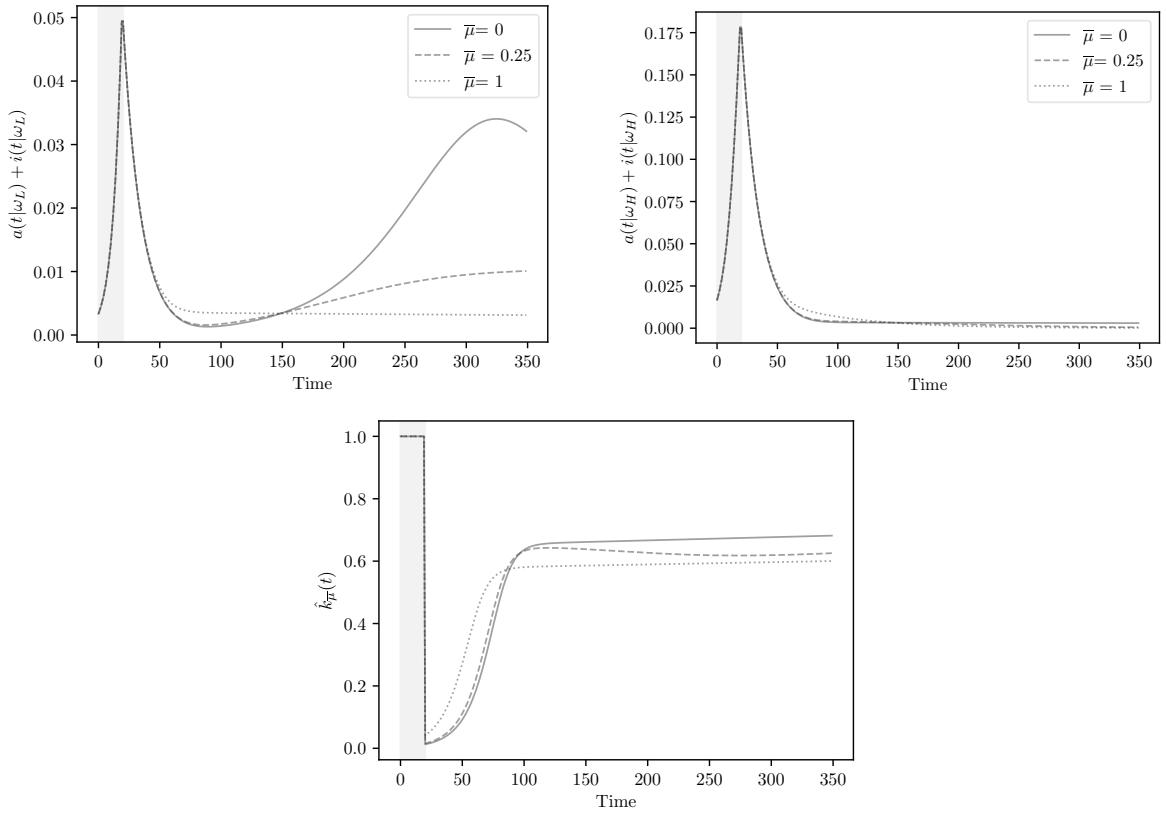

Figure 2.3: Top right: Dynamics of the fraction of infected individuals in ω_L when $\bar{\mu} \in \{0, 0.25, 1\}$. Top left: Dynamics of the fraction of infected individuals in ω_H when $\bar{\mu} \in \{0, 0.25, 1\}$. Below: Dynamics of the equilibrium social activity level $\hat{k}(t)$.

Interestingly, there is a second wave of infection in epidemic ω_L: for each prior $\bar{\mu} \in \{0, 0.25\}$, the proportion of infected decreases from $t = 50$ to $t = 150$ before increasing again. When $\bar{\mu} = 0$, the peak of the second wave is reached at $t = 325$ approximately. When $\bar{\mu} = 0.25$, the peak has not been reached before T. This second wave arises because, after $t = 90$, the social activity level is higher when $\bar{\mu} \in \{0, 0.25\}$ than when individuals form correct anticipations on ω_L. Note that the second wave is particularly high when agents (mistakenly) believe that the epidemic is ω_H with probability 1 (cf. the solid line), because they continuously increase their level of social

activity. On the other hand, when $\bar{\mu} = 0.25$, agents decrease their social activity after $t = 100$ because they anticipate that the fraction of cases will increase again if $\omega = \omega_L$, which results in a flattening of the curve. Surprisingly, the second wave arises only in epidemic ω_L. In epidemic ω_H, uncertainty implies that individuals are more cautious than when they know that $\omega = \omega_H$ for sure, because without uncertainty they would have learned faster that they are likely to be the asymptomatic type and would thus have self-isolate less.

This result is consistent with the dynamics of the ERN, which is interpreted as the fraction of people an infected individual contaminates while infectious. Figure 2.4 suggests that without uncertainty individuals behave in a such a way the ERN is close to one from date 80 to the end. For this reason, there is a single wave in this case. Under uncertainty, the ERN is above one after date 80 when the epidemic is ω_L: each infected individual contaminates more than many individuals, which explains why the infection cases increase after date 80. In epidemic ω_H, the ERN stays below 1 under uncertainty, which is consistant with the fact that there is a single wave for every value of the prior μ_0.

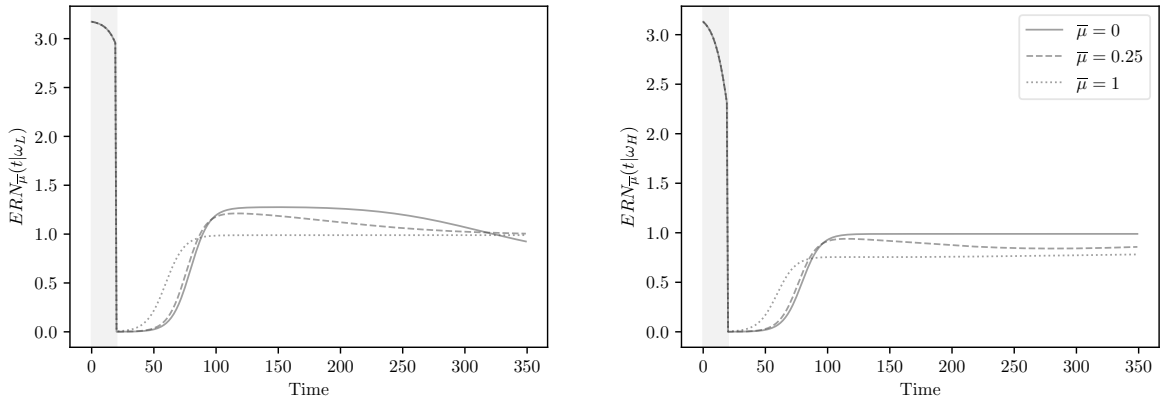

Figure 2.4: Dynamics of the ERN and average ERN in epidemics ω_L and ω_H.

The average social activity level over time, defined as $\bar{k}_{\bar{\mu}} = \frac{1}{T}\int_0^T \hat{k}_{\bar{\mu}}(t)dt$ can be lower under uncertainty than when individuals are confident about the epidemic. For instance, when $\bar{\mu} = 0.6$, $\bar{k}_{\bar{\mu}} = 0.502$ while $\bar{k}_{\bar{\mu}} = 0.534$ and $\bar{k}_{\bar{\mu}} = 0.504$ when $\bar{\mu} = 0$ and 1 respectively (See Figure 2.5).

In epidemic ω_L, the average transmission rate is $TR_{\bar{\mu}}(\omega_L) = 0.46$ when $\bar{\mu} = 1$ and

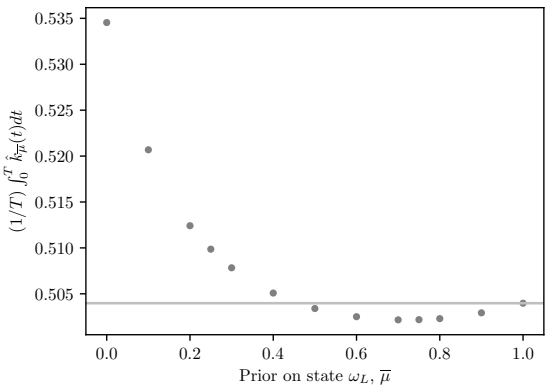

Figure 2.5: Average social activity at the symmetric equilibrium.

$TR_{\bar{\mu}}(\omega_L) = 0.14$ when $\bar{\mu} = 0$. This means that the disease is (much) more transmitted when the population wrongly believes that the epidemic is ω_H. Figure 2.6 suggests that there is a positive relationship between the average transmission rate and the prior in the epidemic ω_L. In contrast, in state ω_H this relationship is non-monotonic in $\bar{\mu}$: the average transmission rate is $TR_{\bar{\mu}}(\omega_H) = 0.35$ when $\bar{\mu} = 0.4$ and $TR_{\bar{\mu}}(\omega_H) = 0.38$ and $TR_{\bar{\mu}}(\omega_H) = 0.37$ in when $\bar{\mu} = 0$ and $\bar{\mu} = 1$, respectively.

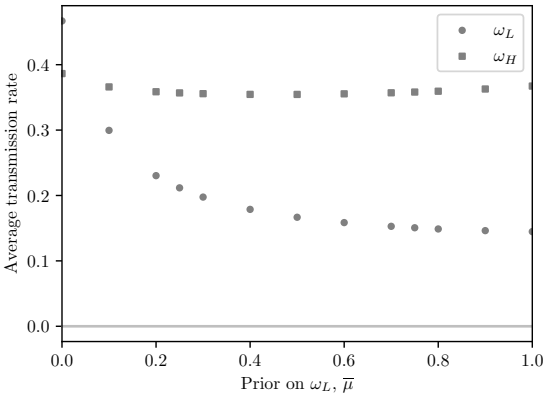

Figure 2.6: Average transmission rate in epidemics ω_H and ω_L.

2.4.4 The value of information

In this section we investigate whether it is always a good idea for a government to give the population all the information they have about the characteristic of an outbreak. We focus on two possible welfare objectives: minimizing the fraction of

deaths and maximizing payoffs.

Figure 2.7 describes the total fraction of deaths for different values of $\bar{\mu}$ in each epidemic. In epidemic ω_L, the fraction of deaths decreases with the prior belief $\bar{\mu}$ that the state is ω_L. When individuals believe that the epidemic is ω_H with probability 1 (total delusion), the fraction of deaths is twice higher than when they know that the state is ω_L. In contrast, in epidemic ω_H the fraction of deaths decreases with uncertainty, since it is 0.112% when $\bar{\mu} = 0.4$ and 0.12% and 0.115% when $\bar{\mu} = 0$ and 1, respectively. In Figure 2.8 one can observe the same pattern for equilibrium payoffs: in epidemic ω_L, the payoffs increase with $\bar{\mu}$, while in ω_H, the payoffs are higher for $\bar{\mu} = 0.4$ than for $\bar{\mu} \in \{0, 1\}$. Therefore, transparency improves welfare - both in terms of deaths and payoffs - when the epidemic is ω_L, while it decreases welfare when $\omega = \omega_H$.

What if the government has to commit to a disclosure policy before knowing the state of the epidemic? Recall that $TD_{\bar{\mu}}(\omega)$ is the fraction of deaths in epidemic ω when the prior is $\bar{\mu}$. The information value in terms of deaths is the fraction of deaths that can be avoided when the government disclose information. It depends on the prior $\bar{\mu}$ and is defined by:

$$IVD_{\bar{\mu}} = - \underbrace{\bar{\mu}TD_1(\omega_L) + (1-\bar{\mu})TD_0(\omega_H)}_{\text{Ex-ante total fraction of deaths without uncertainty}} + \underbrace{\bar{\mu}TD_{\bar{\mu}}(\omega_L) + (1-\bar{\mu})TD_{\bar{\mu}}(\omega_H)}_{\text{Expected fraction of deaths with uncertainty}}$$

As one can see in Figure 2.7, $IVD_{\bar{\mu}} \leq 0$ for every $\bar{\mu} \in (0, 1)$, which suggests that, ex-ante, the value of information is negative when the objective is to reduce the fraction of deaths.

We now address the same question in terms of payoffs. Recall that $v(\hat{k}_{\bar{\mu}}|\omega)$ is the equilibrium payoff in ω when the prior is $\bar{\mu}$. The information value in terms of payoffs is ex-ante payoff gain from knowing whether the epidemic is ω_L or ω_H. It also depends on the prior $\bar{\mu}$ and is defined by:

$$IVP_{\bar{\mu}} = \underbrace{\bar{\mu}v(\hat{k}_1|\omega_L) + (1-\bar{\mu})v(\hat{k}_0|\omega_H)}_{\text{Ex-ante payoff without uncertainty}} - \underbrace{\bar{\mu}v(\hat{k}_{\bar{\mu}}|\omega_L) - (1-\bar{\mu})v(\hat{k}_{\bar{\mu}}|\omega_H)}_{\text{Expected payoff with uncertainty}}$$

In contrast with the information value in terms of deaths, $IVP_{\bar{\mu}}$ is positive for small values of $\bar{\mu}$ and negative for large values of $\bar{\mu}$, as depicted by Figure 2.8. Transparency

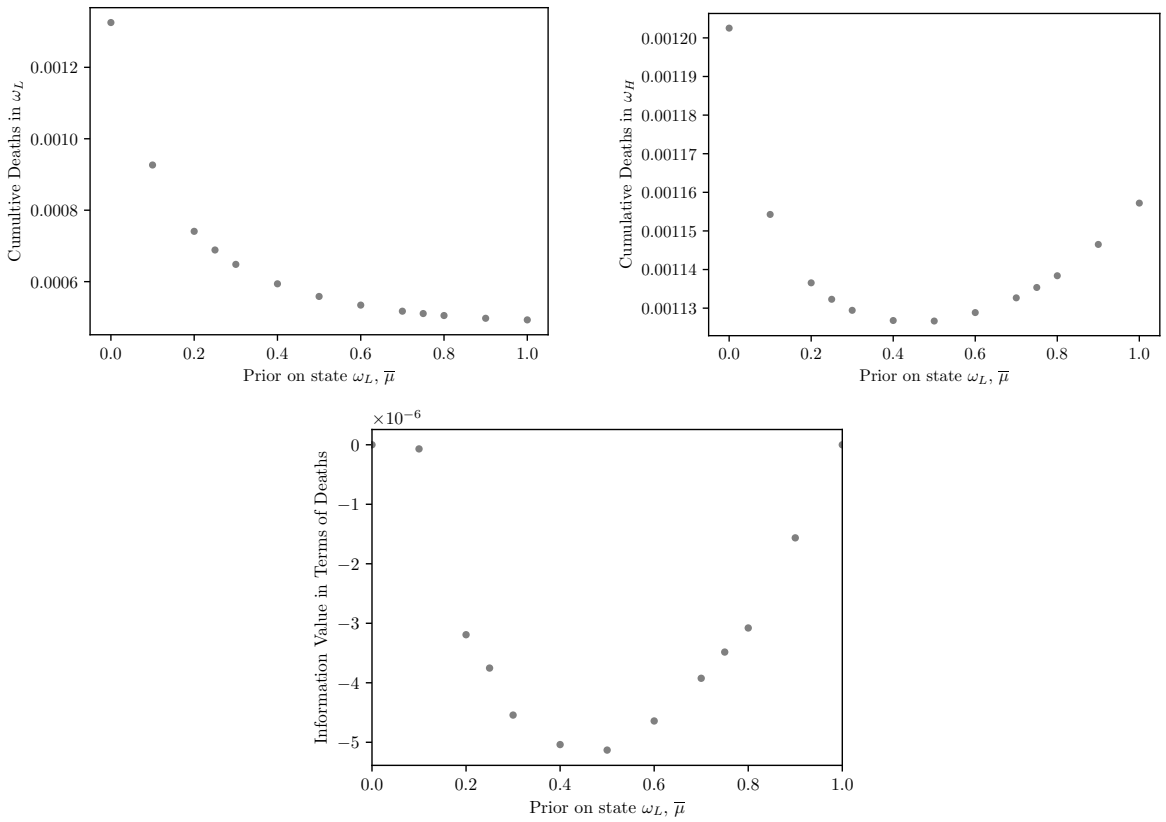

Figure 2.7: Above: Total fraction of deaths in each epidemic. Below: information value in terms of deaths

seems to be ex-ante welfare improving for low prior probabilities but not otherwise.

2.5 The social planner problem

The problem of the social planner is to determine the level of social activity that maximizes the average payoff in the population over the infinite horizon. As the population is homogenous, we restrict the attention to symmetric profiles, i.e., such that $k_j(t) = k(t)$ for every j.

Let us determine the total average payoff of strategy k conditional on some epidemic ω. After time T, every living individual without symptoms gets vaccinated and stops self-isolating, thereby gets payoff 0. Sick individuals continue to bear the flow cost c_S+c_I as long as they have symptoms, and dead individuals bear the cost c_D. Therefore, the average continuation payoff at T conditional on ω is

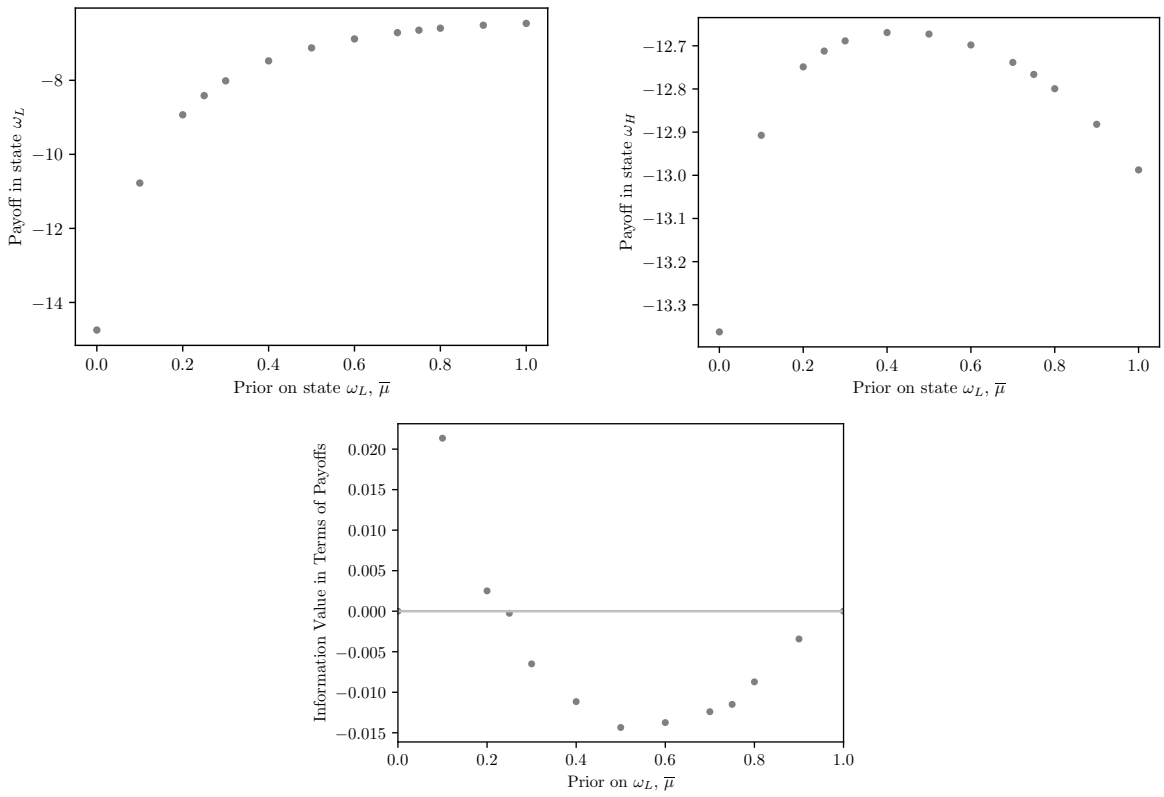

Figure 2.8: Above: expected discounted payoff in epidemic ω_L and ω_H. Below: Information Value in terms of Payoffs

$$W(T \mid \omega) = \int_T^\infty e^{-rt} \left(-(c_S + c_I) i(t \mid \omega) - c_D d(t \mid \omega)\right) dt.$$

After the arrival of the vaccine at time T, the contagiousness rate of the disease drops to $\beta = 0$, hence $\dot{s}(t \mid \omega) = 0 \; \forall \; t \geq T$. Plugging this into (2.3) and (2.5) and integrating between T and $t > T$, we obtain:

$$\begin{aligned} i(t \mid \omega) &= i(T \mid \omega) e^{-\gamma_a (t-T)}, \\ d(t \mid \omega) &= d(T \mid \omega) + \tfrac{\nu}{\gamma_a} i(T \mid \omega)(1 - e^{-\gamma_a (t-T)}). \end{aligned}$$

Plugging this into the latter expression, we obtain:

$$W(T \mid \omega) = -e^{-rT} \left(d(T \mid \omega) \frac{c_D}{r} + i(T \mid \omega) \frac{1}{r + \gamma_a} \left(\frac{c_D}{r} \nu + c_S + c_I \right) \right). \tag{2.13}$$

At each time t before the arrival of the vaccine, the population can be divided into four groups:

1. those who have never had symptoms before t, i.e., susceptible people, asymptomatic infected people and asymptomatic recovered people. They represent a

total fraction $s(t \mid \omega) + \alpha(1 - s(t \mid \omega))$ of the population and, as they spend a fraction $1 - k(t)$ of their day home, bear the flow cost $c_S(1 - k(t))$.

2. those who are infected with symptoms. They represent a fraction $i(t \mid \omega)$ of the population and bear the flow cost $c_S + c_I$.

3. those who had symptoms in the past and have healed from the disease before time t. They represent a fraction $(1 - \alpha)(1 - s(t \mid \omega)) - i(t \mid \omega) - d(t \mid \omega)$ of the population and bear no cost as they do not self-isolate anymore.

4. those who died from the disease before t. They represent a fraction $d(t \mid \omega)$ of the population and bear the flow cost c_D.

Therefore, the total average payoff conditional on ω is

$$W(k \mid \omega) = W(T \mid \omega) + \int_0^T e^{-rt} \left(-c_S(1 - k(t))(\alpha + s(t \mid \omega)(1 - \alpha)) - (c_S + c_I)i(t \mid \omega) - c_D d(t \mid \omega)\right) dt$$

Proposition 10 (The optimal strategy)**.** *The problem of the social planner has a unique symmetric solution $\check{k}$ defined by*

$$\check{k}(t) = \begin{cases} \tilde{k}(t) & \text{if } \tilde{k}(t) \in (0, 1] \\ 1, & \text{otherwise,} \end{cases}$$

where

$$\tilde{k}(t) = \frac{c_S}{2\alpha\beta} \frac{\alpha + (1 - \alpha) \sum_\omega \mu^0(\omega) s(t \mid \omega)}{\sum_\omega s(t \mid \omega) i(t \mid \omega) \left(\frac{1}{1-\alpha}\psi_s(t \mid \omega) - \psi_i(t \mid \omega)\right)},$$

and $\forall\, t \in [0, T]$, $\forall \omega \in \Omega$,

$$\begin{cases} \dot{s}(t \mid \omega) = -\beta \check{k}(t)^2 s(t \mid \omega) \frac{\alpha}{1-\alpha} i(t \mid \omega), \\ \dot{i}(t \mid \omega) = -(1 - \alpha)\dot{s}(t \mid \omega) - \gamma_a i(t \mid \omega), \\ \dot{d}(t \mid \omega) = \nu i(t \mid \omega), \end{cases}$$

$$\begin{cases} \dot{\psi}_s(t \mid \omega) - r\psi_s(t \mid \omega) = & -\check{k}(t)^2 \alpha\beta i(t \mid \omega)(\psi_i(t \mid \omega) - \frac{1}{1-\alpha}\psi_s(t \mid \omega)) + \mu^0(\omega) c_S(1 - \alpha)(1 - k(t))), \\ \dot{\psi}_i(t \mid \omega) - r\psi_i(t \mid \omega) = & -\check{k}(t)^2 \alpha\beta s(t \mid \omega)(\psi_i(t \mid \omega) - \frac{1}{1-\alpha}\psi_s(t \mid \omega)) + \mu^0(\omega) \left(c_S + c_I + \gamma_a \psi_i(t \mid \omega) - \nu\psi_d(t \mid \omega)\right), \\ \dot{\psi}_d(t \mid \omega) - r\psi_d(t \mid \omega) = & \mu^0(\omega) c_D, \end{cases}$$

and $\psi_s(T \mid \omega) = 0$, $\psi_i(T \mid \omega) = -\mu^0(\omega)\frac{1}{r+\gamma_a}\left(\frac{c_D}{r}\nu + c_S + c_I\right)$, *and* $\psi_d(T \mid \omega) = -\mu^0(\omega)\frac{c_D}{r}$.

Proof. See the Appendix. □

2.5.1 Next steps

The algorithm we built for our simulations requires the specification of $\psi_s(0 \mid \omega)$, $\psi_i(0 \mid \omega)$ and $\psi_d(0 \mid \omega)$. These values cannot be determined arbitrarily since HYV is determined by the terminal conditions $\psi_s(T \mid \omega) = 0$, $\psi_i(T \mid \omega) = -\mu^0(\omega)\frac{1}{r+\gamma_a}\left(\frac{c_D}{r}\nu + c_S + c_I\right)$ and $\psi_d(T \mid \omega) = -\mu^0(\omega)\frac{c_D}{r}$. $\psi_s(0 \mid \omega)$, $\psi_i(0 \mid \omega)$ and $\psi_d(0 \mid \omega)$ are related to each other. Our search for terminal values is therefore more complex than in the previous case. The required computing resources being considerable, we will use the servers of Calcul Québec to search for them.

Appendix

2.5.2 Detailed derivation of 2.9

Fix $\omega \in \Omega$ and a strategy k_j for player j. If player j gets symptoms at time τ, her payoff is:

$$\begin{array}{ll} e^{-r\tau}v_I - \int_0^\tau e^{-rs}(1-k_j(s))c_S ds & \text{if } \tau \leq T, \\ -\int_0^T e^{-rs}(1-k_j(s))c_S ds & \text{if } \tau > T. \end{array}$$

As τ is a random variable, player j's expected payoff is:

$$v(k_j \mid \omega) = E[\left(e^{-r\tau}v_I - u(\tau)\right)\mathbb{1}_{\tau \leq T}] - u(T)P(\tau > T),$$

with $u(t) := \int_0^t e^{-rs}(1-k_j(s))c_S ds$.

For $t \leq T$, $P(\tau > t) = 1 - p_0 + p_0 e^{-\int_0^t k_j(s)\beta\bar{k}_A(s|\omega)a(s|\omega)ds}$, which, by integrating (2.6), simplifies to

$$P(\tau > t) = e^{-\int_0^t p_j(s|\omega)k_j(s)\beta\bar{k}_A(s|\omega)a(s|\omega)ds},$$

and implies that τ is distributed with density

$$f_\tau(t) = p_j(t \mid \omega)k_j(t)\beta\bar{k}_A(t \mid \omega)a(t \mid \omega)P(\tau > t).$$

Therefore,

$$\begin{aligned} v(k_j \mid \omega) &= \int_0^T \left(e^{-rt}v_I - u(t)\right) f_\tau(t)dt - u(T)P(\tau > T), \\ &= \int_0^T e^{-rt}v_I f_\tau(t)dt - \int_0^T u(t)f_\tau(t)dt - u(T)P(\tau > T). \end{aligned}$$

Integrating by parts and simplifying, we obtain:

$$\begin{aligned} v(k_j \mid \omega) &= \int_0^T e^{-r\tau}v_I f_\tau(t)dt - [u(t)P(\tau \leq t)]_0^T + \int_0^T u'(t)P(\tau \leq t)dt - u(T)P(\tau > T), \\ &= \int_0^T e^{-r\tau}v_I f_\tau(t)dt - u(T)P(\tau \leq T) + \int_0^T e^{-rt}(1-k_j(t))c_S P(\tau \leq t)dt - u(T)P(\tau > T), \\ &= \int_0^T e^{-r\tau}v_I f_\tau(t)dt - u(T) + \int_0^T e^{-rt}(1-k_j(t))c_S(1-P(\tau > t))dt, \\ &= \int_0^T e^{-r\tau}v_I f_\tau(t)dt - u(T) + u(T) - \int_0^T e^{-rt}(1-k_j(t))c_S P(\tau > t)dt, \\ &= \int_0^T e^{-r\tau}P(\tau > t)\left[v_I p_j(t \mid \omega)k_j(t)\beta\bar{k}_A(t \mid \omega)a(t \mid \omega) - (1-k_j(t))c_S\right]dt. \end{aligned}$$

2.5.3 Proofs for Section 2 and Section 3

Lemma 5. *For every $\omega \in \Omega$, $t \in \mathbb{R}_+$,*

$$\mu_j(t,\omega) = \frac{\mu^0(\omega)/(1-p_j(t \mid \omega))}{\sum_{\omega'}\mu^0(\omega')/(1-p_j(t \mid \omega'))}.$$

Proof. Let $S_j(t)$ stands for the event "j has symptoms in t" and $\bar{S}_j(t^-)$ for the event "j never had symptoms before t". By definition, $\mu_j(t,\omega) = P(\omega \mid \bar{S}_j(t^-))$. By Bayes's rule,

$$P(\omega \mid \bar{S}_j(t^-)) = \frac{P(\bar{S}_j(t^-) \mid \omega)P(\omega)}{P(\bar{S}_j(t^-))} = \frac{P(\bar{S}_j(t^-) \mid \omega)\mu^0(\omega)}{\sum_{\omega'} P(\bar{S}_j(t^-) \mid \omega')\mu^0(\omega')}.$$

As individuals of type θ_a never have symptoms,

$$P(\bar{S}_j(t^-) \mid \omega) = 1 - P(\theta_s) + P(\bar{S}_j(t^-) \mid \omega, \theta_s)P(\theta_s)$$

As $P(\theta_s) = 1 - \alpha$ and $P(\bar{S}_j(t^-) \mid \omega, \theta_s) = e^{-\int_0^t k_j(s)\beta\bar{k}_A(s|\omega)a(s|\omega)ds}$, we can write:

$$P(\bar{S}_j(t^-) \mid \omega) = \alpha + (1-\alpha)e^{-\int_0^t k_j(s)\beta\bar{k}_A(s|\omega)a(s|\omega)ds}.$$

Moreover, integrating (2.6) between 0 and t, we obtain:

$$\begin{cases} p(0 \mid \omega)e^{-\int_0^t k_j(s)\beta\bar{k}_A(s|\omega)a(s|\omega)ds} = p_j(t \mid \omega)e^{-\int_0^t k_j(s)p(s|\omega)\beta\bar{k}_A(s|\omega)a(s|\omega)ds} \\ e^{-\int_0^t k_j(s)p(s|\omega)\beta\bar{k}_A(s|\omega)a(s|\omega)ds} = \frac{1-p(0|\omega)}{1-p_j(t|\omega)} \end{cases}$$

Using the latter identities together with $p(0 \mid \omega) = 1 - \alpha$, we obtain:

$$P(\bar{S}_j(t^-) \mid \omega) = \frac{\alpha}{1 - p_j(t \mid \omega)}.$$

The result follows. □

Lemma 6. *Let τ_H and τ_D be independent random variables distributed according to $f(t) = \gamma e^{-\gamma t}$ and $f(t) = \nu e^{-\nu t}$, respectively. The following equality holds:*

$$E\left[\int_0^{\min\{\tau_H,\tau_D\}} e^{-rt}(c_S + c_I)dt + \frac{c_D}{r}e^{-r\tau_D}\mathbb{1}_{\tau_D<\tau_H}\right] = \frac{1}{r+\gamma+\nu}(c_S + c_I + \nu\frac{c_D}{r}).$$

Proof. Let $g(\tau_H,\tau_D) := \int_0^{\min\{\tau_H,\tau_D\}} e^{-rt}(c_S + c_I)dt + \frac{c_D}{r}e^{-r\tau_D}\mathbb{1}_{\tau_D<\tau_H}$. Straightforwardly,

$$g(\tau_H,\tau_D) = \frac{c_S + c_I}{r}(1 - e^{-r\min\{\tau_H,\tau_D\}}) + \frac{c_D}{r}e^{-r\tau_D}\mathbb{1}_{\tau_D<\tau_H}.$$

The random variable $\min\{\tau_H,\tau_D\}$ is distributed according to $f(t) = (\gamma+\nu)e^{-(\gamma+\nu)t}$. Therefore,

$$E[e^{-r\min\{\tau_H,\tau_D\}}] = \frac{\gamma+\nu}{r+\gamma+\nu}.$$

Moreover,

$$E[e^{-r\tau_D}\mathbb{1}_{\tau_D<\tau_H}] = \int_0^\infty \left(\int_0^{\tau_H} e^{-(r+\nu)\tau_D}\nu d\tau_D\right)\gamma e^{-\gamma\tau_H}d\tau_H = \frac{\nu}{r+\gamma+\nu}$$

Therefore,

$$E[g(\tau_H, \tau_D)] = (c_S + c_I)\frac{1}{r+\gamma+\nu} + \frac{c_D}{r}\frac{\nu}{r+\gamma+\nu}.$$

□

Proof of Proposition 7

The best-response problem of a player is to determine the strategy k that maximizes her expected discounted payoff, with, for every $\omega \in \Omega$, the functions $s(. \mid \omega)$ and $a(. \mid \omega)$ being fixed and defined by the dynamic system:

$$\begin{cases} \forall\, t \in [0,T], \\ \dot{s}(t \mid \omega) = -\beta \bar{k}_S(t \mid \omega) s(t \mid \omega) \bar{k}_A(t \mid \omega) a(t \mid \omega), \text{ with } s(0 \mid \omega) = \bar{s} \in (0,1), \\ \dot{a}(t \mid \omega) = -\alpha \dot{s}(t \mid \omega) - \gamma_a a(t \mid \omega), \text{ with } a(0 \mid \omega) = \bar{a} \in (0,1), \end{cases}$$

Formally, it is the solution of the optimal control problem

$$\begin{cases} \max\limits_{k \in \mathcal{K}} & \int_0^T e^{-rt} \sum\limits_{\omega} \mu^0(\omega) e^{-\int_0^t p(s|\omega)k(s)\beta \bar{k}_A(s|\omega)a(s|\omega)ds} \left(p(t \mid \omega) k(t) \beta \bar{k}_A(t \mid \omega) a(t \mid \omega) v_I - c_S(1-k(t)) \right) dt \\ \text{w.r.t.} & \dot{p}(t \mid \omega) = -p(t \mid \omega)(1 - p(t \mid \omega)) k(t) \beta \bar{k}_A(t \mid \omega) a(t \mid \omega) \text{ and } p(0 \mid \omega) = 1 - \alpha \;\forall\, \omega \in \Omega, \end{cases}$$

where $\mathcal{K}$ denotes the set of piecewise continuous functions from $\mathbb{R}_+$ into $[0,1]$. Making the change of variable $x(t \mid \omega) := \mu^0(\omega) e^{-\int_0^t p(s|\omega)k(s)\beta \bar{k}_A(s|\omega)a(s|\omega)ds}$, with $X(t) := (x(t \mid \omega))_\omega$, and observing that[23]

$$e^{-\int_0^t p(s|\omega)k(s)\beta \bar{k}_A(s|\omega)a(s|\omega)ds} = \frac{\alpha}{1 - p(t \mid \omega)},$$

the player's problem can be rewritten as follows:

$$\mathcal{P}(\mathbf{k}) : \begin{cases} \max\limits_{k \in \mathcal{K}} & \int_0^{+\infty} e^{-rt} F(t, X(t), k(t)) dt \\ \text{w.r.t.} & \dot{x}(t \mid \omega) = -\left(x(t \mid \omega) - \mu^0(\omega)\alpha \right) k(t) \beta \bar{k}_A(t \mid \omega) a(t \mid \omega) \text{ and } x(0 \mid \omega) = \mu^0(\omega) \;\forall\, \omega \in \Omega. \end{cases}$$

with

$$F(t, X(t), k(t)) := \sum_{\omega} \left[(x(t \mid \omega) - \mu^0(\omega)\alpha) k(t) \beta \bar{k}_A(t \mid \omega) a(t \mid \omega) v_I - x(t \mid \omega) c_S (1 - k(t)) \right].$$

As $F(t, X(t), k(t))$ is negative and bounded below by v_I, the objective is well defined. Furthermore, by standard results, the problem admits at least one solution. Applying Pontryagin's maximum principle, the optimal control k^* and the associated trajectory X^* must satisfy the following conditions:

[23] See the proof of Lemma 5.

Lemma 7 (**Necessary conditions**). *If (X^*, k^*) is a solution of $\mathcal{P}(\mathbf{k})$, then there exists a function $\psi : \mathbb{R}_+ \times \Omega \to \mathbb{R}$, C^1 in the first argument, such that:*

(i) $\forall\, \omega,\ \dot{\psi}(t \mid \omega) - r\psi(t \mid \omega) = -H_{x(t|\omega)}(t, X^*(t), k^*(t), \Psi(t))$,

(ii) $H(t, X^*(t), k(t), \Psi(t)) \leq H(t, X^*(t), k^*(t), \Psi(t))$ *for every admissible control* k,

(iii) $\forall\, \omega,\ \psi(T \mid \omega) = 0$,

where $\Psi(t) := (\psi(t \mid \omega))_\omega$ *and* $H(t, X(t), k(t), \Psi(t)) := F(t, X(t), k(t)) + \sum_\omega \psi(t \mid \omega)\dot{x}(t \mid \omega)$ *is the discounted Hamiltonian of the problem.*

The transversality condition (iii) comes from the fact that $x(T \mid \omega)$ is free for every ω.

Observing that
$H(t, X(t), k(t), \Psi(t)) =$

$$\sum_\omega \left[(x(t \mid \omega) - \mu^0(\omega)\alpha)k(t)\beta\bar{k}_A(t \mid \omega)a(t \mid \omega)(v_I - \psi(t \mid \omega)) - x(t \mid \omega)c_S(1 - k(t))\right],$$

the necessary conditions are rewritten as

(i) $\quad \forall\, \omega,\ \dot{\psi}(t \mid \omega) - r\psi(t \mid \omega) = k^*(t)\beta\bar{k}_A(t \mid \omega)a(t \mid \omega)(\psi(t \mid \omega) - v_I) + c_S(1 - k^*(t))$,

(ii) for every admissible control k,
$(k^*(t) - k(t)) \sum_\omega \left[x^*(t \mid \omega)c_S - (x^*(t \mid \omega) - \mu^0(\omega)\alpha)\beta\bar{k}_A(t \mid \omega)a(t \mid \omega)(\psi(t \mid \omega) - v_I)\right] \geq 0.$

As $x(t \mid \omega) = \mu^0(\omega)\alpha/(1 - p(t \mid \omega))$, the latter condition can be more conveniently rewritten as:

$$(ii)\ (k^*(t) - k(t)) \sum_\omega \frac{\mu^0(\omega)}{1 - p(t \mid \omega)} \left[c_S - p^*(t \mid \omega)\beta\bar{k}_A(t \mid \omega)a(t \mid \omega)(\psi(t \mid \omega) - v_I)\right] \geq 0\ \forall\ k.$$

Dividing by $\sum_\omega \mu^0(\omega)/(1 - p(t \mid \omega))$ and using the identity $\mu(t, \omega) = \frac{\mu^0(\omega)(1-p(t|\omega))}{\sum_{\omega'} \mu^0(\omega')(1-p(t|\omega'))}$, condition (ii) reduces to:

$$(ii)\ k^*(t) = \begin{cases} 1, & \text{if } c_S - \sum_\omega \mu(t, \omega)p^*(t \mid \omega)\beta\bar{k}_A(t \mid \omega)a(t \mid \omega)(\psi(t \mid \omega) - v_I) > 0, \\ 0, & \text{if } c_S - \sum_\omega \mu(t, \omega)p^*(t \mid \omega)\beta\bar{k}_A(t \mid \omega)a(t \mid \omega)(\psi(t \mid \omega) - v_I) < 0, \\ \in [0, 1], & \text{if } c_S - \sum_\omega \mu(t, \omega)p^*(t \mid \omega)\beta\bar{k}_A(t \mid \omega)a(t \mid \omega)(\psi(t \mid \omega) - v_I) = 0. \end{cases}$$

Proof of Proposition 8

For all t; consider the strategy profile in which $k_{j'}(t) = \hat{k}(t)\ \forall\ j' \neq j,\ t$ and $k_j(t)$ is arbitrary. Suppose that $\hat{k}(t) \in (0,1)$. Replacing $\hat{k}(t)$ in the Hamiltonian, we obtain: $H(t, X(t), k_j(t), \Psi(t)) = -\sum_\omega x(t \mid \omega)c_S$. It is easy to see that the Hamiltonian is concave with respect to the state variable $X(t)$ and therefore the necessary conditions in Proposition 7 are also sufficient (see e.g. Arrow and Kurz (1970)). Therefore, any $k_j(t) \in (0,1)$ is a best response (and in particular $\hat{k}(t)$ since it belongs to $(0,1)$). Consequently, $\hat{\mathbf{k}}(t)$ is an equilibrium.

Proof of Proposition 9

As a preliminary, let us prove the following lemma:

Lemma 8. *If $\psi : \mathbb{R}_+ \times \Omega \to \mathbb{R}$ satisfies the necessary conditions of Proposition 7, then $\psi(t \mid \omega) \leq 0$ for every $t \in [0,T]$ and $\omega \in \Omega$.*

Proof. Let $\psi : \mathbb{R}_+ \times \Omega \to \mathbb{R}$ such that, for every t and ω,

$$\dot{\psi}(t \mid \omega) - r\psi(t \mid \omega) = k(t)\beta\bar{k}_A(t \mid \omega)a(t \mid \omega)(\psi(t \mid \omega) - v_I) + c_S(1 - k(t)), \qquad (2.14)$$

and $\psi(T \mid \omega) = 0$.

We work towards a contradiction. Fix some epidemic ω. Suppose that there exists $t' < t'' \leq T$ such that $\psi(t \mid \omega) > 0$ for every $t \in [t', t'']$. It follows that $\psi(t \mid \omega) - v_I > 0$ on $[t', t'']$, thus $\psi'(t \mid \omega) > 0$ on $[t', t'']$ by (2.14). As a consequence, $\psi(t \mid \omega) > 0$ in the right neighborhood of t'', which implies $\psi'(t \mid \omega)$ is increasing on the right neighborhood of t''. The argument can be extended to prove that $\psi(t \mid \omega) > 0$ and $\psi'(t \mid \omega) > 0$ for every $t \in [t', T]$. This contradicts $\psi(T \mid \omega) = 0$. □

Fix a player i, a date t and a value $\bar{k}_A(t \mid \omega)$ for each ω. As $\psi(t \mid \omega) < 0$ by Lemma 8, $\psi(t \mid \omega) - v_I < -v_I$. Moreover, $\bar{k}_A(t \mid \omega) \leq 1$ and $a(t \mid \omega) < \alpha$. Finally, $p(t \mid \omega)$ is non increasing in t, thus $p(t \mid \omega) \leq 1 - \alpha$. Therefore, for every t,

$$\begin{aligned}
\beta \sum_\omega \mu(t,\omega)p(t \mid \omega)\bar{k}_A(t \mid \omega)a(t \mid \omega)(\psi(t \mid \omega) - v_I) &< \sum_\omega \mu(t,\omega)p(t \mid \omega)\beta\bar{k}_A(t \mid \omega)a(t \mid \omega)(-v_I), \\
&< (-v_I)\sum_\omega \mu(t,\omega)(1-\alpha)\beta\alpha, \\
&< (-v_I)(1-\alpha)\beta\alpha.
\end{aligned}$$

Suppose that the best response is such that, at some date t, $k_i^*(t) < 1$. If $(1-\alpha)\alpha\beta(-v_I) < c_S$ then $\beta \sum_\omega \mu(t,\omega)p(t \mid \omega)\bar{k}_A(t \mid \omega)a(t \mid \omega)(\psi(t \mid \omega) - v_I)$ is smaller then c_H . According to Proposition 9, $k_i^*(t) < 1$ cannot be a best response. Thus a contradiction. Therefore, $k_i^*(t) = 1$ for all t is a dominant strategy. This proves the result.

Finally, let us determine the players' payoff in the equilibrium where $k^* = 1$. Plugging $k_j(t) = 1$ and $\bar{k}_A(t \mid \omega) = 1$ into the belief dynamics (3), we obtain the players' belief function conditional on ω as the solution of the ODE:

$$\dot{p}(t \mid \omega) = -p(t \mid \omega)(1 - p(t \mid \omega))\beta a(t \mid \omega),$$

with initial condition $p(0 \mid \omega) = 1 - \alpha$. Integrating between 0 and t, we obtain

$$\frac{p(t \mid \omega)}{1 - p(t \mid \omega)} = \frac{1-\alpha}{\alpha} e^{-\int_0^t \beta a(u|\omega)du},$$

and

$$\frac{\alpha}{1 - p(t \mid \omega)} = e^{-\int_0^t \beta p(u|\omega)a(u|\omega)du}.$$

Using the latter findings and plugging $k_j(t) = 1$ into the payoff expression (5) then simplifying, we obtain:

$$v(k^* \mid \omega) = v_I(1-\alpha)\beta \int_0^T e^{-rt} a(t \mid \omega) e^{-\beta \int_0^t \beta a(u|\omega)du} dt.$$

The result is obtained by taking the expectation of the latter expression.

2.5.4 Proofs for Section 5

Proof of Proposition 10.

The problem of the social planner is to determine the strategy that maximizes $E[W(k \mid .)]$ subject to the evolution of the epidemic. As $a(t \mid \omega) = \frac{\alpha}{1-\alpha} i(t \mid \omega)$, the problem depends only on $3\times \mid \Omega \mid$ state variables represented by $X(t) := ((s(t \mid \omega))_\omega, (i(t \mid \omega))_\omega, (d(t \mid \omega))_\omega)$. Formally, it is the solution of the optimal control problem

$$\mathcal{P}^W(k): \begin{cases} \max\limits_{k\in\mathcal{K}} & \int_0^T e^{-rt}F(t,X(t),k(t))dt + E[W_T(k \mid .)] \\ w.r.t., \forall\, \omega \in \Omega, & \dot{s}(t \mid \omega) = -\beta k(t)^2 s(t \mid \omega)\frac{\alpha}{1-\alpha} i(t \mid \omega),\ s(0 \mid \omega) = \bar{s}, \\ & \dot{i}(t \mid \omega) = -(1-\alpha)\dot{s}(t \mid \omega) - \gamma_a i(t \mid \omega),\ i(0 \mid \omega) = \bar{i}, \\ & \dot{d}(t \mid \omega) = \nu i(t \mid \omega),\ d(0 \mid \omega) = \bar{d}, \end{cases}$$

with

$$F(t,X(t),k(t)) := \sum_{\omega} \mu^0(\omega)\left[-c_S(1-k(t))(\alpha+(1-\alpha)s(t \mid \omega)) - (c_S+c_I)i(t \mid \omega) - c_D d(t \mid \omega)\right]$$

As $F(t,X(t),k(t))$ is negative and bounded below, the objective is well defined. Furthermore, by standard results, the problem admits at least one solution. Applying Pontryagin's maximum principle, the optimal control k^* and the associated trajectory X^* must satisfy the following conditions:

Lemma 9 (**Necessary conditions**). *If (X^*, k^*) is a solution of $\mathcal{P}^W(k)$, then there exist functions $\psi_s, \psi_i, \psi_d : \mathbb{R}_+ \times \Omega \to \mathbb{R}$, C^1 in the first argument, such that:*

(i) $\forall\, \omega \in \Omega$,

$$\dot{\psi}_s(t \mid \omega) - r\psi_s(t \mid \omega) = -H_{s(t|\omega)}(t, X^*(t), k^*(t), \Psi(t)),$$

$$\dot{\psi}_i(t \mid \omega) - r\psi_i(t \mid \omega) = -H_{i(t|\omega)}(t, X^*(t), k^*(t), \Psi(t)),$$

$$\dot{\psi}_d(t \mid \omega) - r\psi_d(t \mid \omega) = -H_{d(t|\omega)}(t, X^*(t), k^*(t), \Psi(t)),$$

(ii) $H(t, X^*(t), k(t), \Psi(t)) \leq H(t, X^*(t), k^*(t), \Psi(t))$ *for every admissible control* k,

(iii) $\forall\, \omega \in \Omega$, $\psi_s(T \mid \omega) = \frac{\partial E[W(T|.)]}{\partial s(T|\omega)}$, $\psi_i(T \mid \omega) = \frac{\partial E[W(T|.)]}{\partial i(T|\omega)}$, $\psi_d(T \mid \omega) = \frac{\partial E[W(T|.)]}{\partial d(T|\omega)}$,

where $\Psi(t) := ((\psi_s(t \mid \omega))_\omega, (\psi_i(t \mid \omega))_\omega, (\psi_d(t \mid \omega))_\omega)$ *and*

$$H(t,X(t),k(t),\Psi(t)) := F(t,X(t),k(t)) + \sum_{\omega}\Big(\psi_s(t \mid \omega)\dot{s}(t \mid \omega) + \psi_i(t \mid \omega)\dot{i}(t \mid \omega) + \psi_d(t \mid \omega)\dot{d}(t \mid \omega)\Big)$$

is the discounted Hamiltonian of the problem.

After some simplifications, we observe that

$$H(t, X(t), k(t), \Psi(t)) = -\alpha c_S$$
$$+k(t)^2\alpha\beta\sum_{\omega} s(t \mid \omega)i(t \mid \omega)\left(\psi_i(t \mid \omega) - \frac{1}{1-\alpha}\psi_s(t \mid \omega)\right) + k(t)c_S\left(\alpha + (1-\alpha)\sum_{\omega}\mu^0(\omega)s(t \mid \omega)\right)$$
$$+\sum_{\omega}\mu^0(\omega)\left[-c_S(1-\alpha)s(t \mid \omega) - (c_S + c_I)i(t \mid \omega) - c_D d(t \mid \omega)\right] + i(t \mid \omega)\left[\nu\psi_d(t \mid \omega) - \gamma_a\psi_i(t \mid \omega)\right]$$

If $Z := \sum_{\omega} s(t \mid \omega)i(t \mid \omega)\left(\psi_i(t \mid \omega) - \frac{1}{1-\alpha}\psi_s(t \mid \omega)\right) > 0$, then $H(t, X(t), k(t), \Psi(t))$ is increasing in $k(t)$, thus $k^*(t) = 1$. If $Z < 0$, then $H(t, X(t), k(t), \Psi(t))$ is concave in $k(t)$, hence a candidate for k^* is the solution of $\frac{\partial H(.)}{\partial k(t)} = 0$, i.e.,

$$\tilde{k}(t) = -c_S\frac{\alpha + (1-\alpha)\sum_{\omega}\mu^0(\omega)s(t \mid \omega)}{2\alpha\beta Z}.$$

As $Z < 0$, $\tilde{k}(t) > 0$. If $\tilde{k}(t) > 1$, then $k^*(t) = 1$. If $\tilde{k}(t) < 1$, then $k^*(t) = \tilde{k}(t)$. Therefore,

$$k^*(t) = \begin{cases} \tilde{k}(t), & \text{if } \tilde{k}(t) \in [0,1], \\ 1, & \text{otherwise.} \end{cases}$$

Proceeding as in the proof of Proposition 8, we obtain:

$$\dot{\psi}_s(t \mid \omega) - r\psi_s(t \mid \omega) = -k(t)^2\alpha\beta i(t \mid \omega)(\psi_i(t \mid \omega) - \tfrac{1}{1-\alpha}\psi_s(t \mid \omega)) + \mu^0(\omega)c_S(1-\alpha)(1-k(t)))$$

$$\dot{\psi}_i(t \mid \omega) - r\psi_i(t \mid \omega) = -k(t)^2\alpha\beta s(t \mid \omega)(\psi_i(t \mid \omega) - \tfrac{1}{1-\alpha}\psi_s(t \mid \omega)) + \mu^0(\omega)\left(c_S + c_I + \gamma_a\psi_i(t \mid \omega) - \nu\psi_d(t \mid \omega)\right)$$

$$\dot{\psi}_d(t \mid \omega) - r\psi_d(t \mid \omega) = \mu^0(\omega)c_D$$

Finally, the transversality conditions are, $\forall\omega \in \Omega$:

$\psi_s(T \mid \omega) = 0$;

$\psi_i(T \mid \omega) = -\mu^0(\omega)e^{-rT}\frac{1}{r+\gamma_a}\left(\frac{c_D}{r}\nu + c_S + c_I\right)$;

$\psi_d(T \mid \omega) = -\mu^0(\omega)e^{-rT}\frac{c_D}{r}$.

2.6 More uncertainty

The epidemic is characterized by two features:

1) the initial *epidemic penetration* $(\bar{s}, \bar{i}, \bar{a}, \bar{r}, \bar{d})$, where $\bar{s} \in [0,1]$ is the proportion of individuals who are not immune to the disease at time 0, $\bar{i} \in [0,1]$ is the proportion of

individuals infected with symptoms at time 0, $\bar{a} \in [0,1]$ is the proportion of individuals infected without symptoms at time 0, $\bar{r} \in [0,1]$ is the proportion of individuals who already recovered from the disease at time 0 and are now immune to it and $\bar{d} = 1 - \bar{s} - \bar{i} - \bar{a} - \bar{r} \in [0,1]$ the proportion of dead individuals at time 0;

2) the *medical parameters* of the disease $(\alpha, \beta, \gamma_a, \gamma_s, \nu)$, where $\alpha \in (0,1)$ is the proportion of asymptomatic types in the population, $\beta > 0$ is the contagiousness rate, $\gamma_a > 0$ is the recovery rate of asymptomatic types, and $\gamma_s > 0$ and $\nu > 0$ are the recovery and death rates of symptomatic types, respectively.

The tuple $\omega = \{\bar{s}, \bar{i}, \bar{a}, \bar{r}, \bar{d}, \alpha, \beta, \gamma_a, \gamma_s, \nu\}$ is the *epidemic state*, and we denote by Ω the finite set of possible epidemic states.

The evolution of the epidemics is now:

$$\begin{aligned}
\dot{s}(t \mid \omega) &= -\beta^{\omega} \bar{k}_S(t \mid \omega) s(t \mid \omega) \bar{k}_A(t \mid \omega) a(t \mid \omega) && (2.15)\\
\dot{a}(t \mid \omega) &= -\alpha^{\omega} \dot{s}(t \mid \omega) - \gamma_a^{\omega} a(t \mid \omega), && (2.16)\\
\dot{i}(t \mid \omega) &= -(1-\alpha^{\omega}) \dot{s}(t \mid \omega) - (\gamma_s^{\omega} + \nu^{\omega}) i(t \mid \omega), && (2.17)\\
\dot{r}(t \mid \omega) &= \gamma_a^{\omega} a(t \mid \omega) + \gamma_s^{\omega} i(t \mid \omega), && (2.18)\\
\dot{d}(t \mid \omega) &= \nu^{\omega} i(t \mid \omega), && (2.19)
\end{aligned}$$

The discounted expected payoff conditional on the epidemic being ω is thus:

$$v(k_j \mid \omega) = \int_0^T e^{-rt} e^{-\int_0^t p_j(s|\omega) k_j(s) \beta^{\omega} \bar{k}_A(s|\omega) a(s|\omega) ds} \left(p_j(t \mid \omega) k_j(t) \beta^{\omega} \bar{k}_A(t \mid \omega) a(t \mid \omega) v_I^{\omega} - c_S(1 - k_j(t)) \right) dt.$$

where:

$$v_I^{\omega} = -\frac{1}{r + \gamma_s^{\omega} + \nu} (c_S + c_I + \nu^{\omega} \frac{c_D}{r}) \tag{2.20}$$

The symmetric equilibrium is given by:

Proposition 11 (The symmetric equilibrium)**.** *The game has a unique symmetric equilibrium where all individuals play $\hat{k}$ defined by*

$$\hat{k}(t) = \min \left\{ \frac{c_S}{\beta^{\omega} \sum_{\omega} \mu(t,\omega) p(t \mid \omega) a(t \mid \omega) (\psi(t \mid \omega) - v_I)}, 1 \right\},$$

where

$$\begin{cases} \forall\, t \in [0,T],\ \forall\, \omega \in \Omega, \\ \dot{\psi}(t \mid \omega) - r\psi(t \mid \omega) = \hat{k}^2(t)\beta^{\omega} a(t \mid \omega)(\psi(t \mid \omega) - v_I) + (1 - \hat{k}(t))c_S, \\ \dot{p}(t \mid \omega) = -p(t \mid \omega)(1 - p(t \mid \omega))\beta^{\omega}\hat{k}^2(t)a(t \mid \omega), \\ \dot{s}(t \mid \omega) = -\beta^{\omega}\hat{k}^2(t)s(t \mid \omega)a(t \mid \omega), \\ \dot{a}(t \mid \omega) = -\alpha^{\omega}\dot{s}(t \mid \omega) - \gamma_a^{\omega} a(t \mid \omega), \\ \mu(t,\omega) = \frac{\mu^0(\omega)/(1-p(t|\omega))}{\sum_{\omega'} \mu^0(\omega')/(1-p(t|\omega'))}, \end{cases} \tag{2.21}$$

and $\psi(T \mid \omega) = 0$.

Chapter 3

Swedish Paradox

Dominique Baril-Tremblay[1]

Abstract[2]

Epidemic spreading can be suppressed by the introduction of social distancing measures such as hand washing, mask and lockdowns. Yet, when such measures are relaxed, new epidemic waves and infection cycles may occur. In this paper, with a SIR epidemiological model with vital dynamics, we analyze the effects of infection mitigation strategies on the arising of infection waves. We use SARS-CoV-2 values to calibrate our model and simulate different social distancing scenarios: permanent measures and temporary measures. We show that when the measures are permanent the results are intuitive whereas when they are temporary, for a certain period the cumulative number of infected individuals is greater when temporary distancing measures have been mandated than when none have.

Keywords: SIR model; Self-isolation; COVID-19 epidemic.

JEL codes: C73; D84, I12.

[1]Université Paris 1 - Panthéon Sorbonne, doumbaril@gmail.com.

[2]We have greatly benefited from discussions with Nicolas Klein, Flavio Toxvaerd, Chantal Marlat and Lucie Ménager. We are particularly indebted to Jean-François Blanchette for his support in the programming process of our simulations.

3.1 Introduction

Since the first case reported to the World Health Organization in December 2019, SARS-CoV-2, has spread rapidly across all continents. The key to slowing down the spread of infection is to reduce contact between individuals (Bavel et al. (2020), Min W Fong et al. (2020)). Several countries have chosen to curb the spread of the infection through the adoption of a series of non-pharmaceutical interventions (NPIs), including hand-washing, masks, isolation, social distancing and confinement (Wilder-Smith and Freedman (2020)). However, there is considerable heterogeneity in the scope and stringency in the application of the infection mitigation measures between countries, especially with regard to confinement (Petherick, Kira, et al. (2020)). Sweden made headlines in March 2020. While neighbouring countries adopted strict measures to "flatten the curve", Sweden's state epidemiologist categorically refused to mandate social distancing measures (Born, Dietrich, and Müller (2021), Cho (2020) and Juranek and Zoutman (2020)). Why faced with a similar infectious threat governments have adopted diametrically opposed strategies? Several factors influence government's response to a pandemic threat, such as the local risk assessments, hospital capacity (Kandel et al. (2020)) as well as the nature of the institutions and the cultural context of the country (Matthews Pillemer et al. (2015)).

In this paper, we will explore the effects of different infection mitigation strategies on the onset mechanisms of infection waves in a SIR *(Susceptible - Infected - Recovered)* epidemiological model with vital dynamics (births and deaths). Using this simple model, we will show that under certain conditions Sweden's approach of not mandating infection mitigation measures was the right one.

In our epidemiological model, individuals move from one compartment – susceptible, infected, recovered *(immune)* – to another as the infection progresses. The population regenerates through the process of births and deaths allowing the infection to become endemic. The system exhibits an oscillatory behavior around the endemic equilibrium, which is concretely translated by a succession of infection waves over time.

We used the SARS-CoV-2 values available in March 2020 to calibrate our model.

Our simulations provide insights into the impact of different infection mitigation strategies on the occurrence of different infection waves. We focused our analysis on two types of infection mitigation strategies: permanent and temporary social distancing measures. The persistence of measures over time impacts the rate at which subsequent waves of infection occur. The repercussion of the social distancing measure on the pattern of infection waves is quite intuitive: the higher the level of the social distancing measures, the lower the cumulative number of infected individuals. However, this is not the case when the measures are temporary.

The temporary measures have the effect, in the short term, of slowing the spread of the infection and at the same time protecting the population. However, when they are lifted the previously protected population is exposed to the infection. Since the infection is fuelled by the pool of susceptible individuals, infection waves arise faster. These successive waves of infection lead to a marked increase in the cumulative number of infected individuals. We observe that under certain conditions the cumulative number of infections when there has been temporary social distancing measures is higher than when there were no social distancing measure mandated.

In this article, we will show that under certain specific conditions it is preferable for the social planner not to adopt any confinement measures when facing a new infection if his goal is to reduce the number of cases. We call this phenomenon the Swedish Paradox. The Swedish Paradox is based on the oscillatory behavior of the SIR epidemiological model under certain epidemiological parameters and public containment policies.

Related literature. Our epidemiological model is based on the foundations developed by Kermack and McKendrick (1927). This simple epidemiological model is still valid and is the inspiration for many epidemiological models. These models have been used to study and predict the spread of many diseases such as measles (e.g. Matt J Keeling and Bryan T Grenfell (2002), L. Allen, M. Jones, and Martin (1991)), hepatitis (Shahdoust et al. (2015)), tuberculosis (Azeez et al. (2016)).

For several decades, researchers have developed the literature at the intersection of economics and epidemiology. In the theoretical literature, several papers have analyzed

the effects of social distancing measures in a context of optimal control (e.g. Sethi (1978), F. Chen et al. (2011) Rowthorn and Toxvaerd (2012)) or in a context of individual strategic decision (Reluga (2010), F. Chen (2012), Fenichel et al. (2011), Fenichel (2013), Toxvaerd (2019)). The SARS-CoV-2 pandemic accelerated the development of literature. The authors examined in the optimal control of the pandemic under the hypotheses of the SIR epidemiological model when the population is homogeneous (Kruse and Strack (2020), Eichenbaum, Rebelo, and Trabandt (2022), Alvarez, Argente, and Lippi (2020), C. Jones, Philippon, and Venkateswaran (2021), Glover et al. (2020)) or when the risks for a subpopulation are higher (Acemoglu et al. (2021), Rampini (2020), Bairoliya and İmrohoroğlu (2022)). Toxvaerd (2020), Farboodi, Jarosch, and Shimer (2021) and Brotherhood et al. (2020) studied the problem of individuals who arbitrate the costs and benefits of self-isolation in the SIR model. Baril-Tremblay, Marlats, and Ménager (2021) introduce learning into an SIR epidemiological model and analyze the epidemic dynamics when individuals decide whether or not to self-isolation based on their subjective beliefs. Building on their previous work, Baril-Tremblay, Marlats, and Ménager (2022) introduced uncertainty into their model .

Our research centers around the periodic nature of epidemics causing successive waves of infection to emerge over time. It is important to understand the effects of the various infection mitigation strategies on the arising of future waves in order to predict and control them. Focusing our attention only on getting through the first wave can leave us exposed and unprepared for the following ones.

Periodicity is a normal component of epidemics and has interested researchers for decades (Webster (1799), Soper (1929), Hethcote and Levin (1989), Baryarama, Luboobi, and Mugisha (2005) for example). Researchers have used different mechanisms, endogenous and exogenous, to incorporate oscillatory behavior into epidemiological compartmental models (London and Yorke (1973), Bryan Thomas Grenfell and Roy Malcolm Anderson (1989), Bolker and Bryan Thomas Grenfell (1993), N. M. Ferguson, Nokes, and Roy M Anderson (1996), Hethcote (1997) and Earn et al. (2000)). Although these models allow interesting conclusions to be drawn, they are difficult and mathematically cumbersome to manipulate. Earn (2008) is the first to have laid the

foundations for the natural appearance of oscillatory behavior within an epidemiological model. Greer et al. (2020) formalize the principle by demonstrating that the oscillations arise naturally from the epidemiological model when the model has a population regeneration process either via the birth and death dynamic or via waning immunity (Giannitsarou, Kissler, and Toxvaerd (2021)) Like Greer et al. (2020) we have chosen to adopt a simpler and more flexible model.

In hindsight, Cho (2020) and Born, Dietrich, and Müller (2021) demonstrated that Sweden's state epidemiologist erred in refusing to mandate social distancing measures. Not only could the imposition of stricter social distancing measures have reduced the number of cases by up to 75% (Cho (2020)), a 9-week lockdown could have reduced the death toll by 38% (Born, Dietrich, and Müller (2021)). However, hindsight is 20/20. As we will show later in this paper, Sweden's strategy would have been the right one if the vaccines had arrived much later and if it had been impossible for the social planner to impose permanent social distancing measures.

The remainder of the paper is organized as follows. Section 2 introduces economic and epidemiological models and characterizes the properties of oscillations around endemic equilibrium. In section 3, we analyze the effects of temporary infection mitigation measures and define the Swedish Paradox. In section 4, we calibrate our model to the SARS-CoV-2 epidemiological values available at the beginning of the pandemic and evaluate different scenarios of permanent and temporary measures.

3.2 Models

Several studies show that NPIs are effective in slowing the spread of infection and reducing adverse health outcomes (Born, Dietrich, and Müller (2021), Cho (2020), Flaxman et al. (2020) and Juranek and Zoutman (2020)). The choice of the social planner to implement or not NPIs is based on economic and epidemiological constraints.

3.2.1 Economic model

Time $t \in [0, +\infty)$ is continuous and discounted at rate $r > 0$. A disease is spreading in an initially completely susceptible population, against which a vaccine will be introduced at period $T > 0$. While waiting for the arrival of the vaccine, the social planner can impose NPIs to slow down the progression of the infection.

NPIs reduce contact between individuals and can result in a decrease in social and physical activities leading to a deterioration in the mental health of individuals, while infections lead to a decline in the physical health. When choosing the optimal social distancing level $\kappa_t \in [0, 1]$, the social planner must balance the mental and physical health of her population. We suppose that (κ_t) is the social distancing level at t, ie, the impact of NPIs on the level of contact between individuals at each period. When $\kappa_t = 1$ people double lock themselves at home and when $\kappa_t = 0$, they go about their business as usual. We denote c_H the cost of social distancing measures by units of time and c_I the cost of infection by a unit of time. The social planner imposes a reduction of contacts between individuals by a constant κ proportion. Each period $t \leq T$ the social planner choose κ_t that minimize the value function $v(\kappa_t) = c_H\kappa_t + c_I i_t(\kappa)$, where $i_t(\kappa)$ is the proportion of the population that is infected in each period t[3]. In our model, the infection-related morbidity rate is zero and the performance of the social planner in dealing with the pandemic will only be evaluated on the number of infected individuals. The congestion of health systems due to the SARS-CoV-2 is a real headache for the social planner. Faced with the large number of cases, the social planner is forced to postpone other procedures to free up the necessary resources to take care of individuals infected with the new infection.

In order not to confuse the population, we assume that the social planner chooses a constant social distancing level κ that will be imposed and respected between the exogenous periods $t = \underline{t}$ and $t = \bar{t}$, with $0 \leq \underline{t} < \bar{t} \leq T$. The social planner's response to the pandemic is evaluated at $t = T$.

The choice of κ has a direct effect on the costs of social distancing measures and an indirect effect on the costs of infection. When minimizing her value function, the social

[3]We will discuss this parameter in depth in Section 3.2.2

planner must therefore take into account the effect of his choice of social distancing level on the dynamics of the infection, described in the next section.

3.2.2 Epidemiological model with vital dynamic

To model the spread of the infection in the population is described by a compartmental *Susceptible-Infected-Recovered* (SIR) epidemiological model[4] with stationary vital dynamic (birth and natural deaths).

The population. The model assumes that at time t, a large population $N(t)$ in presence of a non-fatal disease, can be subdivided into three different groups: infected individuals denoted $I(t)$, healthy but susceptible to the disease individuals denoted by $S(t)$, and healthy individuals removed from the susceptible group because they recovered from the disease $R(t)$. The incubation period is neglected: in our model, individuals remain in the S compartment until they are infectious, at which time they switch from the S compartment to the I compartment.

$$N(t) = S(t) + I(t) + R(t)$$

Infection dynamics. We assume the population size to be constant since the time scale for substantial changes to be observed in birth rates (decades) is usually much longer than an epidemic (a few months). Following Kermack and McKendrick (1927) we assume that the birth rate is equal to the natural mortality rate, $\mu > 0$, and that newborns are susceptible which means, there is no vertical transmission from mother to child.

We normalize the population, $1 = s_t + i_t + r_t$ where: $s_t = \frac{S(t)}{N(t)}$, $i_t = \frac{I(t)}{N(t)}$ and $r_t = \frac{R(t)}{N(t)}$. Therefore, s_t is the ratio of healthy individuals on the total population, i_t is the ratio of the infected individuals on the total population, and r_t is the proportion of removed individuals on the total population.

The compartmental diagram in figure 3.1 illustrates the relationship between the different compartments within the SIR epidemiological model with stationary vital

[4]The SIR epidemiological model has been developed by Kermack and McKendrick in a series of paper Kermack and McKendrick (1927).

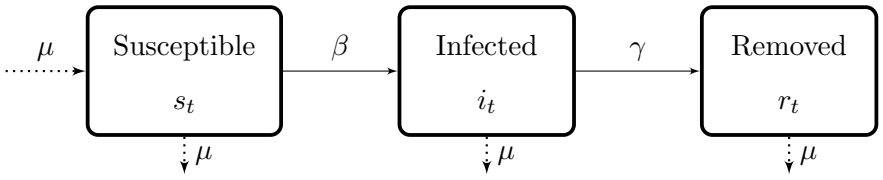

Figure 3.1: Compartmental SIR model with stationary vital dynamic

dynamic framework. Boxes represent the three different compartments. Dashed arrows represent the vital dynamics while solid arrows represent the infection dynamics.

Over time the distribution of individuals among each group varies. Under the homogenous mixing hypothesis, individuals move from the susceptible to the infected group, at the rate $\beta \in [0, 1]$, when a susceptible individual comes in contact with an infected individual. Conversely, some individuals will heal, moving from the infected group to the immunized group at the rate $\gamma > 0$, the recovery rate. The differential equations describing the dynamics of the system under all these assumptions have the following form:

$$\begin{aligned} \dot{s} =& -\beta\kappa i s + \mu(1-s) \\ \dot{i} =& \beta\kappa i s - (\gamma+\mu) i \\ \dot{r} =& \gamma i - \mu r \end{aligned} \tag{3.1}$$

where $s(0) > 0$, $i(0) > 0$, $r(0) \geq 0$ and $s(0) + i(0) + r(0) = 1$. Individual face short outbreak with lifelong consequences. Since at any point in time, $s + i + r = 1$, the system can be summarized by :

$$\begin{aligned} \dot{s} =& -\beta\kappa i s + \mu(1-s) \\ \dot{i} =& \beta\kappa i s - (\gamma+\mu) i \end{aligned} \tag{3.2}$$

for any social distancing policy κ.

The transmission rate $\beta = b\kappa$ embed two distinct sub-processes: the social behaviour i.e. the number and nature of contacts between individuals κ, and the biological contagion process $b \in [0, 1]$ which is the probability that appropriate contact[5] between two individuals will result in an infection. By choosing a level of contact κ economic agents

[5]Different infections have different modes of transmission, and the nature of the contacts that can lead to infection differs from one infection to another.

can influence the dynamics of the infection. This choice parameter is the thread that connects the economic model and the epidemiological model.

The previous equations describe the dynamics of a population facing an infection. Depending on the epidemiological parameters of the model, an epidemic may spread or die out. To determine the epidemiological importance of an infection, we will look at the expected number of secondary infection cases caused by a single typical infective case during his entire period of infectivity in a wholly susceptible population, the *basic reproduction number* (BRN)[6], denoted R_0. R_0 is a dimensionless threshold parameter: if $R_0 > 1$ the epidemics take off and if $R_0 < 1$ the epidemic dies out. In the SIR compartmental model with vital dynamics, in the presence of a non-fatal disease, the basic reproduction number is expressed as:

$$R_0 = \frac{\beta}{(\gamma + \mu)}. \tag{3.3}$$

This dimensionless parameter plays an important role in characterizing the equilibriums points of the system (3.2).

Equilibriums points. Since the equation system (3.2) is nonlinear, to further our analysis we will linearize the system around the equilibrium points. Therefore, we are going to identify the equilibria and define the conditions for which they are asymptotically stable. The asymptotic stability of an equilibrium means that for given initial conditions, a point remains close to equilibrium following a disturbance and approaches the equilibrium when $t \to \infty$. An equilibrium point is unstable if it is not stable.

The equation system (3.2) is at the equilibrium when $\dot{s} = \dot{i} = 0$. Rearranging the terms of the second equation such that, $\dot{i} = (\gamma + \mu)i(R_0\kappa s - 1)$, we see that $\dot{i} = 0$ when $i = 0$ or when $R_0\kappa s = 1$. By substituting $i = 0$ in the first equation of the system of equation (3.2), we see that when $i = 0$, $\dot{s} = 0$, when $s = 1$. Naturally, when there are no infected individuals in the population, the infection cannot spread and all individuals remain susceptible. To find the second equilibrium, we substitute $s = \frac{1}{(R_0\kappa)}$ into the first equation. We find that when $s = \frac{1}{(R_0\kappa)}$, $\dot{s} = 0$, when $\frac{\mu}{\mu+\gamma}(1 - \frac{1}{\kappa R_0})$.

[6]The basic reproduction number was first introduced by Dietz (1975) and Hethcote (1975), see Wang et al. (2016), Anderson and May (1992) for useful illustration of the concept.

The system admits two equilibriums points: a disease-free equilibrium (dfe) and an endemic equilibrium (ee).

$$(s_{dfe}, i_{dfe}) = (1, 0) \tag{3.4}$$

$$(s_{ee}, i_{ee}) = (\frac{1}{\kappa R_0}, \frac{\mu}{\mu+\gamma}(1 - \frac{1}{\kappa R_0})) \tag{3.5}$$

We will use the approach proposed by Matt J. Keeling and Rohani (2008)[7], and analyze the eigenvalues to determine the stability of the balance points. A stable system is one in which all eigenvalues have a real part less than zero.Since we are dealing with a system with two equations we will have two eigenvalues per equilibrium.

The eigenvalues *Lambda* are the solutions of $det(J - \Lambda \boldsymbol{I}) = 0$ where

$$\begin{aligned} J &= \begin{pmatrix} \frac{\partial \dot{s}(s^*,i^*)}{\partial s^*} & \frac{\partial \dot{s}(s^*,i^*)}{\partial i^*} \\ \frac{\partial \dot{i}(s^*,i^*)}{\partial s^*} & \frac{\partial \dot{i}(s^*,i^*)}{\partial i^*} \end{pmatrix} \\ &= \begin{pmatrix} -\mu - \beta\kappa i^* & -\beta\kappa s^* \\ \beta\kappa i^* & \beta\kappa s^* - (\gamma+\mu) \end{pmatrix} \end{aligned} \tag{3.6}$$

is the Jacobian matrix of first order partial derivatives of the equation system (3.2) around the equilibrium (s^*, i^*). To find the eigenvalues, we will replace (s^*, i^*) in J by the equilibria (s_{dfe}, i_{dfe}) and (s_{ee}, i_{ee}) and solve the caracteristic polynomial associated.

At the disease-free equilibrium, the Jacobian matrix takes the following form:

$$J_{dfe} = \begin{pmatrix} -\mu & -\beta\kappa \\ 0 & \beta\kappa - (\mu+\gamma) \end{pmatrix}. \tag{3.7}$$

The eigenvalues of the matrix (3.7) are the roots of the quadratic equation:

$$\begin{aligned} |J_{dfe} - \Lambda \mathbf{I}| = \left| \begin{pmatrix} -\mu & -\beta\kappa \\ 0 & \beta\kappa - (\mu+\gamma) \end{pmatrix} - \begin{pmatrix} \Lambda & 0 \\ 0 & \Lambda \end{pmatrix} \right| = 0 \\ (-\mu - \Lambda)(\beta\kappa - (\mu+\gamma) - \Lambda) = 0. \end{aligned} \tag{3.8}$$

The eigenvalues of this matrix are $-\mu$ and $\beta\kappa - (\mu+\gamma)$. Thus as long as $\beta\kappa < (\mu+\gamma)$ i.e. $R_0\kappa = \frac{\beta\kappa}{\gamma+\mu} < 1$, every real parts of the eigenvalues are negative and the disease-free equilibrium is asymptotically stable.

[7] You will find the approach in chapter 2 in box 2.4

At the endemic equilibrium, the Jacobian matrix takes the following form:

$$J_{ee} = \begin{pmatrix} -\mu\kappa R_0 & -(\mu+\gamma) \\ \mu(\kappa R_0 - 1) & 0 \end{pmatrix} \tag{3.9}$$

The eigenvalues of the matrix (3.9) are the roots of the quadratic equation:

$$\begin{aligned} |J_{ee} - \Lambda\mathbf{I}| = \left| \begin{pmatrix} -\mu\kappa R_0 & -(\mu+\gamma) \\ \mu(\kappa R_0 - 1) & 0 \end{pmatrix} - \begin{pmatrix} \Lambda & 0 \\ 0 & \Lambda \end{pmatrix} \right| = 0 \\ \Lambda^2 + \mu\kappa R_0 \Lambda + \mu(\kappa R_0 - 1)(\mu+\gamma) = 0, \end{aligned} \tag{3.10}$$

which are:

$$\Lambda = \frac{-\mu\kappa R_0 \pm \sqrt{\mu^2(\kappa R_0)^2 - 4\mu(\kappa R_0 - 1)(\mu+\gamma)}}{2}. \tag{3.11}$$

Knowing that the infection period $1/\gamma$ is significantly shorter than the life expectancy $1/\mu$, we will neglect the quadratic terms in μ as suggested by L. J. Allen et al. (2008). The eigenvalues of the matrix (3.9) are therefore approximately:

$$\Lambda \approx \frac{-\mu\kappa R_0}{2} \pm \sqrt{-\mu(\kappa R_0 - 1)(\gamma+\mu)}. \tag{3.12}$$

The eigenvalues of matrix (3.9) have a negative real part $(-\mu(\kappa)R_0)/2$, and an imaginary part $\sqrt{-\mu((\kappa)R_0 - 1)(\gamma+\mu)}$. Therefore the endemic equilibrium exist when $R_0\kappa > 0$ and the system tends asymptotically towards the endemic equilibrium via oscillatory dynamics. The characterization of these oscillations is the warp and woof of our analysis of social distancing strategies.

Interestingly, the epidemiological parameterization and the level of confinement both influence the equilibrium points asymptomatic stability. Moreover, the condition which ensures instability of the disease-free equilibrium is the same which ensure the stability of the endemic equilibrium, thusly the SIR epidemiological model exhibit a threshold behavior.

3.2.3 Oscillations

Oscillations around the endemic equilibrium create successive waves of infection over time. From a public health policy perspective, it is essential to understand and anticipate these infection waves. The number of periods that elapse between two successive waves of infection is called the pseudo-period (Taylor (2005)).

Since the real part of the eigenvalues is negative, the SIR epidemiological model with vital dynamic at the endemic equilibrium is therefore analogous to a damped oscillator[8]. Since the system has a damped oscillatory behavior, the amount of time it takes for one complete cycle of motion is called a pseudo-period. It is denoted by T and, following Matt J. Keeling and Rohani (2008)[9], is obtained by multiplying the inverse of the complex part of the eigenvalues by 2π:

$$T = \frac{2\pi}{\sqrt{\mu(\kappa R_0 - 1)(\gamma + \mu)}}. \tag{3.13}$$

The pseudo-period depends only on the social distancing level and the epidemiological parameters. When $\kappa R_0 > 1$, $\frac{\partial T}{\partial \kappa} = -\frac{R_0 \pi}{\sqrt{\mu(\mu+\gamma)(\kappa R_0 - 1)^3}} < 0$. The higher the social distancing level κ, the shorter the pseudo-period T, therefore, the highere the social distancing level, the closer the subsequent infection waves are.

Everything we have described so far assumes that the social distancing level is constant and permanent, which means that the social distancing measures are the same between the announcement period $\underline{t} < T$ and the introduction of a vaccine at a period T. This type of stringent social distancing measure can be difficult for the social planner to justify and implement.

3.3 Temporary social distancing measures

Non-pharmaceutical interventions are socially (Ferry et al. (2021)) and economically (Kong and Prinz (2020), Sheridan et al. (2020)) unsettling. The effectiveness of these

[8] For more information on damped oscillators, see Goldstein, Poole, and Safko (2002)

[9] see Chapter 2, box 2.4

transmission mitigation measures depends on the extent to which the population adheres to them (Cho (2020), Flaxman et al. 2020, Born, Dietrich, and Müller (2021)). Despite their importance for public health, we observe a decrease in adherence to NPIs either because individuals have a biased infection perceived risk (Cava et al. (2005)), strong financial pressure (Bodas and Peleg (2020), Atchison et al. (2021)) or policy-induced fatigue (Smith et al. (2020), Petherick, Goldszmidt, et al. (2021), Di Domenico et al. (2021), Pépin et al. (2020)). Subsequently, transmission mitigation measures can be difficult to implement up to the vaccine arrival at period T. Hence, the social planner may wish to impose temporary infection intigation measure for a short period.

We assume that the social planner mandate social distancing measure temporarily between periods $\underline{t}$ and $\bar{t}$, where $0 < \underline{t} < \bar{t} < T$. Consider two social distancing levels: $\kappa_0 \in]0, 1]$ and $\kappa_1 \in [0, 1]$ where $\kappa_0 > \kappa_1$ and $\kappa_1 R_0 > \kappa_0 R_0 \geq 1$[10]. The social distancing measures are implemented as follows:

$$\kappa(t) \begin{cases} k_0 & \text{if } t \in [\underline{t}, \bar{t}[\\ k_1 & \text{if } t \in [\bar{t}, T[. \end{cases} \tag{3.14}$$

Since, as demonstrated previously in the section (3.2.2), the endemic equilibrium is asymptotically stable for any κ, as long as $\kappa R_0 > 1$, we know that between the periods $\underline{t}$ and $\bar{t}$, the system tends towards the endemic equilibrium $(s_{ee}(\kappa_0), i_{ee}(\kappa_0)) = (\frac{1}{\kappa_0 R_0}, \frac{\mu}{\mu+\gamma}(1 - \frac{1}{\kappa_0 R_0}))$. However, when the social distancing level changes at period $\bar{t}$, the endemic equilibrium shifts and the system will oscillate towards the new endemic equilibrium $(s_{ee}(\kappa_1), i_{ee}(\kappa_1)) = (\frac{1}{\kappa_1 R_0}, \frac{\mu}{\mu+\gamma}(1 - \frac{1}{\kappa_1 R_0}))$.

The oscillatory behavior of the system is affected by two elements: the social distancing level κ and the epidemiological parameters that are assumed to be constant. Thus, when the social distancing level changes, the pseudo-periods and the amplitude of the oscillations shift. When the social distancing level goes from κ_0 to κ_1 the pseudo-periods of the oscillations will change from $T(\kappa_0) = \frac{2\pi}{\sqrt{\mu(\kappa_0 R_0 - 1)(\gamma+\mu)}}$ to $T(\kappa_1) = \frac{2\pi}{\sqrt{\mu(\kappa_1 R_0 - 1)(\gamma+\mu)}}$. The oscillations quietly stabilize around the new endemic equilibrium and the pseudo-period slowly adjusts. This stabilization process is at the origin of the Swedish Paradox.

[10] We are only interested in the case where the infection is endemic

3.3.1 Swedish Paradox

Temporary social distancing measures are not always the strategy that minimizes the number of infected individuals. While they reduce the number of infected individuals when implemented, they also have the effect of shortening the pseudo-period between oscillations and thus the delay between different infection waves. Their effects are felt long after the social distancing measures have been lifted. The rhythm and trajectory of the oscillatory system towards the endemic equilibrium is influenced by these temporary measures. The early arrival of infection waves means that, during certain periods, the cumulative number of infected individuals is greater when temporary distancing measures have been imposed than when they have not. We have named this phenomenon the Swedish Paradox.

3.4 Illustration

The purpose of this section is to illustrate the impact of different social distancing strategies on the oscillations of the SIR epidemiological model with vital dynamics, and to highlight the different lessons we can draw for future public policies implementation.

3.4.1 Calibration

Following Fenichel et al. (2011), we assume that individuals discount time at rate $r = 0.99986\%$, and that initially the population is distributed among epidemiological compartments such as $s(0) = 0.99$, $i(0) = 0.01$ and $r(0) = 0$.

The social planner's response may not occur as soon as the new infection break out. He could take a few periods to assess the situation or the first cases may go unnoticed (Baril-Tremblay, Marlats, and Ménager (2022)). This is very much in line with what happened when SARS-CoV-2 first appeared. We assume that the social planner announces the start of social distancing measures 25 days after the first case is detected, at period $\underline{t} = 25$ and the end of social distancing measures at period

$T = 20000$ for the scenarios where social distancing measures are permanent and in period $\bar{t} = 375$ for the scenarios where social distancing measures are temporary.

Estimates of epidemiological parameter values today are not necessarily the same as they were at the beginning of the SARS-CoV-2 pandemic for two main reasons. First, as the epidemic progresses, we learn more and more about the new infection, thus epidemiological parameter estimation become more refined. Second, variants appear. Since our initial motivation is to understand Sweden's decision not to impose social distancing measures, in March 2020, we will use estimates calculated with the data available at that time.

We will use the estimates provided by A. Remuzzi and G. Remuzzi (2020), i.e. $R_0 = 2.76$ and an average infection duration of 15 days. From the average infection duration, we obtain directly $\gamma = 1/15$. The demographic dynamic is estimated by the inverse of the discount rate which is $\mu = 0.00014$. The transmission rate β is difficult to estimate since it is not directly observable. We will use the estimate of R_0, γ and μ to infer it's the value. In our model, $R_0 = \beta/(\gamma + \mu)$ and therefore $\beta = R_0(\gamma + \mu) = 0.184$.

Finally, to simplify the analysis, we will arbitrarily assume that $c_H = 0$ and $c_I = 1$. The social planner's value function can be rewritten as: $v(k, i(k)) = c_I \int_0^T i_t(\kappa)dt$ and to maximize the latter it simply suffices to minimize the number of infected individuals between $t = 0$ and $t = T$.

3.4.2 Permanent social distancing

We will first assume that social distancing measures are permanent. We will focus our attention on the case that respects the asymptotic stability condition for the endemic equilibrium, i.e. $\kappa R_0 > 1$. Given the previously defined calibration, the scenarios of interest are those for which $\kappa < (1 - R_0)/R_0 = 0.6377$. We have selected three scenarios: no measure ($\kappa = 0$), a low level of social distancing ($\kappa = 0.25$) and a medium level of social distancing ($\kappa = 0.50$).

The endemic equilibrium associated with each scenario is: $(s_{ee}(\kappa = 0), i_{ee}(\kappa = 0)) = (0.36232, 0.00134)$, $(s_{ee}(\kappa = 0.25), i_{ee}(\kappa = 0.75)) = (0.48309, 0.00108)$ and $(s_{ee}(\kappa =$

$0.5), i_{ee}(\kappa = 0.5)) = (0.72464, 0.00058)$. As shown in figure 3.2, all three endemic equilibriums are asymptomatically stable. The higher the social distancing level, the higher the proportion of susceptible individuals and the lower the proportion of infected at the endemic equilibrium.

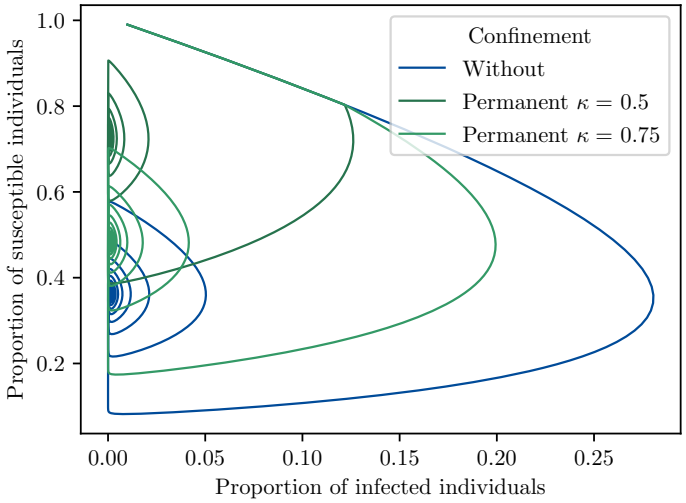

Figure 3.2: Asymptotic stability of equilibriums under permanent social distancing measures.

The different scenarios of social distancing lead to different oscillatory patterns. As can be seen from the left panel of figure 3.3, the higher the initial social distancing level, the smaller the amplitude of the first infection wave. When the level of social distancing is high ($\kappa = 0.5$), the first wave reaches its maximum prevalence 0.12617 at time 34, while with a low level of social distancing ($\kappa = 0$), the first wave reaches its maximum prevalence 0.19937 at time 47.

Moreover, the right panel of figure 3.3 shows that the lower the social distancing level, the faster the second wave of infection appends. The peak of the second wave of infection occurs at $t = 5869$ when $\kappa = 0$, at $t = 7700$ when $\kappa = 0.25$ and at $t = 14088$ when $\kappa = 0.5$. Note: in the scenario where there is no social distancing measures, four waves of infection occur before there is a second wave of infection in the scenario where the social distancing level is high.

The system goes through a transition phase in which the pseudo-periods are longer than predicted by the model. After this transition phase the system becomes marginally

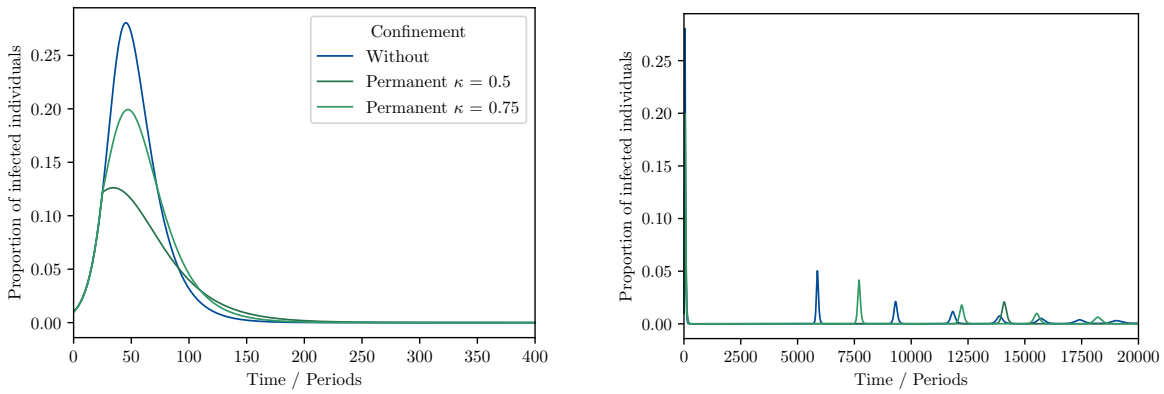

Figure 3.3: Proportion of the population infected each period between periods 0 and 400 (left panel) and between periods 0 and 20000 (right panel).

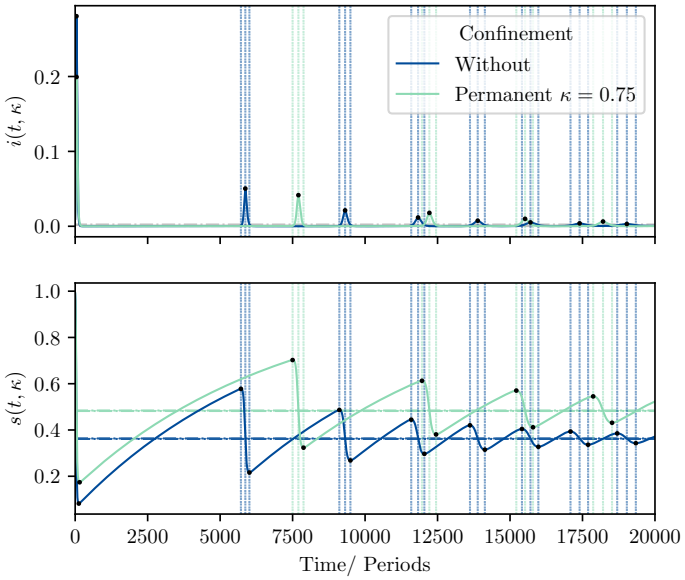

Figure 3.4: Top panels: proportion of the population infected each period. Bottom panel: proportion of the population susceptible each period. *Position markers mark the maximum and minimum of each oscillation of the susceptible curve as well as the maximum of each wave of the infected curve. Dashed lines have been added to make it easier to visually track values from one panel to another.*

stable and the pseudo-periods are $T(\kappa = 0) = 1550$, $T(\kappa = 0.75) = 1988$ and $T(\kappa = 0.5) = 3337$, which are the length predicted by the model.

As can be seen in figure 3.4, waves of infection are closely related to the process of susceptible population growth. In the absence of infection, the pool of susceptible individuals grows to a point where the epidemic pick up steam. After this point, infections increase at the expense of the pool of susceptible individuals which decreases

at a great speed. When the proportion of susceptible individuals crosses the endemic equilibrium, the epidemic loses speed. The epidemic subsides and the pool of susceptible individuals resumes growth until the next wave of infection.

Over time, subsequent phases of infection increase the cumulative number individual who has been infected. When social distancing measures are permanent, as illustrated in 3.5, these waves of infection are monotonically non-decreasing and do not intersect.

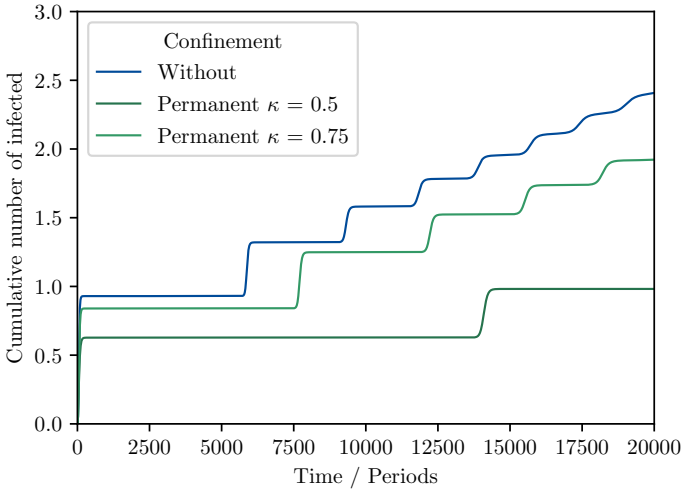

Figure 3.5: Cumulative number of infected individual.

The analysis of the effect of permanent social distancing policies on the dynamics of the SIR epidemiological model with vital dynamics is quite straight forward. The coordinates of the endemic equilibrium are permanently influenced by the level of social distancing imposed by the social planner and the system tends asymptotically towards these equilibriums. Ultimately, the higher the level of social distancing, the longer the waves of infection are spaced out in time and the lower the cumulative number of infected individuals.

3.4.3 Temporary social distancing measures

Temporary social distancing measures offer a more interesting analytical framework than permanent social distancing measures for studying the effects of social distancing policies on infection dynamics. The imposition of temporary social distancing measures

slows down the progression of the infection for a short period. However, when these measures are lifted, the epidemic, fueled by the pool of susceptible individuals, resumes and the infection waves follow one another more rapidly than in the scenario without social distancing measures or with permanent social distancing measures.

We will illustrate this mechanism, by comparing three levels of social distancing measures. As in the section 3.4.2, we will focus our attention on the values of κ which respect the condition $\kappa R_0 > 1$, thus $\kappa < 0.6377$. In the first scenario, the social planner will choose not to implement any social distancing measures ($\kappa = 0$), while in the other two scenarios, measures are mandated temporarily. We assume that the levels of social distancing are respectively $\kappa = 0.75$ and $\kappa = 0.5$ between the periods $t = \underline{t} = 25$ and $t = \overline{t} = 375$, then $\kappa = 0$ after the period $t = \overline{t} = 375$ for all scenarios.

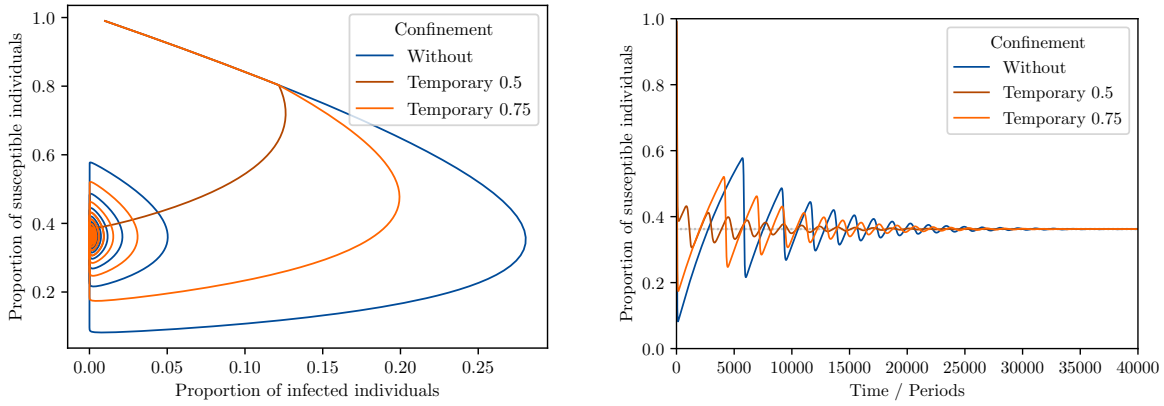

Figure 3.6: Convergence of the various endemic equilibriums according to different social distancing scenario.

As illustrated in the left panel of figure 3.6, between periods $t = \underline{t} = 25$ and $t = \overline{t} = 375$, the orange curves, representing the two scenarios where social distancing measures are temporary, begin their spiral of convergence towards their respective endemic equilibrium, i.e.: $(s_{ee}(\kappa = 0.75), i_{ee}(\kappa = 0.75)) = (0.48309, 0.00108)$ and $(s_{ee}(\kappa = 0.5), i_{ee}(\kappa = 0.5)) = (0.72464, 0.00058)$. However, at the end of the temporary social distancing measures, their course is abruptly redirected to the endemic equilibrium $(s_{ee}(\kappa = 0), i_{ee}(\kappa = 0)) = (0.36232, 0.00134)$. Thus, in all three scenarios the system oscillates around the same endemic equilibrium, the endemic equilibrium without social distancing (see right panel of figure 3.6).

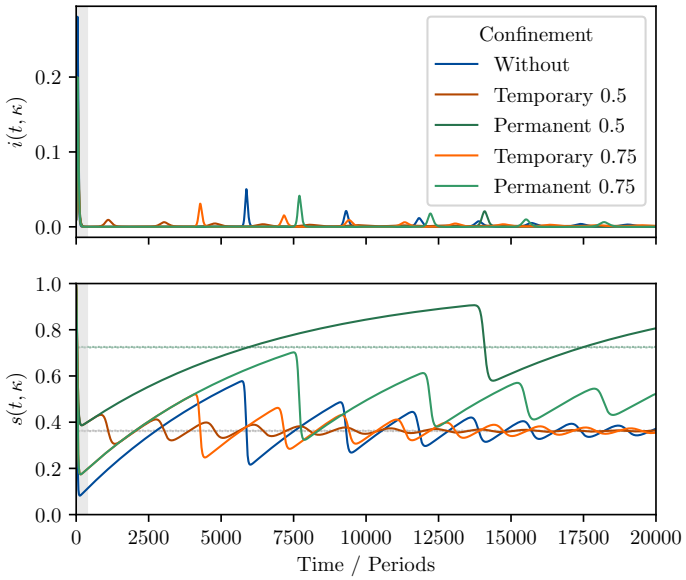

Figure 3.7: Top panel: proportion of the population infected each period. Botton panel: proportion of the population susceptible each period. The horizontal dotted line mark the endemic equilibrium position for each scenario.

The system goes through a transition phase where the pseudo-periods depend on the level of susceptible individual with respect to the endemic equilibrium. As briefly described previously, the infection waves feed from the pool of susceptible individuals. Thus, the proportion of susceptible individuals at the end of the temporary social distancing measures impacts the speed at which the epidemic will resume. As illustrated in figure 3.7, when the social distancing level is low $\kappa = 0.5$ (the dark orange curve), the proportion of susceptible individuals at the end of restrictions is $s(t = 374, \kappa = 0.5) = 0.3993$ and the second infection peaks at $t = 609$. As an indication, when the same measures are implemented permanently, the peak of the second wave is reached much later, at $t = 14088$. Similarly, when the level of social distancing is high $\kappa = 0.75$ (the light orange curve), the proportion of susceptible individuals at the end of the social distancing measures is $s(t = 374, \kappa = 0.25) = 0.1966$. The pool of susceptible individuals takes longer to reach its critical level, but eventually the second wave arises and peaks at $t = 4279$ whereas when these measures are permanent the second wave peaks at $t = 7700$. Note that when the system tends to infinity, the pseudo-periods are the same for the three scenarios, ie $T(\kappa = 0) = 1550$.

As figure 3.8 shows, the dynamic between the proportion of susceptible individuals

and the wave of infection is the same when social distancing measures are temporary as when they are permanent.

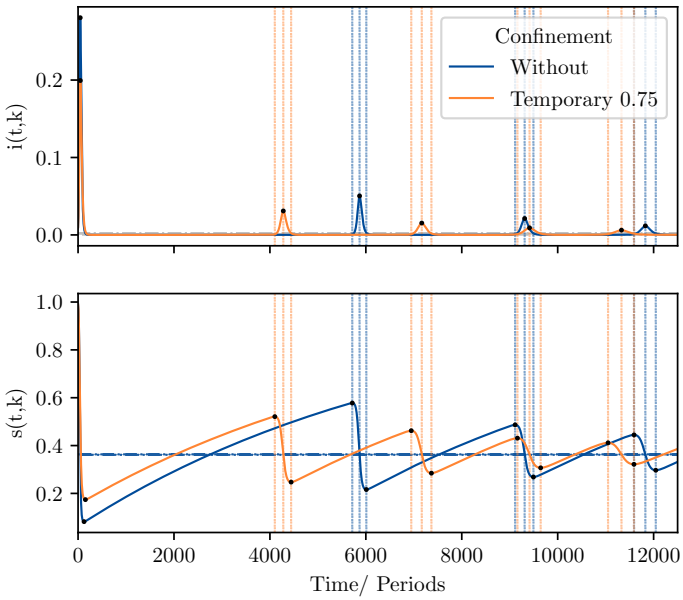

Figure 3.8: Top panels: proportion of the population infected each period. Bottom panel: proportion of the population susceptible each period. *Position markers mark the maximum and minimum of each oscillation of the susceptible curve as well as the maximum of each wave of the infected curve. Dashed lines have been added to make it easier to visually track values from one panel to another.*

The cumulative number of infected individuals increases in stages. When a wave occurs, it leads to a sharp increase in the number of infected individuals. Successive waves of infection cause the cumulative number of infected individuals to constantly increase. As can be seen in figure 3.9, at certain periods, the curves of the different scenarios intersect. When the orange curves pass above the blue curve the cumulative number of infected individuals is greater when the social planner has temporarily imposed social distancing measures than when there have been no measures. It is this phenomenon that we have called the Swedish Paradox.

3.4.4 Swedish Paradox

As described in the previous sections, under certain conditions, waves of infection occur faster when temporary social distancing measures have been imposed than when

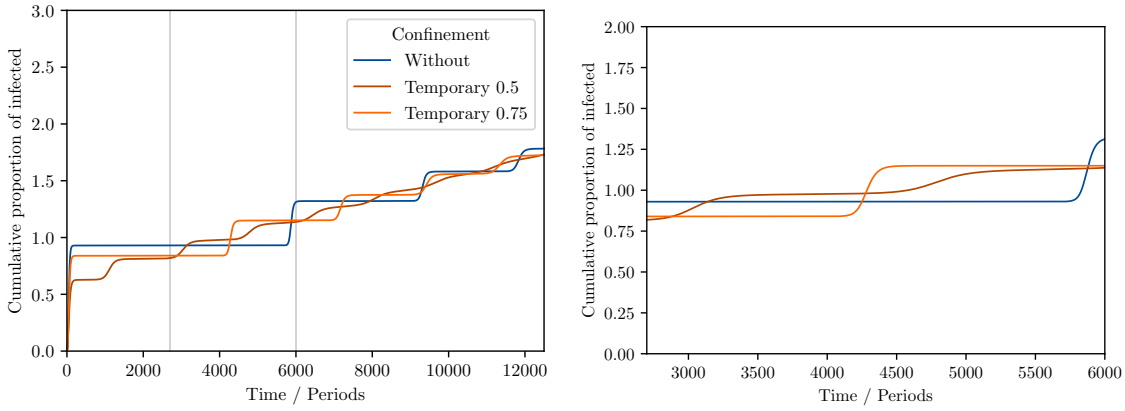

Figure 3.9: Graphic illustration of the Swedish Paradox by comparing the cumulative number of infections without social distancing measures (blue) to different scenarios of temporary social distancing measures (orange) for periods 0 to 12000 (right panel) and for periods 2700 to 6000 (left panel).

they have not. This results in the cumulative number of infections when temporary social distancing measures were in place being greater than the cumulative number of infections when social distancing measures were not in place for certain periods. We call this phenomenon the Swedish Paradox. Given the oscillatory dynamics of the SIR epidemiological model with vital dynamics, this phenomenon is repeated several times. In our example shown in Figure DynaB12, it is repeated 8 times, i.e., when the periods are colored yellow.

The social planner who wishes to minimize the number of people infected before a vaccine arrives will need to consider the Swedish paradox when choosing the optimal social distancing strategy. The social planner who wishes to minimize the number of people infected before a vaccine arrives will need to consider the Swedish paradox when choosing the optimal social distancing strategy. In the example in 3.10, if the vaccine arrives at a time in the interval $t \in [4251 - 5880]$ the social planner will minimize the number of infected individuals by not mandating any social distancing measures vs. temporary measures. A pessimistic social planner who believes that the vaccine will take 11.65 years and 16.11 years to reach the market, will choose not to impose social distancing measures.

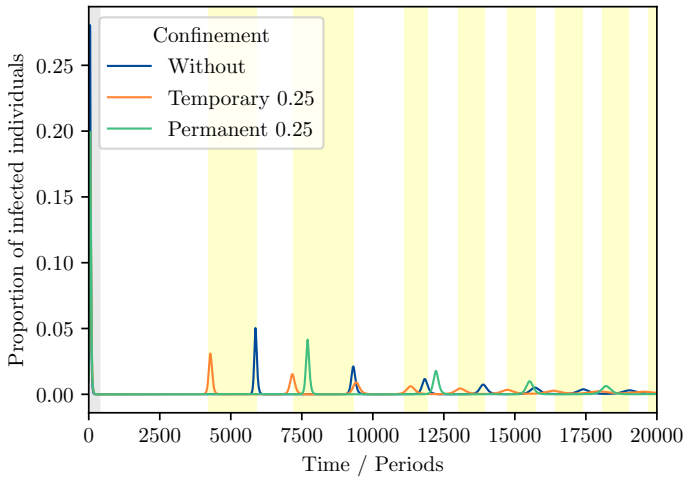

Figure 3.10: Graphic illustration of the recurrence of Swedish Paradox phases in relation to the oscillations of the proportion of infected between periods 0 and 20000. *Yellow zone indicate where the cumulative number of infected individual is higher after a phase of temporary social distancing measures than the cumulation number of infected individual without social distancing measures*

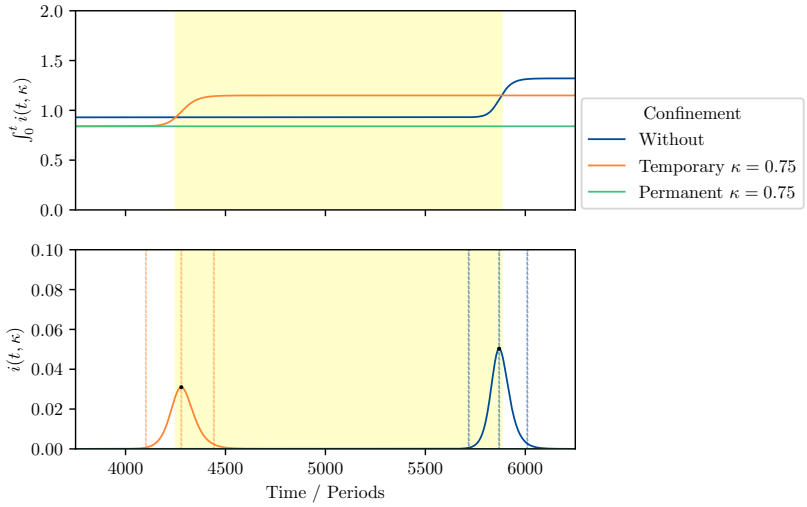

Figure 3.11: Graphic illustration of the relationship between the cumulative proportion of infected (top panel), proportion of infected (bottom panel) during a phase of Swedish Paradox (yellow zone).

3.5 Discussion

In this paper we considered the effects of different social distancing strategies on the dynamics of the SIR epidemiological model with vital dynamics. We chose this model because unlike more complex epidemiological models, this model displays an oscillatory behavior without having to resort to exogenous or endogenous mechanisms. The

damped oscillations around the endemic equilibrium generate several successive waves of infection. These waves appear as the population regenerates via vital dynamics. Under the assumptions of the model, the regeneration of the population is not large enough to compensate for the depletion of the pool of susceptible individuals. Therefore the amplitude of the oscillations decreases with time, without, however, being completely wear off.

Analyzing the two social distancing strategies allows us to come to completely different conclusions. When the social distancing policy is permanent, the oscillations perfectly follow the intuitions of the model. The greater the level of social distancing, the smaller the cumulative number of infected individuals. This principle does not necessarily apply social distancing measures are temporary.

Infection mitigation measures require a fundamental shift in human behavior. The social planner can find it difficult to enforce them and therefore wish to lift them after a certain number of periods. Social distancing measures slow down the infiltration of the infection into the susceptible individuals population thereby protecting a larger proportion of the pool of susceptible individuals. When the measures are lifted, the pool of susceptible individuals takes only a few periods to regenerate to the level required for the infection to resume. When temporary social distancing measures have been mandated, subsequent waves of infection arrive faster than when no measures have been mandated. Therefore, for certain periods, the cumulative number of infected individuals is greater when there have been temporary social distancing measures than when there have not been. The social planner who wishes to minimize the cumulative number of infected individuals must take into account this phenomenon, called the Swedish Paradox, and anticipate the expected time of arrival of the vaccine.

Other factors can influence the oscillatory dynamics of the SIR epidemiological model, such as decreasing immunity. Our research is only a first step towards understanding the mechanisms behind the successive waves of infection and should be deepened in the future. In order to ensure that public policy recommendations reflect a fair and global analysis, it is essential to choose the carefully the model time range when using an epidemiological model that displays oscillatory behaviors.

Bibliography

Acemoglu, Daron et al. (2021). "Optimal targeted lockdowns in a multigroup SIR model". *American Economic Review: Insights* 3.4, pp. 487–502.

Ahituv, Avner, V Joseph Hotz, and Tomas Philipson (1996). "The responsiveness of the demand for condoms to the local prevalence of AIDS". *Journal of Human Resources*, pp. 869–897.

Aiello, Allison E et al. (2010). "Mask use, hand hygiene, and seasonal influenza-like illness among young adults: a randomized intervention trial". *The Journal of infectious diseases* 201.4, pp. 491–498.

Allen, Linda JS et al. (2008). *Mathematical epidemiology*. Vol. 1945. Springer.

Allen, LJS, MA Jones, and CF Martin (1991). "A discrete-time model with vaccination for a measles epidemic". *Mathematical biosciences* 105.1, pp. 111–131.

Alvarez, Fernando E, David Argente, and Francesco Lippi (2020). *A simple planning problem for covid-19 lockdown*. Tech. rep. National Bureau of Economic Research.

Arrow, Kenneth J and Mordecai Kurz (1970). "Optimal growth with irreversible investment in a Ramsey model". *Econometrica: Journal of the Econometric Society*, pp. 331–344.

Atchison, Christina et al. (2021). "Early perceptions and behavioural responses during the COVID-19 pandemic: a cross-sectional survey of UK adults". *BMJ open* 11.1, e043577.

Azeez, Adeboye et al. (2016). "Seasonality and trend forecasting of tuberculosis prevalence data in Eastern Cape, South Africa, using a hybrid model". *International journal of environmental research and public health* 13.8, p. 757.

Bairoliya, Neha and Ayşe İmrohoroğlu (2022). "Macroeconomic consequences of stay-at-home policies during the COVID-19 pandemic". *European Economic Review*, p. 104266.

Baril-Tremblay, Dominique, Chantal Marlats, and Lucie Ménager (2021). "Self-isolation". *Journal of Mathematical Economics* 93, p. 102483.

Baril-Tremblay, Dominique, Chantal Marlats, and Lucie Ménager (2022). "Self-isolation under uncertainty". *Working Paper*.

Baryarama, Flugentius, Livingstone S Luboobi, and Joseph YT Mugisha (2005). "Periodicity of the HIV/AIDS epidemic in a mathematical model that incorporates complacency".

Bavel, Jay J Van et al. (2020). "Using social and behavioural science to support COVID-19 pandemic response". *Nature human behaviour* 4.5, pp. 460–471.

Bodas, Moran and Kobi Peleg (2020). "Self-isolation compliance in the covid-19 era influenced by compensation: Findings from a recent survey in israel: Public attitudes toward the covid-19 outbreak and self-isolation: a cross sectional study of the adult population of israel". *Health Affairs* 39.6, pp. 936–941.

Bolker, Ben M and Bryan Thomas Grenfell (1993). "Chaos and biological complexity in measles dynamics". *Proceedings of the Royal Society of London. Series B: Biological Sciences* 251.1330, pp. 75–81.

Born, Benjamin, Alexander M Dietrich, and Gernot J Müller (2021). "The lockdown effect: A counterfactual for Sweden". *Plos one* 16.4, e0249732.

Britton, Tom, Frank Ball, and Pieter Trapman (2020). "A mathematical model reveals the influence of population heterogeneity on herd immunity to SARS-CoV-2". *Science* 369.6505, pp. 846–849.

Brotherhood, Luiz et al. (2020). "An economic model of the Covid-19 epidemic: The importance of testing and age-specific policies".

Buitrago-Garcia, Diana et al. (2022). "Occurrence and transmission potential of asymptomatic and presymptomatic SARS-CoV-2 infections: Update of a living systematic review and meta-analysis". *PLoS medicine* 19.5, e1003987.

Carnehl, Christoph, Satoshi Fukuda, and Nenad Kos (2022). "Time-varying Cost of Distancing: Distancing Fatigue, Holidays and Lockdowns". *arXiv preprint arXiv:2206.03847*.

— (2023). "Epidemics with behavior". *Journal of Economic Theory* 207, p. 105590.

Cava, Maureen A et al. (2005). "Risk perception and compliance with quarantine during the SARS outbreak". *Journal of Nursing Scholarship* 37.4, pp. 343–347.

Chen, Frederick (2012). "A mathematical analysis of public avoidance behavior during epidemics using game theory". *Journal of theoretical biology* 302, pp. 18–28.

Chen, Frederick et al. (2011). "Public avoidance and epidemics: insights from an economic model". *Journal of theoretical biology* 278.1, pp. 107–119.

Cho, Sang-Wook (2020). "Quantifying the impact of nonpharmaceutical interventions during the COVID-19 outbreak: The case of Sweden". *The Econometrics Journal* 23.3, pp. 323–344.

Cowling, Benjamin J, Sheikh Taslim Ali, et al. (2020). "Impact assessment of non-pharmaceutical interventions against coronavirus disease 2019 and influenza in Hong Kong: an observational study". *The Lancet Public Health* 5.5, e279–e288.

Cowling, Benjamin J, Kwok-Hung Chan, et al. (2009). "Facemasks and hand hygiene to prevent influenza transmission in households: a cluster randomized trial". *Annals of internal medicine* 151.7, pp. 437–446.

Dangerfield, Ciara et al. (2022). "Challenges of integrating economics into epidemiological analysis of and policy responses to emerging infectious diseases". *Epidemics* 39, p. 100585.

Dasaratha, Krishna (2020). "Virus dynamics with behavioral responses". *arXiv preprint arXiv:2004.14533*.

Delamater, Paul L et al. (2019). "Complexity of the basic reproduction number (R0)". *Emerging infectious diseases* 25.1, p. 1.

Di Domenico, Laura et al. (2021). "Adherence and sustainability of interventions informing optimal control against the COVID-19 pandemic". *Communications medicine* 1.1, pp. 1–13.

Earn, David JD (2008). "A light introduction to modelling recurrent epidemics". *Mathematical epidemiology*. Springer, pp. 3–17.

Earn, David JD et al. (2000). "A simple model for complex dynamical transitions in epidemics". *science* 287.5453, pp. 667–670.

Eichenbaum, Martin S, Sergio Rebelo, and Mathias Trabandt (2022). "The macroeconomics of testing and quarantining". *Journal of Economic Dynamics and Control* 138, p. 104337.

Farboodi, Maryam, Gregor Jarosch, and Robert Shimer (2021). "Internal and external effects of social distancing in a pandemic". *Journal of Economic Theory* 196, p. 105293.

Favero, Carlo A, Andrea Ichino, and Aldo Rustichini (2020). "Restarting the economy while saving lives under Covid-19".

Fenichel, Eli P (2013). "Economic considerations for social distancing and behavioral based policies during an epidemic". *Journal of health economics* 32.2, pp. 440–451.

Fenichel, Eli P et al. (2011). "Adaptive human behavior in epidemiological models". *Proceedings of the National Academy of Sciences* 108.15, pp. 6306–6311.

Ferguson, Neil et al. (2020). "Report 9: Impact of non-pharmaceutical interventions (NPIs) to reduce COVID19 mortality and healthcare demand". *Imperial College London* 10.77482, pp. 491–497.

Ferguson, Neil M, D James Nokes, and Roy M Anderson (1996). "Dynamical complexity in age-structured models of the transmission of the measles virus: epidemiological implications at high levels of vaccine uptake". *Mathematical biosciences* 138.2, pp. 101–130.

Ferry, Finola et al. (2021). "The impact of reduced working on mental health in the early months of the COVID-19 pandemic: Results from the Understanding Society COVID-19 study". *Journal of Affective Disorders* 287, pp. 308–315.

Flaxman, Seth et al. (2020). "Estimating the effects of non-pharmaceutical interventions on COVID-19 in Europe". *Nature* 584.7820, pp. 257–261.

Fong, Min W et al. (2020). "Nonpharmaceutical measures for pandemic influenza in nonhealthcare settings—social distancing measures". *Emerging infectious diseases* 26.5, p. 976.

Giannitsarou, Chryssi, Stephen Kissler, and Flavio Toxvaerd (2021). "Waning immunity and the second wave: Some projections for SARS-CoV-2". *American Economic Review: Insights* 3.3, pp. 321–38.

Glover, Andrew et al. (2020). *Health versus wealth: On the distributional effects of controlling a pandemic*. Tech. rep. National Bureau of Economic Research.

Goldstein, Herbert, Charles Poole, and John Safko (2002). *Classical mechanics*.

Greer, Meredith et al. (2020). "Emergence of oscillations in a simple epidemic model with demographic data". *Royal Society open science* 7.1, p. 191187.

Grenfell, Bryan Thomas and Roy Malcolm Anderson (1989). "Pertussis in England and Wales: an investigation of transmission dynamics and control by mass vaccination". *Proceedings of the Royal Society of London. B. Biological Sciences* 236.1284, pp. 213–252.

Gudbjartsson, Daniel F et al. (2020). "Humoral immune response to SARS-CoV-2 in Iceland". *New England Journal of Medicine* 383.18, pp. 1724–1734.

Han, Dongsheng et al. (2020). "COVID-19: Insight into the asymptomatic SARS-COV-2 infection and transmission". *International Journal of Biological Sciences* 16.15, p. 2803.

Hethcote, Herbert W (1997). "An age-structured model for pertussis transmission". *Mathematical biosciences* 145.2, pp. 89–136.

Hethcote, Herbert W and Simon A Levin (1989). "Periodicity in epidemiological models". *Applied mathematical ecology*. Springer, pp. 193–211.

Jefferson, Tom et al. (2022). "Transmission of Severe Acute Respiratory Syndrome Coronavirus-2 (SARS-CoV-2) from pre and asymptomatic infected individuals: a systematic review". *Clinical Microbiology and Infection* 28.2, pp. 178–189.

Jones, Callum, Thomas Philippon, and Venky Venkateswaran (2021). "Optimal mitigation policies in a pandemic: Social distancing and working from home". *The Review of Financial Studies* 34.11, pp. 5188–5223.

Juranek, Steffen and Floris Zoutman (2020). "The effect of social distancing measures on intensive care occupancy: Evidence on COVID-19 in Scandinavia". *NHH Dept. of Business and Management Science Discussion Paper* 2020/2.

Kandel, Nirmal et al. (2020). "Health security capacities in the context of COVID-19 outbreak: an analysis of International Health Regulations annual report data from 182 countries". *The Lancet* 395.10229, pp. 1047–1053.

Keeling, Matt J and Bryan T Grenfell (2002). "Understanding the persistence of measles: reconciling theory, simulation and observation". *Proceedings of the Royal Society of London. Series B: Biological Sciences* 269.1489, pp. 335–343.

Keeling, Matt J. and Pejman Rohani (2008). *Modeling Infectious Diseases in Humans and Animals*. Princeton University Press.

Kellam, Paul and Wendy Barclay (2020). "The dynamics of humoral immune responses following SARS-CoV-2 infection and the potential for reinfection". *The Journal of general virology* 101.8, p. 791.

Kermack, W.O. and A.G. McKendrick (1927). "Contribution to the Mathematical Theory of Epidemics". *Proceedings of the Royal Society A* 115; 138; pp. 700–721, 55–83, 94–122.

Kong, Edward and Daniel Prinz (2020). "Disentangling policy effects using proxy data: Which shutdown policies affected unemployment during the COVID-19 pandemic?" *Journal of Public Economics* 189, p. 104257.

Kremer, Michael (1996). "Integrating behavioral choice into epidemiological models of AIDS". *The Quarterly Journal of Economics* 111.2, pp. 549–573.

Kruse, Thomas and Philipp Strack (2020). "Optimal control of an epidemic through social distancing". *Available at SSRN 3581295*.

Lewis, Rhyd (2007). "Metaheuristics can solve sudoku puzzles". *Journal of heuristics* 13.4, pp. 387–401.

Li, Qun et al. (2020). "Early transmission dynamics in Wuhan, China, of novel coronavirus–infected pneumonia". *New England journal of medicine*.

Liu, Kai et al. (2020). "Clinical features of COVID-19 in elderly patients: A comparison with young and middle-aged patients". *Journal of Infection* 80.6, e14–e18.

London, Wayne P and James A Yorke (1973). "Recurrent outbreaks of measles, chickenpox and mumps: I. Seasonal variation in contact rates". *American journal of epidemiology* 98.6, pp. 453–468.

Matthews Pillemer, Francesca et al. (2015). "Predicting support for non-pharmaceutical interventions during infectious outbreaks: a four region analysis". *Disasters* 39.1, pp. 125–145.

Matthies, Konstantin and Flavio Toxvaerd (2022). "Rather doomed than uncertain: risk attitudes and transmissive behavior under asymptomatic infection". *Economic Theory*, pp. 1–44.

Mizumoto, Kenji et al. (2020). "Estimating the asymptomatic proportion of coronavirus disease 2019 (COVID-19) cases on board the Diamond Princess cruise ship, Yokohama, Japan, 2020". *Eurosurveillance* 25.10, p. 2000180.

Nishiura, Hiroshi et al. (2020). "Estimation of the asymptomatic ratio of novel coronavirus infections (COVID-19)". *International journal of infectious diseases* 94, pp. 154–155.

Pépin, Jean Louis et al. (2020). "Wearable activity trackers for monitoring adherence to home confinement during the COVID-19 pandemic worldwide: data aggregation and analysis". *Journal of medical Internet research* 22.6, e19787.

Petherick, Anna, Rafael Goldszmidt, et al. (2021). "A worldwide assessment of changes in adherence to COVID-19 protective behaviours and hypothesized pandemic fatigue". *Nature Human Behaviour* 5.9, pp. 1145–1160.

Petherick, Anna, Beatriz Kira, et al. (2020). "Variation in government responses to COVID-19". *Blavatnik Centre for Government Working Paper, University of Oxford*.

Phelan, Thomas and Alexis Akira Toda (2022). "Optimal epidemic control in equilibrium with imperfect testing and enforcement". *Journal of Economic Theory* 206, p. 105570.

Philipson, Tomas J and Richard A Posner (1993). *Private choices and public health: The AIDS epidemic in an economic perspective*. Harvard University Press.

Piret, Jocelyne and Guy Boivin (2021). "Pandemics throughout history". *Frontiers in microbiology* 11, p. 631736.

Pollán, Marina et al. (2020). "Prevalence of SARS-CoV-2 in Spain (ENE-COVID): a nationwide, population-based seroepidemiological study". *The Lancet* 396.10250, pp. 535–544.

Rachel, Łukasz et al. (2020). *An analytical model of covid-19 lockdowns*. CFM, Centre for Macroeconomics.

Rampini, Adriano A (2020). *Sequential lifting of COVID-19 interventions with population heterogeneity*. Tech. rep. National Bureau of Economic Research.

Reluga, Timothy C (2010). "Game theory of social distancing in response to an epidemic". *PLoS computational biology* 6.5, e1000793.

Remuzzi, Andrea and Giuseppe Remuzzi (2020). "COVID-19 and Italy: what next?" *The lancet* 395.10231, pp. 1225–1228.

Richardson, Safiya et al. (2020). "Presenting characteristics, comorbidities, and outcomes among 5700 patients hospitalized with COVID-19 in the New York City area". *Jama* 323.20, pp. 2052–2059.

Rowthorn, Bob RE and Flavio Toxvaerd (2012). "The optimal control of infectious diseases via prevention and treatment".

— (2020). "The optimal control of infectious diseases via prevention and treatment".

Sanyaolu, Adekunle et al. (2020). "Comorbidity and its impact on patients with COVID-19". *SN comprehensive clinical medicine* 2, pp. 1069–1076.

Sethi, Suresh P (1978). "Optimal quarantine programmes for controlling an epidemic spread". *Journal of the Operational Research Society*, pp. 265–268.

Shahdoust, Maryam et al. (2015). "Predicting hepatitis B monthly incidence rates using weighted Markov chains and time series methods".

Sheridan, Adam et al. (2020). "Social distancing laws cause only small losses of economic activity during the COVID-19 pandemic in Scandinavia". *Proceedings of the National Academy of Sciences* 117.34, pp. 20468–20473.

Silverio, Angelo et al. (2020). "Timing of national lockdown and mortality in COVID-19: The Italian experience". *International Journal of Infectious Diseases* 100, pp. 193–195.

Singh, Awadhesh Kumar et al. (2020). "Diabetes in COVID-19: Prevalence, pathophysiology, prognosis and practical considerations". *Diabetes & Metabolic Syndrome: Clinical Research & Reviews* 14.4, pp. 303–310.

Smith, Louise E et al. (2020). "Factors associated with adherence to self-isolation and lockdown measures in the UK: a cross-sectional survey". *Public Health* 187, pp. 41–52.

Soper, Herbert E (1929). "The interpretation of periodicity in disease prevalence". *Journal of the Royal Statistical Society* 92.1, pp. 34–73.

Taylor, John R (2005). *Classical Mechanics. 3 "E ed.*

Toxvaerd, Flavio (2019). "Rational disinhibition and externalities in prevention". *International Economic Review* 60.4, pp. 1737–1755.

— (2020). "Equilibrium social distancing". *Working Paper.*

— (2022). "Silent Spreaders: Behavior and Equilibrium Under Asymptomatic Infection". *Working Paper.*

Van Dorp, Lucy et al. (2020). "Emergence of genomic diversity and recurrent mutations in SARS-CoV-2". *Infection, Genetics and Evolution* 83, p. 104351.

Verity, Robert et al. (2020). "Estimates of the severity of COVID-19 disease". *MedRxiv*, pp. 2020–03.

Wang, Bolin et al. (2020). "Does comorbidity increase the risk of patients with COVID-19: evidence from meta-analysis". *Aging (albany NY)* 12.7, p. 6049.

Webster, Noah (1799). *A Brief History of Epidemic and Pestilential Diseases: With the Principal Phenomena of the Physical World, which Precede and Accompany Them, and Observations Deduced from the Facts Stated...* Vol. 2. Hudson & Goodwin.

Wilder-Smith, Annelies and David O Freedman (2020). "Isolation, quarantine, social distancing and community containment: pivotal role for old-style public health measures in the novel coronavirus (2019-nCoV) outbreak." *Journal of travel medicine.*

Xiao, Meng et al. (2020). "Antiphospholipid antibodies in critically ill patients with COVID-19". *Arthritis & Rheumatology* 72.12, pp. 1998–2004.

Yan, Y et al. (2020). *Do face masks create a false sense of security? a COVID-19 dilemma. MedRxiv, 2020.05. 23.20111302.*

Yan, Youpei et al. (2021). "Measuring voluntary and policy-induced social distancing behavior during the COVID-19 pandemic". *Proceedings of the National Academy of Sciences* 118.16, e2008814118.

Zeng, Hui et al. (2020). "Antibodies in infants born to mothers with COVID-19 pneumonia". *Jama* 323.18, pp. 1848–1849.

Zhang, Sheng et al. (2020). "Estimation of the reproductive number of novel coronavirus (COVID-19) and the probable outbreak size on the Diamond Princess cruise ship: A data-driven analysis". *International journal of infectious diseases* 93, pp. 201–204.

Zhao, Shi et al. (2020). "Estimating the serial interval of the novel coronavirus disease (COVID-19): a statistical analysis using the public data in Hong Kong from January 16 to February 15, 2020". *Frontiers in Physics* 8, p. 347.

Zhou, Fei et al. (2020). "Clinical course and risk factors for mortality of adult inpatients with COVID-19 in Wuhan, China: a retrospective cohort study". *The lancet* 395.10229, pp. 1054–1062.